SEPT. - DEC. 2007
Volume XIII Number III
ISSN 0859 144X

THE ASEAN JOURNAL OF RADIOLOGY

Published by The Radiological Society and
The Royal College of Radiologists of Thailand,
Bangkok, Thailand

SEPT. - DEC. 2007
Volume XIII Number III
ISSN 0859 144X

THE ASEAN JOURNAL OF RADIOLOGY

Published by The Radiological Society and
The Royal College of Radiologists of Thailand,
Bangkok, Thailand

Started through an educational grant from Bracco Since 1995

www.bracco.com

Chief Editor

Professor Kawee Tungsubutra
Kaweevej Hospital, 318 Tarksin Road, Dhonburi, Bangkok 10600, Thailand.

Asean Journal of Radiology.
Instructions for Authors.

1. The Asean Journal of Radiology publishes the papers on Radiological Sciences, such as research work, review articles, case reports, innovations in Medical Sciences related to all branches of Radiology, and letters to the editor. The aforementioned materials can be written in English only.

2. The authors have to submit 2 copies of the manuscript and a diskette: **to Prof. Dr. Kawee Tungsubutra.** 318 Kaweevej Hospital, Tarksin Road, Dhonburi, Bangkok 10600, Thailand.

3. The original copy to be submitted must be typed in a double space on one side of the page of 8.1/2" x 11.1/2" paper.

4. The format of the article must include :
   a. Title page and address of the author (s)
   b. Abstract
   c. Introduction (Background)
   d. Material and Method
   e. Results and discussion (Tables and Illustrations)
   f. Acknowledgement (if any)
   g. References (Follow the Vancouver style developed by ICMJE)

5. We will provide 5 copies of reprints for the author (s) who submit (s) an article for publication in the Asean Journal.

6. The illustrations and tables must be clearly prepared with legends in English as they are the art works to be reproduced.

7. The authors are reponsible for the contents of the article as to its facts and findings.

8. Ethics.

Paper reporting studies which might be interpreted as human experimentation (e.g. controlled trials) should conform to the standards of the Declaration of Helsinki (see British Medical Journal 1964: 2: 177) and should indicate that, approval that such studies may proceed, has been granted by the local or hospital Ethics Committee.

When reporting experiments on animals indicate whether the institution's or the National Research Council's guide for, or any national law on, the care and use of laboratory animals was followed.

THE ASEAN JOURNAL OF RADIOLOGY

Volume XIII Number III SEPT. - DEC. 2007

CONTENTS

THE ASEAN JOURNAL OF RADIOLOGY

Volume XIII Number III SEPT. - DEC. 2007

CONTENTS

COMPUTED TOMOGRAPHY OF BRAIN IN EPILEPTIC PATIENTS

Supang SINTHUNYATHUM, M.D.,[1] Pipat CHIEWVIT, M.D.[2]

ABSTRACT

Objective: To assess the yields of imaging findings of computed tomography (CT) of the brain and to detect CT findings in epileptic patients.

Materials and Methods: Study in 63 epileptic patients admitted in Phrachomklao Hospital, Phetchaburi, Thailand during January 2004-June 2007. CT scan with intravenous contrast administration was performed in all patients. The radiologic findings were assessed by one radiologist.

Results: 63 epileptic patients with an average age of 37 years (range 1-92 yrs). 35 were males, and 28 females. They were stratified into three age groups, including young age (1-30 years old), middle age (31-50 years old) and elderly (over 50 years old). Most common CT finding in all aging groups were idiopathic (non-related finding or normal finding), found in young age group = 64%, middle age group = 62.5% and elderly group = 50%; Total cases with idiopathic findings = 38/63 = 60.31%. The causes of epilepsy could be identified in 25 cases, 39.69% in this report. The causes could be identified easier and better in the elderly group in comparison with in the young and middle age groups. The result of this study was compared with the result of MRI in epileptic adult patients: experience in Ramathibodi Hospital.[1]

Conclusion: CT is important in the diagnosis of epilepsy and assessment of the disease, which may be treatable but it is not standard investigation for epileptic patients in comparison with EEG and MRI. The yield of CT is for detecting the cause in some patients such as stroke in elderly patients, vascular abnormality in young adult (AVM), cerebral infection, brain tumor and some congenital lesions.

INTRODUCTION

Seizure: A paroxysmal event due to abnormal, excessive, hypersynchronous discharges from an aggregation of central nervous system (CNS) neurons. Depending on the distribution of discharges, this abnormal CNS activity can have various manifestations, ranging from dramatic convulsive activity to experiential phenomena. The incidence and prevalence of seizures approximately 5 to 10% of the population will have at least one seizure during their lifetime[3,7] with the highest incidence occurring on early childhood and late adulthood.[7]

Epilepsy: describes as a condition of "recurrent seizure" due to a chronic, underlying process.

The cause of seizures[7] :

Neonates (< 1mo) Perinatal hypoxia and ischemia
Intracranial hemorrhage and trauma
Acute CNS infection
Metabolic disturbances

[1] Division of Radiology, Phrachomklao Hospital.
[2] Division of Diagnostic Radiology, Department of Radiology, Siriraj Hospital.

	Drug withdrawal
	Developmental disorders
	Genetic disorders
Infants and children (>1mo,< 12mo)	
	Febrile seizures
	Genetic disorders
	CNS infection
	Developmental disorders
	Trauma
	Idiopathic
Adolescents:	Trauma
(12-18 years)	Genetic disorders
	Infection
	Brain tumor
	Illicit drug use
	Idiopathic
Young adults:	Trauma
(18-35 years)	Alcohol withdrawal
	Illicit drug use
	Brain tumor
	Idiopathic
Older adults:	Cerebrovascular disease
(>35 years)	Brain tumor
	Alcohol withdrawal
	Metabolic disorders
	Alzheimer's disease and other degenerative CNS disease
	Idiopathic

The evaluation and management of patients with epilepsy are essential for qualily of life. Although many studies, the majority of epileptic patients by CT imaging have unknown etiology.

At present, there are many investigations and modalities available for diagnosis and searching for the causes of epilepsy including electro-encephalography (EEG), computed tomography (CT); magnetic resonance imaging (MRI), single photon emission computed tomography (SPECT) as well as positron emission tomography (PET).

Although computed tomography (CT) is not considered standard for evaluation of the patients with epilepsy, CT is still useful in limited investigations in provincial hospital or when MRI is contraindicated. Compared to MRI, CT suffers from, by lesser soft tissue contrast, lack of multi-planar capability and beam hardening artifact at the skull base.[4]

The purpose of this study was to review epileptic patients referred to CT imaging of the brain at Phrachomklao Hospital to detect the causes related or non related to the seizure and assess the diagnostic yield of CT imaging for epileptic patients.

MATERIALS AND METHODS

A study was done in 63 epileptic patients admitted in the Departments of Medicine and Pediatrics, Phrachomklao Hospital during January 2004-June 2007. Children with febrile convulsion were excluded. They had underwent CT study.

The CT scan was performed by axial 5 mm. at the posterior fossa and 10 mm. slice thickness of the rest, using SHIMADZU SCT- 4800 TCZ. Intravenous contrast study was given to all patients. The radiologic findings were assessed by one radiologist.

RESULTS

There were 63 epileptic patients, with an average age of 37 years (range 1-92 yrs). 35 were males, and 28 females. Patients were stratified into three age groups.

Table 1 Number of patients with different ages

	Group	Number of patients
1	young age (1 – 30 years)	25
2	middle age (31 – 50 years)	24
3	elderly (over 50 years)	14
	total	63

Table 2 CT findings categories and details.

CT findings categories	CT findings
1. Idiopathic (non related findings or normal findings)	Hyperostosis frontalis, interna, Brain atrophy (compatible with aging), Normal CT finding
2. Vascular disease	Brain infarction, AVM, Hypertensive encephalopathy
3. Infection	Toxoplasmosis, HIV encephalopathy.
4. Degenerative disease	Brain atrophy (uncompatible with aging)
5. Congenital	Cerebral dysgenesis(open-lip schizencephaly) Encephalomalacia
6. More than 1 categories	Combined two findings of 2-5

Table 3 Findings classified in age group

Age	Idiopathic (Non related or normal findings)	Abnormal CT findings related to epilepsy	Number of patients
1 – 30 yrs	16 (64%)	9	25
31 – 50 yrs	15 (62.5%)	9	24
over 50 yrs	7 (50%)	7	14
Total	38 (60.31%)	25	63

Table 4 Abnormal CT findings related to epilepsy

Age	Congenital	Vascular	Degenerative	Infection	More than 1 categories	Total
1 – 30 yrs	1	2	5	-	1*	9
31 – 50 yrs	-	3	3	2	1**	9
over 50 yrs	-	6	1	-	-	7
Total	1	11	9	2	2	25

* (congenital coincident with brain atrophy)
** (brain atrophy coincident with brain infarction)

In the present study, the most common CT finding in each age groups was indeterminate or non -specific and was classified as an idiopathic (table 3)

As in Table 4, CT finding in one patient in congenital group is cerebral dysgenesis (open-lip schizencephaly) (Fig. 1)

Vascular anomalies was found in 11 patients, 6 showed cerebral infarction, 2 hypertensive hemorrhage and 3 AVM. (Fig. 3)

9 patients had degenerative disease, hemiatrophy was found in 1 patient, focal brain atrophy in 2 patients, and diffuse brain atrophy (uncompatible with aging) in 6 patients. Those with diffuse brain atrophy compatible with aging were not included in these groups. They were classified as idiopathic group.

Findings in 2 patients were related to HIV infection and one of them was multiple nodular enhancements with dramatic responsive to treatment of toxoplasmosis. (Fig. 2) The other showed HIV encephalopathy.

Two patients had more than 1 categories, one with brain atrophy found coincident with brain infarction, the other had brain atrophy coincident with congenital disease (encephalomalacia).

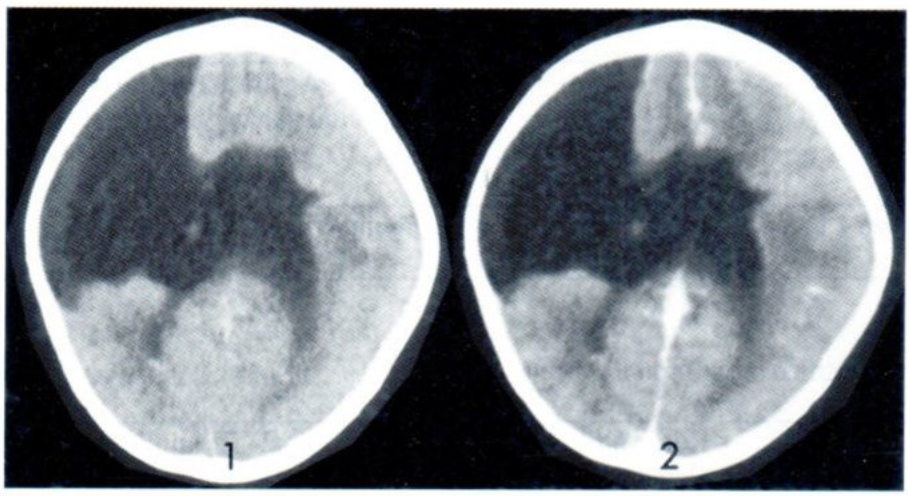

Fig. 1 NECT (1) and CECT (2) study of a one-year old girl, revealed a wedge-shaped fluid-filled space, replacing in the areas of right lateral fronto-parietal cerebral hemisphere and communicating with right lateral ventricle, suggestive of CNS congenital anomalies likely to be "Open-lip schizencephaly".

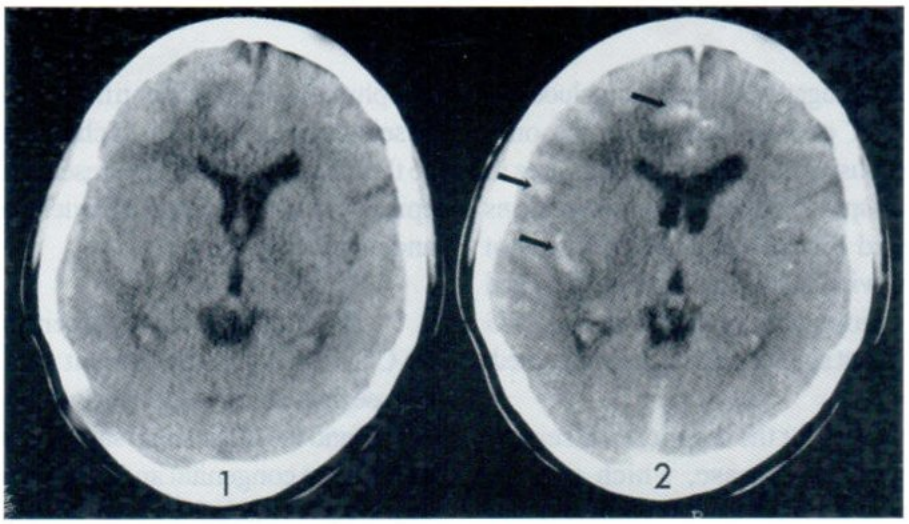

Fig. 2 NECT (1) and CECT (2) study of a HIV positive patient, revealed multiple small enhanced nodules at right fronto-parietal lobe with mild perifocal edema. She was dramaticly responsive to treatment of toxoplasmosis.

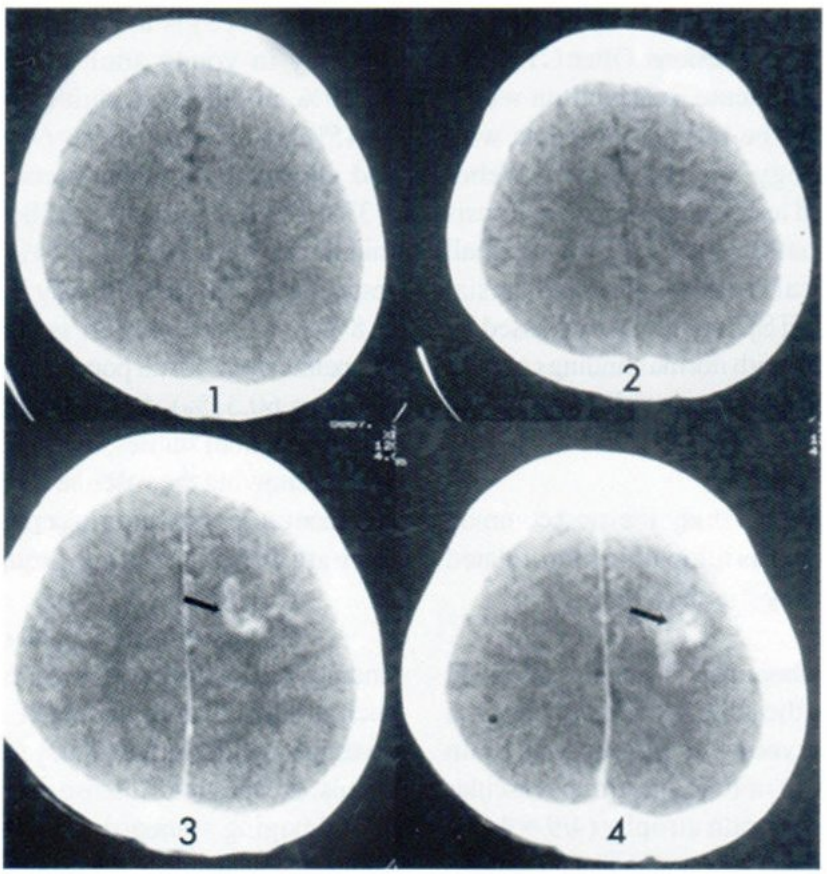

Fig. 3 NECT (1,2) and CECT (3,4) study of a 32 year-old male patient with epilepsy, revealed no gross abnormality of NECT brain study, but serpentine vascular configuration enhancement at left parietal vertex at CECT, suggestive of AVM.

DISCUSSION

Epileptic investigations in patients include CT, MRI, EEG, SPECT or PET but CT is the only available modality using for röentgen diagnoses in Phrachomklao Hospital. The other investigations which are standard for epileptic patients are not available in the provincial hospital such as EEG and MRI, therefore, comparison of diagnoses by EEG and MRI in the present study could not be performed.

CT is essential for the diagnosis of seizure and assessment of the disease, which may be treatable; however it is not standard investigation for epileptic patients due to its limitation from lesser soft tissue contrast, lack of multi-planar capability and beam hardening artifacts,[4] as compare to the MRI study. However, CT is readily useful in patients with acute presentations such as intracranial hemorrhage, brain infarct and mass lesions as well as obvious malformations and calcified lesions. Often CT serves as first line imaging in acute presentation where urgent treatment may be merited. Patients with hemispheric pathology such as Sturge-Weber syndrome or calcified lesions of tuberous sclerosis may adequately evaluated with CT. However, small tumors, subtle cortical malformation and mesial temporal sclerosis (MTS) may be easily missed by CT. In general patients with normal findings or with lesions judged incompletely characterized by CT will then proceed to MRI.[4,5]

Thus, in the present study, the most common CT finding in all groups is idiopathic (non-related finding or normal findings) as the table 3.

Regarding to abnormal CT findings classified in each age group, as the table 4, the most common cause of epilepsy in young age group was brain atrophy (6/9 = 66%). In middle age group, vascular abnormality as well as brain atrophy (4/9 = 44%) and in elderly group, vascular abnormality (6/7 = 86%) (Hypertensive hemorrhage and brain infarction) were most common.

Among the abnormal CT findings, brain atrophy could not be identified as the obvious cause of seizure but it is a result of chronic seizure findings, so the elderly group in the present study, the cause of epilepsy could be identified better than the young age and middle age groups.

The definite causes of seizure demonstrating by CT imaging in the present study was vascular disease (hypertensive encephalopathy, brain infarction, AVM) and the other small samples in the other aging group were congenital and HIV infection (the risk of seizure was 38% in HIV positive patient).[8] The other common causes but no examples in the present study were cranial trauma, brain tumor, CNS infections, etc.

Compared to the report of MRI of brain in epileptic adult patients in Thailand,[1] mesial temporal sclerosis (MTS) is the most common etiology of epilepsy in young adult (15-34 yrs) = 11/42 = 26.19%, middle age adult (35-64 yrs) = 14/41 = 34.15% but the older adult (>64 yrs) vascular disease and idiopathic were equally common etiologies, 3/8 = 37.50%. The idiopathic of both young adult and middle adult is only 3/42 (7.14%) and 2/41 (4.88%), respectively. The idiopathic by MRI of all population = 8/91 = 8.79% which is much less than the idiopathic by CT of all population in the present study (38/63 = 60.31%). Among the abnormal imaging findings of both studies, the similar findings of both reports showing the vascular diseases were the most common cause of seizure in older age group, eventhough there are differences in age groups of both studies.

By this comparison, all cases of normal CT findings and some abnormal cases of all aging groups such as brain atrophy should be referred for further investigation such as MRI study for evaluation in more details, except stroke disease in elderly patients. MRI is an imaging standard for routine evaluation of epileptic patients. MRI could detect pathologic abnormalities with more sensitivity and accuracy than CT. Therefore, while epileptogenic lesions are visible by CT, the advantages of MRI is more pronounced in pathological conditions such as focal cortical

dysplasia, migrational anomalies and mesial temporal sclerosis (MTS). However; this comparison of MRI findings in seizure patients in Ramathibodi Hospital and CT findings in seizure patients of the present study is not based on the same population. Furthermore, many CT and MRI modalities have varies efficiency and could give in more or lesser information for each one.

MTS is the most common syndrome associated with complex partial seizures. MRI can detect the characteristic of hippocampal sclerosis appearing as increased signal on T2-weighted image associated with small temporal lobe and enlarged temporal horn of lateral ventricle, meanwhile CT is insensitive to MTS.[6] Recognition of this syndrome is especially important because it tends to be refractory to treatment with anticonvulsants but responds extremely well to surgical intervention.[7] MTS accounts for majority of patients undergoing temporal lobe surgery.[6]

For the present study; in the author's opinion,

1. Epilepsy in stroke diseases appear to be adequately evaluated with CT imaging.

2. CT imaging in elderly epileptic patients in present study could identify the causes of epilepsy better than in young age and middle age groups and is most useful to be performed, as compared to the other age groups.

3. Normal CT findings in all epileptic patients are suggested to have further investigation such as MRI, EEG.

CONCLUSIONS

CT imaging is not only important in the diagnosis of epilepsy and assessment of the disease, but also for identifying its etiology, which may be treatable. However; it is not standard investigation for epileptic patient in comparison with the EEG and MRI.

It is still useful in a provincial hospital for detecting the causes of epilepsy in some patients such as stroke diseases, cerebral infection, brain tumor or some congenital lesions.

Therefore; normal CT findings or unidentified causes of seizure in CT findings should be referred for further investigation such as MRI because detection of the causes and management of the patients with seizure are essential for quality of life.

ACKNOWLEDGEMENTS

The author would like to thank Dr. Witaya Petdachai for reviewing the manuscript.

REFERENCES

1. Solosrungruang A, Laothamatas J, Chinwarun Y. Magnetic Resonance Imaging of the brain in epileptic adult patients: experience in Ramathibodi Hospital. J Med Assoc Thai 2007; 90 (4): 762-73.
2. Wongladarom S, Laothamatas J, Visudtibhan A, et al. Magnetic Resonance Imaging of the brain in epileptic pediatric patients: review of the experience in Ramathibodi Hospital. J Med Assoc Thai 2004; 87 (9): 1092-9.
3. Schoenenberger RA. Indication for computed tomogram of the patients with first umcomplicated generalized seizure. BMJ 1994; 309 : 986-9.
4. Bradley WG, Shey RB. MR Imaging evaluation of seizures. Radiology 2000; 214 (3) : 651-6.
5. Hallam DK. Investigating Epilepsy; CT and MRI in Epilepsy. Nepal Journal of Neuroscience 2004; 1: 64-72.
6. Osborn AG, Salzman KL, Katzman GL, et al. Mesial temporal sclerosis In, Diagnostic Imaging Brain 2nded, Amirsys 2004, I 10-50-53.

7. Lowenstein DH, Seizure and Epilepsy In, Braunwald E., Fauci AS., Kasper DL., Hauser SL., Longo DL., Jameson JL., editors; Harrison"s principle of medicine, 15th ed McGraw-Hill; 2001, 2354-69.

8. Gumbo T, Kodzirange G, Mielke J, et al. Cryptococus neoformans meningoencephalitis in African children with acquired immunodeficiency syndrome. Pediatr Infect Dis J 2002; 21: 54-6.

CASE REPORT: PRIMARY RETROPERITONEAL VENOUS HEMANGIOMA MIMICKING RETROPERITONEAL LYMPHADENOPATHY IN PHRACHOMKLAO HOSPITAL

Supang SINTHUNYATHUM, M.D.,[1] Pipat CHIEWVIT, M.D.[2]

ABSTRACT

A 35 year-old male patient presented with abdominal pain. Ultrasound (u/s) and computed tomography (CT) suspected to be caused by distal CBD stone obstruction and additional incidental findings of a large retroperitoneal hypodense nodule at para aortic region, appearing to engulf the left renal vein, suggestive of lymphadenopathy. A diagnosis of paraaortic lymphadenopathy was made based on U/S and three studies of CT findings to be hypodense, non-enhancing lesion of the mass which was atypical for hemangioma. However; upon laparoscope resection, histopathologically examination revealed retroperitoneal soft tissue mass to be a venous hemangioma. Retroperitoneal venous hemangioma is a very rare condition, which accurate preoperative diagnosis is very difficult.

CBD = Common Bile Duct

INTRODUCTION

Hemangioma is a slowly growing benign vascular tumor which is rarely originating in retroperitoneum. It is the most common vascular tumor in the childhood aging group, occurring in 10-12 % of children with one year of age and involving upto 30 % of those with very low birth weight (less than 1000 g). The skin and soft tissue are the organs most commonly involved, particularly in the areas of head and neck (60 %) and the trunk (25 %). The other organs involvement are visceral organs, most frequently are the liver (64%), central nervous system (52 %), gastrointestinal tract (52 %), lung (52 %), eyes (32 %), mouth and tongue (44 %) and rarely at retroperitoneum. Females are more often affected than males.[2]

Special clinical manifestations are hemangiomatosis,[6, 7] which are rare occasions. A child may present with multiple cutaneous hemangiomas with or without visceral involvement .When the lesions are limited to the skin, the condition is known as benign neonatal hemangiomatosis (BNH). When there is visceral involvement, it is denominated as disseminated or diffuse neonatal hemangiomatosis (DNH).

Histologically: hemangiomas are subdivided into five categories, depending on the predominant type of vascular channel identifiable. These subdivisions include capillary, cavernous, arteriovenous, venous and mixed variations.[8,9]

1. capillary hemangiomas are the most common. They are usually diagnosed during the first few years of life and found in the skin, subcutaneous tissue, or vertebral bodies. Microscopically, capillary hemangiomas are composed of a disordered array of capillary-sized vessels. Most of these hemangiomas spontaneously involute.

[1] Division of Radiology, Phrachomklao Hospital.
[2] Division of Diagnostic Radiology, Department of Radiology, Siriraj Hospital.

2. Cavernous hemangiomas are larger and deeper and occur later in life. They are often affect the skin and liver,[4] composed of dilated, blood-filled space lined by flattened endothelium. Calcification is common. They do not spontaneously involute and therefore may require surgical intervention.

3. Arteriovenous hemangiomas may be deep or superficial. They represent an abnormal communication between arteries and veins, and can cause a variable degree of shunting.

4. Venous hemangiomas typically involve deep structures, generally found in adults and most frequently are located in the deep soft tissue, such as retroperitoneum, mesentery and muscles of lower extremities. They are composed of thicker-walled vessels containing smooth muscle cells. They often have slow blood flow, and pheboliths may be presented.

5. mixed type

Almost all retroperitoneal hemangiomas are of the cavernous type; the venous type is very rare.[1] Accurate preoperative diagnosis of this tumor is very difficult.

Symptoms secondary to retroperitoneal hemangioma are usully vague and appear late in the course of the disease, secondary to compression. Back pain, epigastrium disturbance and postprandial sensation.[3]

CASE REPORT

A 35 years old male patient with a history of a minute gallstone presented with sudden abdominal pain, off and on for 1 week, with no palpable mass.

Physical examination: Normal

Laboratory tests: all of blood and urine are normal including coagulation test, tumor markers such as CA (125), CA (199), and urine metanephrine and normetanephrine except for HBs Ag positive.

Ultrasound of abdomen

: Mild dilatation of both intrahepatic bile ducts and CBD (measuring about 1.2 cm.) without demonstrable the cause of obstruction. The gallbladder is fairly distension, with no identifiable stone.

: A large hypoechogenic mass, about 4x5 cm. at left para-aortic area, medial to left kidney.

CT (first study at private imaging center, 3 days after ultrasound study).

: Minimally dilated intrahepatic bile ducts of both lobes liver and CHD (1.5cm), no demonstrable obstructed cause.

: The gallbladder appears to have minimal smooth wall thickening, no opaque stone.

: A non enhanced retroperitoneal mass appearing as encasement of the left renal vein with an impression of left paraaortic mass to be enlarged node.

CT (second study at private hospital after first CT study 5 days and the patient had marked improvement of abdominal pain)

: Normal appearance of liver without intrahepatic duct dilatation or CBD, CHD dilatation. Normal gallbladder without stone.

: A large non-enhanced lobulated retroperitoneal mass at left paravertebral region near left renal hilum with few areas of internal hemorrhage. Differential diagnosis is included tumor such as mesenchymal tumor, nerve tumor, duodenal GIST or enlarged node.

CT (third study* at another government hospital after second CT study 1 month)

: Liver is of normal, no intrahepatic duct dilatation. The gallbladder is normal distension, without evidence of stone.

: 6.9x4.6 cm. retroperitoneal lobulated non enhanced mass at left paraaortic area with pressure effect to left renal vein. Differential diagnosis to be necrotic lymph node, neuroendocrine tumor or sarcoma.

Laparoscope resection at another government hospital (the same hospital of the* third CT study)

: A retroperitoneal soft tissue mass measuring 5.5x4x3 cm. surrounding and floating in the old blood.

: Cholecystectomy.

Histopathology findings :

: Macroscopic characteristics showed a piece of irregular-shaped brown mass.

: Microscopic exam showed fibrofatty tissue containing clumps of dilated vein like vascular units with variable irregular smooth muscle walls.

Diagnosis : Soft tissue mass (retroperitoneum) :Venous hemangioma

Gallbladder : Chronic cholecystitis.

The patient had follow up ultrasound study 7 months after laparoscope resection, showing no residual tumor.

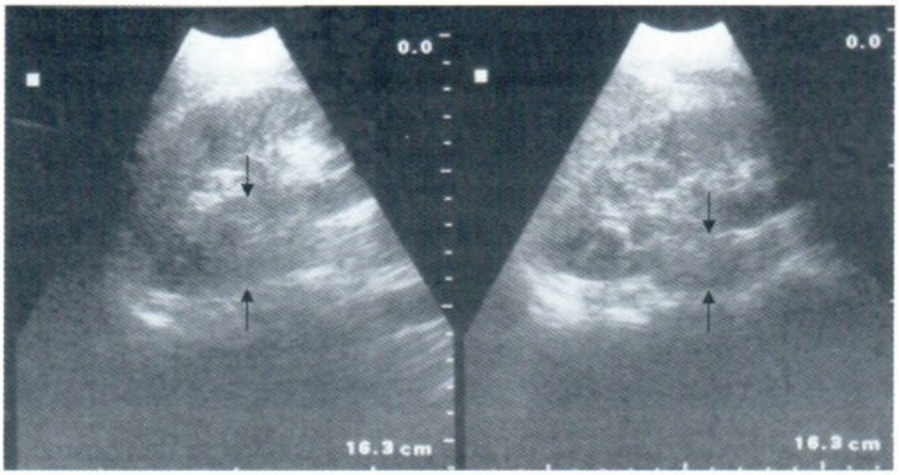

Fig. 1 Ultrasound finding revealed a large hypoechogenic mass, about 4x5 cm. at left para aortic area at medially aspect of left kidney.

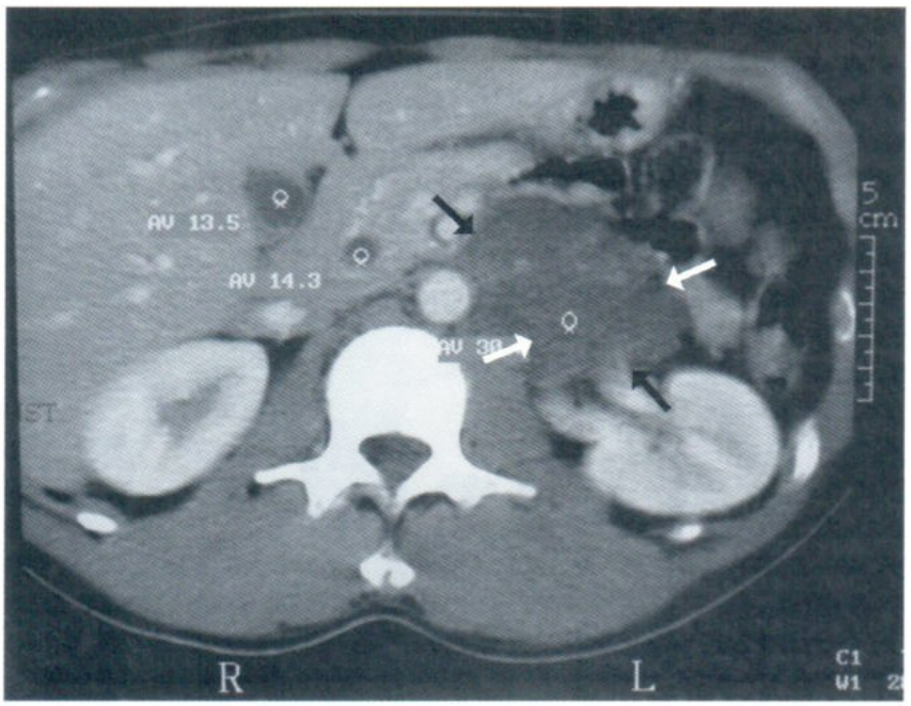

Fig. 2 First CECT study revealed a non enhanced retroperitoneal mass appearing as encasement of left renal vein with an impression of left para aortic mass likely to be enlarged node. Mild dilatation of intrahepatic bile ducts and distal CBD, no demonstrable obstructed cause.

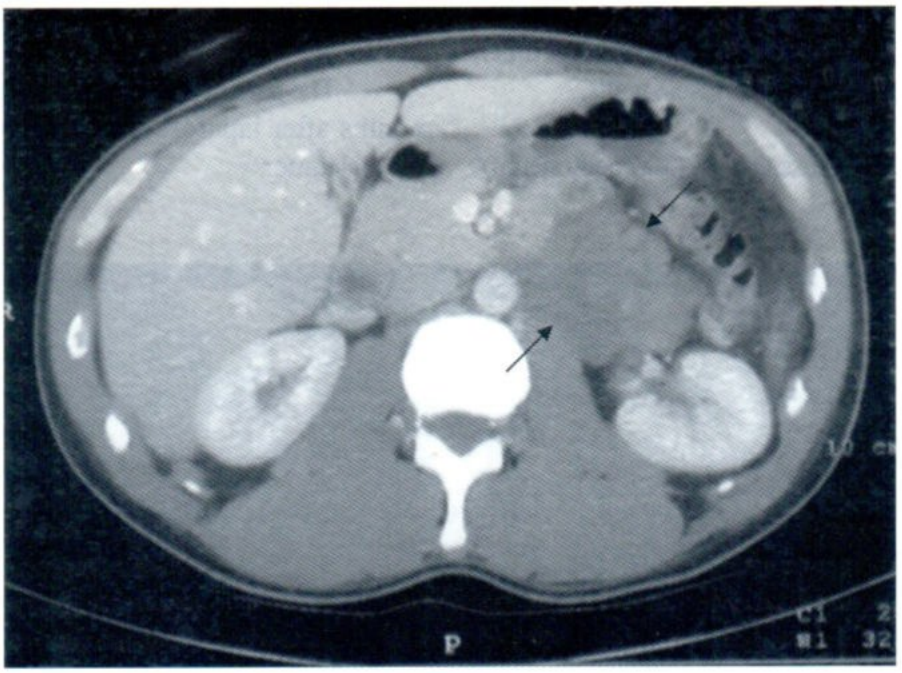

Fig. 3 Follow up second CECT study revealed no longer demonstrated distal CBD dilatation as compare to the previous first CT study. The patient had been marked improvement of the abdominal pain. No significant change of retroperitoneal hypodense mass.

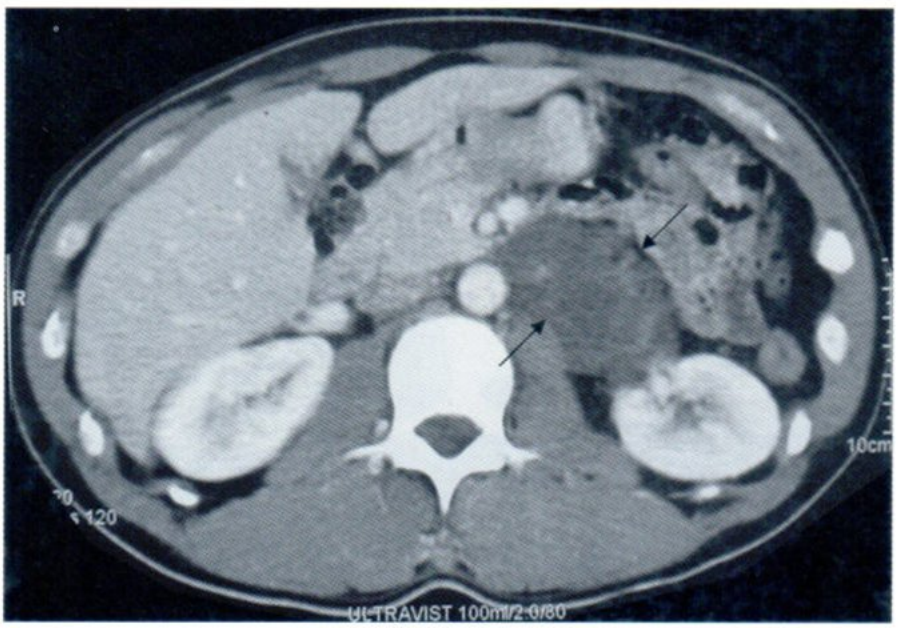

Fig. 4 Third CECT study revealed no significant change as compare to the second CT study.

DISCUSSION

Retroperitoneal primary tumor are relatively rare. It is accounted for approximately 0.07% to 0.6% of all tumors.[3] About 80% of it is malignant. Benign retroperitoneal tumors are infrequent and hemangioma is a rather exception. Among them, cavernous hemangioma is the most prevalent but venous hemangioma is unusual Most hemangioma presents at birth. Some regresses spontaneously and others grow, usually more rapidly during puberty or pregnancy. It is suggested that its growth is a result of thrombosis and obstruction of outflow of blood.[1,3]

Retroperitoneal venous hemangioma never become malignant, but the high incidence of rupture and/or bleeding make total resection to be the treatment of choice. Resection could be performed through laparoscopy as it is highly beneficial to the patient, who has been evaluated to be of low tendency of bleeding.

In the present study, the patient is a middle -aged male. He had a history of a minute gallstone at previous ultrasound finding for many years ago. He presented with sudden abdominal pain. Ultrasound and first CT study demonstrated mild degree of intrahepatic bile ducts and CBD dilatation without demonstrable the obstructed cause, suspected to be CBD stone obstruction, but incidental finding of a large retroperitoneal non-enhanced hypodense mass. However; he had marked improvement of abdominal pain in the following day after first CT study. Follow up second and third CT studies had no longer seen intrahepatic bile ducts and CBD dilatation, which possibly to be caused by passing of CBD stone. There is no significant change in size and characteristics of the large retroperitoneal para aortic mass of all three CT studies. No evidence of venous obstruction of the patient before. Although, the characteristic ultrasound finding of hemangioma appeared as a soft tissue mass with high-flow pattern on Doppler, intense contrast enhancement on CT finding and high signal intensity on T2-weighted images on MRI study, seem to be helpful for preoperative diagnosis.[2] But this was the same findings as hypervascular malignant tumors which are much more prevalent than benign retroperiteneal venous hemangioma.

In addition, atypical findings in this patient, ultrasound exam showed a large hypoechogenic mass, located at paraaortic regions. Three CT studies showed the same findings of a non-enhanced mass at paraaortic with evidence of firm attachment to adjacent organs and appearing as encasement the left renal vein. The studies had been performed by different CT machines and radiologists but the similar impression on each U/S and CT studies was para aortic lymphadenopathy or malignant tumor.

Atypical imaging findings in this patient suggest retroperitoneal lymphadenopathy due to a large hypodense (>2 cm), non-vascular enhancing lesion with appearing as blood vessel invasion at para aortic area that more likely to be malignant retroperitoneal lymphadenopathy. However; laparoscopy observation of the mass showed poorly vascular tumor with low tendency of malignancy and bleeding; therefore, laparoscopy resection of the mass was performed, and histopathologically finding revealed the retroperitoncal soft tissue mass to be venous hemangioma. Laparoscope cholecystectomy is also performed at the same time and pathologically diagnosis is chronic cholecystitis.

Follow up U/S seven months after laparoscopic resection showed no residual para aortic mass and no evidence of recurrent intrahepatic bile ducts and CBD dilatation.

CONCLUSIONS

Retroperitoneal venous hemangioma is very rare condition, typically CT findings show highly vascular tumor with intense contrast enhancement. In this patient, atypical CT finding was non-enhanced mass at para aortic region mimicing retroperitoneal lymphadenopathy and incidental finding of the mass caused by abdominal pain secondary to passing of CBD stone. However; laparoscopic resection was

successfully made because of low tendency of bleeding and the patient recovered well with good health. Ultrasound follow up 7 months, S/P laparoscope showed no residual or recurrent of the mass.

ACKNOWLEDGEMENTS

The author would like to thank Dr. Witaya Petdachai for reviewing the manuscript and the publication of this manuscript with illustrations has been approved by the patient.

REFERENCES

1. Igarashi J, Hanazaki K. Retroperitoneal venous hemangioma. AJG 1998; 93: 2292-3.
2. Vasudevan S, Cumbie T, Dishop M, et al. Retroperitoneal hemangioma of infancy. J. Ped Surg 2006; 41 : E 41-4.
3. Martin R, Zarranz J, Fernandez M, et al. Laparoscopic resection of retroperitoneal venous hemangioma. J Urol. 2004; 171: 336.
4. Farbes T. Retroperitoneal hemorrhage secondary to a ruptured cavernous hemangioma. Can J. Surg 2005; 48: 78.
5. Murphy M, Fairbain K, Parman L, et al. Musculoskeletal angiomatous lesions, radiologic-pathologic correlation. Radiographics 1995; 15: 4.
6. Wannanukul S, Voramethkul W, Nuchprayoon I, et al. Diffuse Neonatal hemangiomatosis. J Med Assoc thai 2006; 89: 1297-303.
7. Ronan S, Sdomon L. Benign neonatal eruptive hemangiomatosis in identical twins. Pediatric Dermatology 1984; 1: 318 -21.
8. Nishino M, Hayakawa K, Minami M, et al. Primary retroperitoneal neoplasms : CT and MR Imaging findings with anatomic and pathologic diagnostic clues. Radiographics 2003; 23: 45-57.
9. Olsen KI, Stacy GS, Montag A. Soft tissue cavenous hemangioma. Radiographics 2004; 24: 49-54.

ACCURACY FOR DETECTION OF BREAST CANCER BY MAMMOGRAPHY AND ULTRASOUND AT UDONTHANI REGIONAL CANCER CENTER

N. MUNPOLSRI[1] MD, (diagnostic radiology)
S. WISET NANN[1] MSc(radiology)

Objective; To determine the accuracy for detection of breast cancer by mammography and ultrasonography compared with histopathology and unchanged follow up mammographic reports in 2 years.

Material and Method: Retrospective study of 1,756 mammographic reports with BIRADS classification into BIRADS 1 for negative study, BIRADS 2 for benign findings, BIRADS 3 for probably benign lesion, BIRADS 4 for suspicious malignancy and BIRADS 5 for highly suggestive of malignancy. All patients had confirmed diagnoses with tissue histopathology or unchanged mammographic reports within 2 years.

Results: The overall sensitivity was 88.00%, specificity 98.93% and accuracy 98.48% which is very high compatible with other studies.

Keywords: Mammography, Ultrasound, Breast cancer, histopathology.

Breast cancer is the second most common malignancy of women with an incidence of about 17.2 per 100,000 female population of Thailand.[1] Early detection of breast cancer can provide curative treatments with deceased morbidity and morbidity of the patients suffering from breast cancer. Now-a-day, these are multiple tools for early detection of breast cancer, but the most recommended one is mammography. Since 1996, Udonthani Regional cancer center is a unit of the Ministry of Public Health of Thailand provided for the people in the 9 provinces of the north Eastern part of Thailand in duding our neighboring country-Loas for early cancer detection, screening for massed in the breasts and also offering appropriate treatment. The provinces in the aforementioned included, Udonthani, KhonKaen, Kalasin, Nakonpranom, Mahasarakam, Loei, Sakonnakorn, Naongkai, Nongbualumphu, including Laos. Every years there are a large member of woman who had symptoms of abnormalities in the breast attending our center.

We would like to present to you our analysis of the result of 2,000 mammography, studied from the people having breast symptoms for mammography, aging from 16-81 yeast old since 2004 to 2006. The sensitivity, specificity and accuracy of mammography reports were analysed using BIRADS classification[2] in comparison with histopathology or unchanged followed up mammography in 2 years. The results of this study may help us to plan for further development in diagnostic procedures or treatment of breast cancer.

MATERIAL AND METHODS

From Jan 2004- Dec 2006, the collected data of 2,000 women caming to Udonthani Regional Cancer Center for mammography (screening and/or diagnostic mammography were analysed). About 1,756 patients (87.80 %) the diagnoses were proven by tissue diagnosis and the other group with unchanged of the mammographic results of a followed up after 2

[1] Devision of diagnostic radiology, Udonthani Regional Cancer Cener.
Correspondence to; Munpolsri N. Devision of Diagnostic Radiology, Udonthani Regional Cancer Center, Udonthani 41330. Thailand.

years interval. The accuracy of the diagnosis of the two groups were compared.

At least two standard positions of mammography were performed (CC: craniocaudal view and MLO; mediolateral oblique view) and additional position for more information if indicated. The mammographic machines are GE-Senograph DMR and 7.5 MHz linear probe ultrasound-GE logic 400.

The result of mammographic reports were classified into category of Breast Imaging Reporting and Data Systems of American College of Radiology (BIRADS)[2,3] by experience radiologists at Udonthani Regional Cancer Center. Negative study were classified as BIRADS I, benign findings were classified as BIRADS II, probably benign findings were classified as BIRADS III, suspicious lesion of malignancy were classifies as BIRADS IV and highly suggestive of malignancy were classified as BIRADS V. The BIRADS O (incomplete study) and BIRAD VI (known case of malignancy) were excluded from the study.

The statistical result such as sensitivity, specificity and accuracy of the study were determine by histopathology (fine needle aspiration, core needle biopsy or excision) or by unchanged mammographic report within 2 years.

In the groups of BIRADS I , II were recommended for annual follow up mammography. Group of BIRADS III were recommended for short interval follow up and in group pf BIRADS IV and V were recommended for definite tissue diagnosis and proper management.

RESULTS

There were 1,756 mammographic reports to be studied with the ages range from 16-81 years old, average age about 46.328 years and high peak of age incidence range is between 40-49 years. (the lowest age is 16 years old came form Lao with bloody nipple discharge, diagnosed as BIRADS 4 and had proved to be intraductal papillaoma)

Age	Number of patients
<30	19
30-34	49
35-39	230
40-44	451
45-49	458
50-54	273
55-59	147
60-64	71
65-69	35
70-74	23
>74	7

Table 1 Age distribution of the patients.

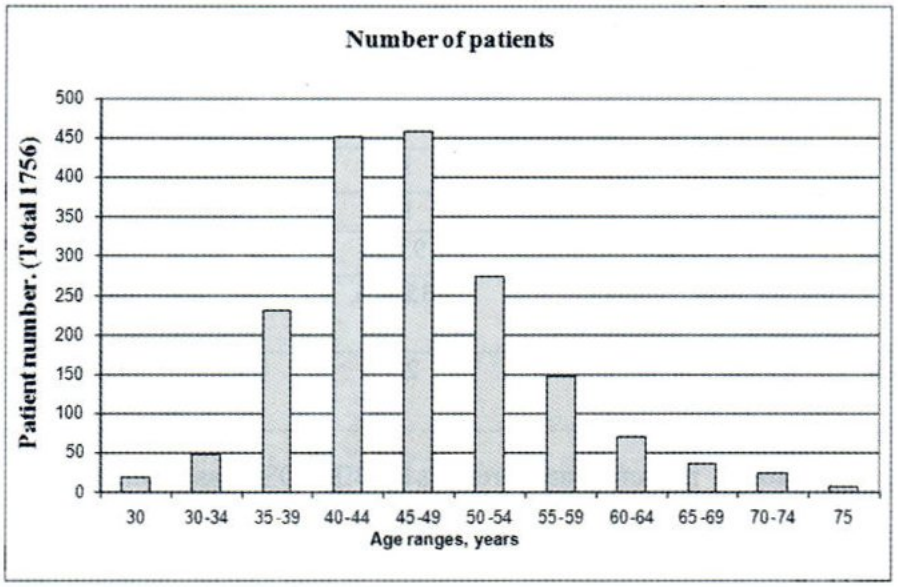

Graph 1 number of patients distribution by age groups.

Area (Provinces)	Number of patient	
	persons	%
Responsible area [9 provinces in Northeast of Thailand]	1,616	92.03
Out off responsible area	60	3.42
Laos	80	4.55

Table 2 percentage of patients in and out of responsilble area

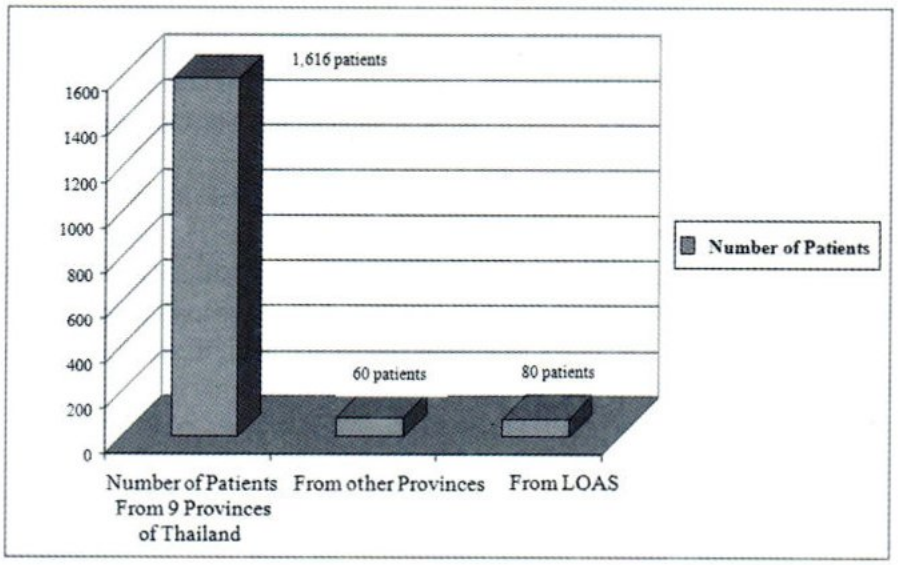

About 92.03 % (1616 persons) of patients lived in the upper part of North-East of Thailand, in the responsible area of Udonthani Regional Cancer Center.

Mammographic reports	Histopathology or 2 years followed up mammography				Total
	Benign		Malignancy		
	number	%	number	%	number
BIRADS I Negative Studies	847	100	0	0	847
BIRADS II Benign	695	100	0	0	695
BIRADS III Probably Benign	121	93.08	9	6.92	130
BIRADS IV Suspicious of Malignancy	17	35.426	31	64.58	48
BIRADS V Highly Suggestive of Malignancy	1	2.78	35	97.22	36

Table 3 mammographic reports by BIRADS classification

In 847 patients of BIRADS I revealed 2.27 % were tissue proven as fibrocystic change(15), fibrosis (5), and unchanged mammographic report in 2 years for 97.63 % (827)

In 695 patients of BIRADS II revealed 5.47 % were tissue proven as fibrocystic change (15), fibroadenoma (18), fibroadenosis (3), inflammation (2) and 94.53% unchanged mammographic reports in 2 years (567)

In 130 patients of BIRADS III revealed 23.08 % (30) were tissue proven as malignancy (9), lipoma (1), fibrocystic change (11), fibroadenoma (8), benign phylloides tumor (1) and unchanged mammographic reports in 2 years 76.92 % (100)

In 48 patients of BIRADS IV revealed 64.58 % were tissue proven as malignancy (31), benign intraductal papilloma (2), fat necrosis (1), fibrocystic change (3), fibroadenoma (10), abscess (1)

In 36 patients of BIRADS V revealed 97.22 % (36) were tissue proven as malignancy (35) and lobulated contour fibroadenoma (1)

All data was statistically analysis. In group of BIRADS I, II, III regarded as negative for malignancy, where as BIRADS IV, V were regarded as positive for malignancy.

True Positive (TP) means the patients in BIRADS IV, V who were diagnosed as malignancy in mammography and proven to be malignancy by histopathology.

TP = 31+35=86

True Negative (TN) means the patients in BIRADS I, II, III were diagnosed as benign and confirmed to be benign or normal

TN = 847+695+121 =1,163

False negative (FN) means the patients who were diagnosed as non-malignancy in BIRADS I, II, III, but proven to be malignancy by histopathology

FN = 0+0+9 = 9

False Positive (FP) means the patients who were diagnosed as malignancy in BIRADS IV, V but proven to be benign condition by histopathology

FP = 17+1 =18

Negative Predictive Value (NPV)= TN/total negative malignancy on mammography Positive Predictive Value (PPV) = TP/ total positive malignancy on mammography

Mammographic reports	Positive Predictive Value (%)	Negative Predictive Value (%)
BIRADS I Negative Studies	-	100
BIRADS II Benign	-	100
BIRADS III Probably Benign	-	86.43
BIRADS IV Suspicious of Malignancy	64.58	
BIRADS V Highly Suggestive of Malignancy	97.22	

Table 4 PPV and NPV of each BIRADS classification

Mammographic reports	Positive Predictive Value (%)	Negative Predictive Value (%)
Benign (BIRADS I, II, III)	-	99.46
Malignancy (BIRADS IV, V)	78.57	-

Table 5 overall PPV and NPV

Sensitivity = TP/ (TP+TN) True Positive/ (True Positive+True Negative)
= 66/ (66+9)
= 88.00 %

Specificity = TN / (TN+FP) True Negative/ (True Negative+False Positive)
= 1,663/ (1,663+18)
= 98.93 %

Accuracy = (TN+TP)/ total number of study True Negative+True Positive/ total number of study
= (1,663+66) / 1,756
= 98.46 %

DISCUSSION

Mammography was recommended for the standard screening method of breast cancer (with addition sonographic examination depend on density of breast tissue[4,5] According to BIRADS classification it is easily helpful to make decision for further management of the patient after mammography having been taken. The groups of BIRADS I,II,III were defined as normal or negative for malignancy (benign condition) which in this study proved to be about 99.46 % for overall NPV in BIRADS I, II, III and 78.57 % for overall PPV for malignancy in BIRADS IV, V., high value.[6,7]

There was 87.80% of patients in this study had regular followed up of mammography and/or taken tissue for histopathology, means that the patients were alert and having awareness for detection of breast cancer.

The common benign disorders of breasts in this study are fibrocystic change and fibroadenoma, where as the malignant disorder is the infiltrative ductal carcinoma.

This study showed high sensitivity (88.00%),

specificity (98.93%) and accuracy (98.46%) similar to another studies,[8-11] so it is supported that the mammography is useful to be the screening tool for breast cancer which is not too expensive, but give high sensitivity, specificity and accuracy. However the sensitivity, specificity and accuracy are depends on multiple factors such as good technology of machines (mammography and ultrasound), well trained radiologic technicians, well trained and experience of radiologist.[12]

REFERENCES

1. Martin N, Cheirsilp A. Breast cancer. Cancer in Thailand Vol. III.1995-1997; 47-48.
2. American College of Radiology. ACR BIRADS-Mammography. In ACR Breast imaging reporting and data system atlas. 4th ed. Reston,VA: American College of Radiologt; 2003
3. Lehman C, Holt S, PeACOCK s,White E, urban N. Use of the American College of Radiology BIRADS guidelines by community radiologists: concordance of assessments and recommendations assigned to screening mammograms. AJR Am I Roentgenol 2. 2; 179: 15-20.
4. Skaane P. The additional value of US to mammography in the diagnosis of breast cancer. A prospective study. Acta radiol 1994; 40: 486-490.
5. Feig SA. The role of ultrasound in a breast imaging center. Semin Ultrasound CT MRI 01989; 10: 90-105
6. Kompas DB. The positive predictive value of mammography. AJR 1992; 158: 521-6
7. Lacquement MA, Mitchell D, Hollingsworth AB. Positive predictive value of the Breast Imaging Reports and Data Systems. J Am Coll Surg. 1999; 189: 34-40.
8. Hirunpat S, Tanomkiat W, Rungrat K, Aroakupakul N. Accuracy of the Mammographic Report Category according to BIRADS J. Med. Assoc. Thai 2005; 88(1): 62-65
9. Charnvises S. The accuracy of mammography; a comparison with fine needle aspiration cytology. J Med Assoc Tahi 1996; 79: 27-30
10. Elmore JG, Wells CK, Howars DH. Dose Diagnostic accuracy in mammography depend on radiologists' experiences?. J Womens Health 1998; 7: 443-9
11. Azzarelli A, Guzzon A, Pilotti S, Quag; iuoli V, Bono A. et al. Accuracy of breast cancer diagnosis by physical, radiologic and cytologic combined examination., Tumori 1983; 69: 137
12. Elmore JG, Wells CK, Howars DH. Dose Diagnostic accuracy in mammography depend on radiologists's experiences?. J Womens Health 1998; 7: 443-9.

ESTIMATION OF GLOMERULAR FILTRATION RATE IN RENAL TRANSPLANTED PATIENTS: COMPARISON BETWEEN ^{99m}TECHNETIUM DTPA GAMMA CAMERA TECHNIQUE AND PLASMA CLEARANCE TECHNIQUE

Jettana CHAROENRAT, M.D.[1], Krisana ROYSRI, M.D.[1]
Charoonsak SOMBOONPORN, M.D.[1]

ABSTRACT

OBJECTIVE: To find the correlation of glomerular filtration rate (GFR) derived from ^{99m}technetium diethylenetriaminepentaacetic acid (^{99m}Tc DTPA) renography with gamma camera technique and plasma clearance technique in renal transplanted patients and to find the relationship between GFR values from the two techniques.

DESIGN: Descriptive study design with prospective data collection.

SETTING: Department of Radiology, Srinagarind Hospital, Khon Kaen University.

MATERIALS AND METHODS: Ten renal transplanted patients (12 studies) were enrolled into the study between October 2004 and July 2005. GFR was estimated by two different methods, gamma camera technique and plasma clearance technique, using 99mTc DTPA. GFR values derived from the two methods were correlated. The relationship between GFR values from the two techniques is then determined.

RESULTS: We found that there was a fair correlation of the GFR values between the two techniques ($r = 0.69$).

CONCLUSION: Although the GFR value from gamma camera technique may be lower than that of the standard plasma clearance technique, GFR by this method is reliable enough in determining renal function in patients post renal transplantation.

INTRODUCTION

Glomerular filtration rate (GFR) is the most commonly used parameter in determining excretory renal function both in patients with native kidneys and transplanted kidneys. Several techniques have been developed for the estimation of GFR; however some techniques have their own limitations. Although inulin clearance remains the gold standard as a GFR measurement, it requires a steady-state plasma concentration and urine collection, is time-consuming and is also expensive.[1] Endogenous serum creatinine

[1] Department of Radiology, Faculty of Medicine, Khon Kaen University, Thailand
Author for correspondence: Charoonsak Somboonporn, MD
Address: Department of Radiology, Faculty of Medicine, Khon Kaen University, 40002 Thailand
Phone: 043 363 895 **Facsimile:** 043 202 472 **E-mail address:** charoonsak_s@yahoo.com

clearance, another method for GFR estimation, is not accurate, especially in patients with reduced renal function, due to a compensatory increase in tubular secretion of creatinine.[2] In addition, serum creatinine level depends on muscle mass and is not usually elevated out of the normal range until the GFR has fallen by at least 50%.[3-4]

There are two methods of GFR estimation using radiopharmaceuticals, plasma clearance technique and gamma camera renography. However, the former needs multiple blood samplings and counting for radioactivity. Therefore, gamma camera technique has been more widely used in evaluation of GFR in the clinical practice. Due to most of the data using this method are from the study in native kidneys, we aim to evaluate the correlation of GFR derived from ^{99m}Tc DTPA renography with gamma camera technique and the standard plasma clearance technique in renal transplanted patients.

MATERIALS AND METHODS

The study was approved by the local ethic committee before patient recruitment. Ten renal transplanted patients referred for radionuclide renal function study at Nuclear Medicine Division, Department of Radiology, Srinagarind Hospital between October 2004 and July 2005 were included into the study. Two patients underwent 2 studies giving the total number of 12 studies.

In each patient GFR was studied both by gamma camera technique and plasma clearance technique using ^{99m}Tc DTPA as the radiotracer.

GFR estimation by gamma camera technique

If not contraindicated, the patient was hydrated before commencing the study. Most of the patients had urinary catheter in place. If these were not the cases, they were asked to empty bladder before the study.

After a bolus injection of approximately 3 mCi of ^{99m}Tc DTPA into the anticubital vein of the patient lying in the supine position, the pelvic renal graft dynamic images were acquired using a large field of view, parallel-hole, low-energy collimator equipped with gamma camera (ADAC Genesys, USA) in the anterior projection. A 1-minute pre and post injection counting the radioactivity of the syringe were also performed. In addition, at the end of anterior dynamic imaging of the renal graft, a 1-minute static view of the graft was imaged in the lateral projection and the distance between the center of the graft to the anterior skin surface was measured as a renal depth for subsequent GFR estimation. This renal depth value was later used for attenuation correction in determining the GFR values by Gates technique. The GFR of the gamma camera technique was automatically calculated by the computer program using Gates equation.[5] In brief, the regions of interest were placed at the renal graft and perirenal region inferolaterally to create time-activity curve of each region (Figure 1). Then the net renal curve was acquired by subtraction of the normalized background activity from the renal activity curve. Finally, the area under net renal curve during 2-3 minutes post injection was used to determine the GFR value.

At the end of renal image acquisition, image at the injection site was acquired in every patient. If evidence of radiotracer leakage is found, that particular patient would be excluded from the study.

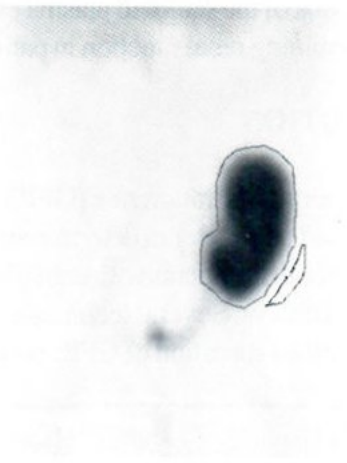

Fig.1 Region of interest of the renal graft and perirenal background.

GFR estimation by plasma clearance technique

During the patient lying for image acquisition in the gamma camera technique, 5-ml of blood was drawn from an anticubital vein of the opposite arm at 10, 20, 30, 60, 120, and 180 minutes after radiotracer injection and collected in the heparinized tube and each specimen was then centrifuged for separation of the plasma. Two-ml plasma was pipetted from each tube and counted for radioactivity. The same was done to the ^{99m}Tc DTPA standardized tube, for the control standard activity.

Plasma radioactivity of each blood sample from 6 points of time of each patient was plotted on a semilogarythmic graph by the Y-axis representing the log scale of the radioactivity and the X-axis representing the linear scale of time, in minute (Figure 2). GFR, or the ^{99m}Tc DTPA clearance, was determined by double exponential analysis with curve peeling technique (Figure 3).

The clearance was calculated by the following equation:

$$GFR = Q0 \times S1 \times S2 / (A1 \times S2) + (A2 \times S1)$$

Q_0 = total amount of 99mTc DTPA injected
= (pre - postinjected syringe weight in gram) x count rate of the standard x 20,000
S_1 = slope of the first exponential function
= 0.693 / T1/2 of the first exponential function
S_2 = slope of the second exponential function
= 0.693 / T1/2 of the second exponential function
A_1 = intercept of the first exponential function
A_2 = intercept of the second exponential function

Correlation of GFR

The two GFR values derived from both techniques were correlated by interclass correlation and regression analysis.

RESULTS

Ten patients, 4 women and 6 men, were studied. The mean age was 42 years (range 15-58). The time between transplantation operation and the time of GFR study ranged from 1 to 7 days (mean 4). GFR values from the two techniques in each patient were shown in Table 1. GFR value by gamma camera method varied from 6.0 to 65.4 ml/minute (mean 26.2), whereas GFR value by plasma clearance technique varied from 25.0 to 85.3 ml/minute (mean 53.4).

Correlation between GFR estimated by gamma camera technique and plasma clearance technique was 0.69 and standard error of estimate was 15.2 ml/minute (Figure 4).

By using regression analysis, the new equation to show the relationship between GFR value of the gamma camera technique (GFR_{ga}) and of the plasma clearance technique (GFR_{pl}) was as followed:

$$GFR_{pl} \text{ in ml/minute} = GFR_{ga} \text{ in ml/minute} \times 0.883 + 30.2$$

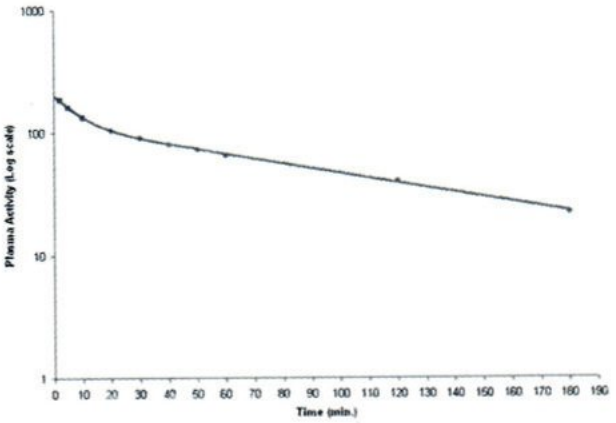

Fig.2 Plasma disappearance curve.

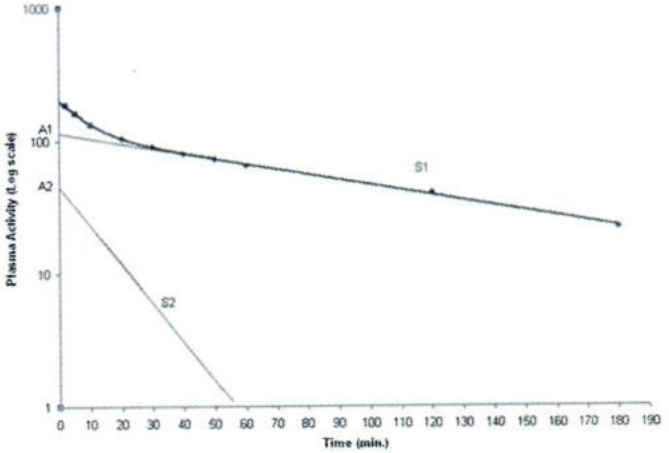

Fig.3 Curve peeling technique

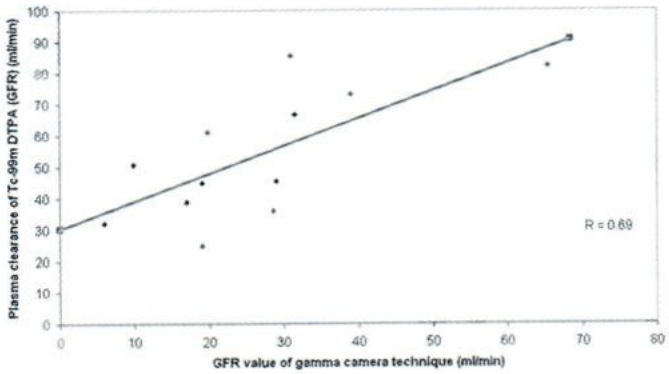

Fig.4 Correlation between GFR values estimated by gamma camera technique and plasma clearance technique.

Table 1 The GFR values derived from both techniques, gamma camera and plasma clearance techniques, using ^{99m}Tc DTPA.

Patient	GFR value by gamma camera technique (ml/min)	GFR value by plasma clearance technique (ml/min)
1	65.4	82.0
2	29.0	45.3
3	9.8	50.8
4	19.9	60.9
5	31.0	85.3
6	31.5	66.7
7	19.0	25.0
8	28.6	36.0
9	39.0	73.0
10	17.0	38.7
11	19.0	45.0
12	6.0	32.0

DISCUSSION

There have been studies showing a fairly good correlation between the GFR derived from gamma camera technique and from plasma clearance technique (r 0.79-0.89).[6-7] However, all of these studies have been conducted in patients with native kidneys. Whether this correlation is still good in the renal transplanted patients still remains unknown.

In this study we found that there was a fair correlation between the GFR values derived from plasma clearance technique and gamma camera renography technique using ^{99m}Tc DTPA in renal transplanted patients (r = 0.69). It should be noted that the GFR value of the gamma camera method was lower than that of the plasma clearance method in every patient studied. This suggests that the GFR estimation from gamma camera technique may not be appropriate for directly applying to the renal transplanted patients. Further regression analysis demonstrated the new equation that showed relationship of the GFR between the two methods. This relationship is useful in converting GFR derived from gamma camera technique, which is widely used in routine clinical practice, into that from a more accurate plasma clearance technique, which demands multiple blood taking and is time consuming.

Estimation of GFR by ^{99m}Tc DTPA gamma camera method using Gates equation bases on the fractional renal accumulation of ^{99m}Tc DTPA during the renal parenchymal phase after tracer injection.[5] By this method, a few parameters influencing the estimated GFR value have to be considered to explain the difference of GFR derived from the two methods. The first one is the fractional renal uptake. The fractional renal uptakes which most correlated with GFR and were used for GFR estimation of Gates equation, were the uptake during 2-3 minutes after ^{99m}Tc DTPA injection. This period of fractional renal uptake derived from the study of native kidneys of Gates model may not be appropriately to be applied to the transplanted kidneys as in our study population. The second factor is the acquisition of renal depth for calculation of attenuation correction. The gamma camera technique with Gates model calculates renal depth from height and weight of the patient giving the distance between the mid-point of kidney to the posterior skin surface at the back. In our study we were aware of this rationale of acquiring renal depth that may not be appropriate in calculating the renal depth of the renal graft while the image acquisition was performed in the anterior pelvic projection. Furthermore, soft tissue swelling at the early post -transplanted period can increase the renal depth; hence applying height and weight should not be accurately applied to this circumstance in measuring the renal depth. Another factor that needs to be considered is the position of the background region of interest to calculate background subtraction.

Since the GFR of plasma clearance technique is basically more accurate than that of the gamma camera technique and GFR derived from gamma camera technique with Gates model may have some limitations in renal transplanted kidney, we propose the relationship to calculate the GFR of plasma clearance technique from that of the gamma camera technique.

However, our study had some limitations. The number of GFR studies is small and the GFR values of these patients were not widely distributed. Most of them were in the low ranges and therefore could not represent a normal distribution of renal transplanted patients with varying renal function. In addition, all of the patients studied were in the early postoperative period, within the first week of transplantation. The result in particular the relationship equation of GFR between the two methods may not be generalized for applying to patients of late follow-up of the renal function. Furthermore, we did not measure the labeling efficiency of ^{99m}Tc DTPA that can affect the accuracy of the acquired GFR value.

We suggest that further researches need to be done in a large scale to evaluate the GFR from these two studies in renal transplanted patients. The fractional renal accumulation of varying time after

^{99m}Tc DTPA injection that most correlates with the GFR value of Gates model should be identified. In addition, the effect of renal depth derived from height and weight method and from the direct measurement of the lateral renal image on the GFR values should be explored.

CONCLUSION

In summary, we have found, in a limited number of patients, a fair correlationship of GFR derived from gamma camera technique and from plasma clearance technique in patients with early post renal transplantation. We also proposed the relationship equation to calculate a more accurate GFR estimation from GFR derived from gamma camera technique commonly performed in our routine clinical practice.

REFERENCES

1. Price M. Comparison of creatinine clearance to inulin clearance in the determination of glomerular filtration rate. J Urol 1972; 107(3): 339-40.
2. Jagenburg R, Attman PO, Aurell M, Bucht H. Determination of glomerular filtration rate in advanced renal insufficiency. Scand J Urol Nephrol 1978;12(2):133-7.
3. Brochner-Mortensen J, Rodbro P. Selection of routine method for determination of glomerular filtration rate in adult patients. Scand J Clin Lab Invest 1976;36(1):35-43.
4. Sawyer WT, Canaday BR, Poc TE, Webb CE, Porter RS, Gal P, et al. A multicenter evaluation of variables affecting the predictability of creatinine clearance. Am J Clin Pathol 1982; 78(6): 832-8.
5. Gates GF. Glomerular filtration rate: estimation from fractional renal accumulation of ^{99m}Tc DTPA (stannous). AJR Am J Roentgenol 1982; 138(3): 565-70.
6. Itoh K. Comparison of methods for determination of glomerular filtration rate: ^{99m}Tc DTPA renography, predicted creatinine clearance method and plasma sample method. Ann Nucl Med 2003; 17(7): 561-5.
7. Delpassand ES, Homayoon K, Madden T, Mathai M, Podoloff DA. Determination of glomerular filtration rate using a dual-detector gamma camera and the geometric mean of renal activity: correlation with the ^{99m}Tc DTPA plasma clearance method. Clin Nucl Med 2000; 25(4):258-62.

CORRELATION BETWEEN EARLY AND LATE RADIOIODINE THYROID UPTAKE IN NORTHEASTERN THAI GRAVES' DISEASE PATIENTS

Krisana ROYSRI, MD,[1]
Charoonsak SOMBOONPORN, MD[1]

ABSTRACT

A retrospective study was undertaken at the Department of Radiology, Faculty of Medicine, Khon Kaen University to determine the correlation between early (3-hrs) and late (24-hrs) radioiodine (^{131}I) thyroid uptake in hyperthyroid Graves' disease patients who were referred for the first ^{131}I treatment. Nine hundred and sixty-nine patients residing in the Northeastern Thailand were enrolled into the study. Their clinical background regarding age, sex, province of residence, indication for ^{131}I treatment, and estimated thyroid gland weight were presented. Thyroid uptake test results of all subjects were analyzed for the correlation between early (Eup) and late (Lup) uptake value. Fairly good correlation between Eup and Lup was found ($r = 0.6$, $P < 0.001$). The best fitted regression equation was the logarythmic model: $Lup = 7.8 + 17.3 \ln Eup$. These data are useful in the prediction of 24-hrs ^{131}I uptake value from the 3-hrs value in order to reduce a visit in performing thyroid uptake test before ^{131}I treatment.

Key word: Correlation, Thyroid uptake, Graves' disease, Radioiodine treatment

Eup = Early uptake
Lup = Late uptake

INTRODUCTION

^{131}I has been recognized as an effective, safe and convenient isotope, using for the treatment of hyperthyroidism for more than 50 years.[1-2] Apart from toxic adenoma and toxic multinodular goiter, Graves' disease is the most common cause of primary hyperthyroidism. Estimation of appropriate dose of ^{131}I for individual Graves' disease patient is usually calculated from the size of thyroid gland and the result of radioiodine thyroid uptake test, which is the ratio of amount of ^{131}I uptake in thyroid gland at early (3-6 hrs) or late (24-hrs) periods of time after drinking of ^{131}I solution and the total amount of orally administered radioiodine, expressed as a percentage dosages. Good correlation between the early uptake value (Eup) and the late uptake value (Lup) were reported by some researchers and a predicted 24-hrs uptake value was then established in order to be used instead of the measured 24-hrs uptake value. This can reduce the time and cost of the second visit in undertaking a 24-hrs uptake measurement.[3-5]

Because of the varying amount of daily iodine diet in the population of various regions in the world, resulting in a varying thyroid uptake value, both

[1] Department of Radiology, Faculty of Medicine, Khon Kaen University, Thailand
Author for correspondence: Charoonsak Somboonporn, MD Department of Radiology, Faculty of Medicine, Khon Kaen University, 40002 Thailand
Phone: 043 363 895 Facsimile: 043 202 472 E-mail address: charoonsak_s@yahoo.com

in normal and hyperthyroid individuals, the predicted 24-hrs uptake value conducted at one place may not be suitably applied at another place. We therefore conducted the study to find the correlation between Eup and Lup of hyperthyroid Graves' disease patients referred for the first ^{131}I treatment and then to obtain the appropriate regression model to predict 24-hrs uptake value from 3-hrs value.

PATIENTS AND METHODS

Patients

We retrospectively studied the medical records of 1,029 consecutive Graves' disease patients, residing in the Northeastern provinces, referred for ^{131}I treatment at the Division of Nuclear Medicine, Department of Radiology, Faculty of Medicine, Khon Kaen University from June 1994 to August 2000. The clinical diagnosis of Graves' disease was supported by the elevation of serum thyroxin or triiodothyronine with or without serum thyrotropin measurement. Patients with a prior history of ^{131}I therapy or any type of thyroidectomy were excluded. Data regarding age, gender, province of residence, indication for ^{131}I treatment, estimated thyroid gland weight by palpation, and result of ^{131}I thyroid uptake test were recorded.

Radioiodine thyroid uptake test

Patients with contraindications of ^{131}I treatment, pregnancy and lactating, were firstly excluded before selecting the patients for the test. Anti-thyroid drug (ATD), if taken, was discontinued at least 5-7 days in all cases before the test. Drugs or foods known to interfere with iodine uptake were refrained for an appropriate period of time. At least 4-hours fasting on the first day of the test was recommended to all subjects.

Radioactivity of 20 microcuries (μCi) of the standard ^{131}I NaI solution, supplied by the Office of Atomic Energy for Peace, Thailand, were counted before and after ingestion, and then radioactivity at the 10-cm distance from the subject's neck extended by a pillow under the shoulders were measured at 3 and 24 hours later. Background radioactivity was corrected by measuring the activity at the 10-cm distance from the subject's thigh at the level of 10-cm above knee joint. Time-decay correction was also computed. All measurements were performed by the external counter probe system of Elscint Company, model DTR-4A. Thyroid uptake value was calculated according to the following equation:

$$\%\ \text{thyroid uptake of } ^{131}I = \frac{\text{neck counts - background}}{\text{standard counts - background}} \times 100$$

Statistical analysis

A personal computer with an SPSS program for Windows was used for statistical analysis. The continuous variables were shown as mean, standard deviation and range. Pearson correlation was used to show the correlation between 3-hrs and 24-hrs uptake values. The least square fit method was used to determine the best fit regression model of these values. Scatter plots of 3-hrs against 24-hrs uptake values and the regression line were shown.

RESULTS

Of 1,029 subjects, 46 were excluded due to having previous history of thyroidectomy and another 14 subjects were excluded due to having an incomplete history. The rest 969 subjects were enrolled for analysis. Female to male ratio was 776: 193 (4:1). Mean age was 40.9 ± 11.7 years (range 14-75). All subjects were from the provinces in the Northeastern Thailand: 31.3% from Khon Kaen, 9.2% from Udorn Thani, 9.2% from Chaiyaphum,

7.0% from Leoi, 6.8% from Mahasarakam, 6.3% from Sakonnakorn, and few subjects from various other provinces including Kalasin, Nakornratchasima, Roi-Ed, Nongkai, Yasothorn, Nongbualumphu, Petchaboon, Nakornphanom, Ubonratchathani, Bureerum, Mukdaharn, Surin, and Srisagate.

Various indications for ^{131}I therapy were noted: 23 cases (2.4%) were new cases without prior ATD treatment; 831 cases (85.8%) were failed to ATD treatment; and 115 cases (11.9%) has disease relapse after ATD withdrawal.

Mean estimated thyroid gland weight was 44.4 ± 23.5 g (range 20-200). Mean 3-hrs uptake value was 68.8 ± 20.7 % dose (range 11.1-98.7) and mean 24-hrs uptake value was 79.7 ± 11.1 % dose (range 33.5-98.8). Fairly good correlation between Eup and Lup was found ($r = 0.6$, $P < 0.001$).

ATD = Antithyroid drug

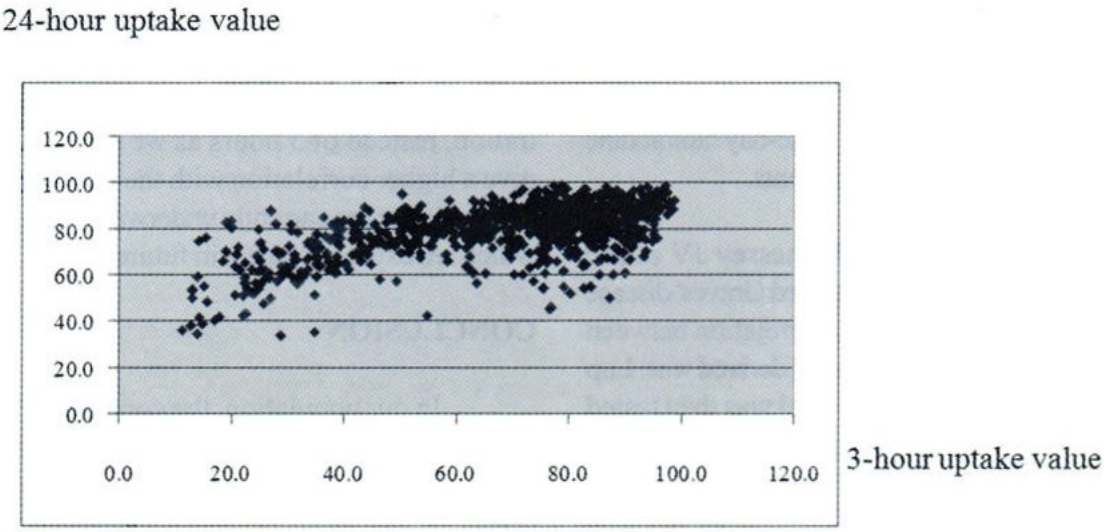

Fig.1 shows the scatter plots of 3-hour and 24-hour 131I thyroid uptake value showing a logarythmic relationship between the two variables. The best appropriated regression equation was: Lup = 7.8 + 17.3 ln (Eup).

DISCUSSION

Since its introduction in the mid-1940s, ^{131}I therapy has become the most widely used treatment for adults with hyperthyroid Graves' disease in the United States.[6] However, there has been no consensus concerning the optimal ^{131}I dose or the most satisfactory method of dose calculation. Although a fixed dose regimen is being used in many institutes, calculation of an administered dose for each individual patient according to the thyroid gland weight, avidity of thyroid gland for iodine measured by ^{131}I thyroid uptake test, and biologic half-life of ^{131}I in the gland is still performed in many nuclear medicine laboratories. However, calculation of biologic half-life is time consuming and often inaccurate.[7] One common approach in determining ^{131}I dosage for the treatment of Graves' disease is from the following formula:

$$\text{Dose}_{\text{admin}} = \frac{100\ \mu\text{Ci of } 131\text{I/ g TW x estTW x } 10}{\%\text{ dose of 24-hour } ^{131}\text{I uptake}}$$

$\text{Dose}_{\text{admin}}$ = administered dose of ^{131}I in milli curies, mCi
estTW = estimated thyroid gland weight (in g)

Since the thyroid uptake pattern including the 24-hrs thyroid uptake value is needed to calculate the administered dose, the patients have to come to the hospital for two consecutive days. In order to omit the second visit, a prediction of Lup from the Eup has been proposed. In a retrospective study in 27 Graves' disease patients of Hayes AA et al,[3] the best fit regression model to predict the Lup at 20-28 hours from the Eup at 3-6 hours was: Lup = - 55.7 + 73.2 log Eup. The authors used this relationship to find the correlation between the measured Lup and the predicted Lup in another 24 patients. Very high correlation was obtained (r = 0.94). Moreover, ^{131}I dose calculation based on these two Lup values showed a very high correlation (r = 0.97). The authors proposed the use of predicted Lup for the same-day radioiodine treatment for Graves' disease patients.

A similar study by Hennessey JV et al [4] performed in 51 previously untreated Graves' disease patients confirmed a very high correlation between Eup and Lup. The regression model derived was: Lup = 28.94 + 0.584 (Eup). This model was then tested in another 21 Graves' disease patients and showed that the measured Lup and the predicted Lup correlated well to each other ($r = 0.85, P < 0.001$), resulting in a very small difference in the mean ^{131}I administered dose.

Vemulakonda US et al.[5] retrospectively studied in 35 Graves' disease patients and found the regression model from the Eup value at 4 hours in predicting the Lup at 24 hours as: Lup = - 38.618 + 65.216 log Eup and the ^{131}I administered dose predicted from the Eup studied in another 34 Graves' disease patients also correlated well with the dose calculated from the measured Lup (r = 0.82204).

Our study revealed that 3-hrs uptake value correlated fairly well with the 24-hrs uptake value in the logarythmic pattern. It should be noted that the degree of correlation in our study was not as high as those from the previous studies mentioned above. This might be in part due to some of our Graves' disease subjects had a rapid turnover pattern of uptake, in which the Lup was lower than the Eup.

Although conducted in the retrospectively manner, our study included the largest number of sample size, 969 Graves' disease patients, so far published in the literatures. In particular, all patients were from the local residents. This regression model therefore is highly appropriate to apply for Graves' disease patients living in the Northeastern part of Thailand.

Further study should be carried out to apply the regression from this study into a new group of population to test the difference of ^{131}I administered dose calculated from the measured and predicted 24-hrs uptake value. In addition, a different time for Eup such as 4 or 6 hours after a tracer dose administration, instead of 3 hours as we had done, might give a higher correlation with the Lup at 24 hours. These studies are currently underway at our Institute, which we expect to report in future.

CONCLUSION

In our population, the correlation between 3-hrs and 24-hrs thyroid uptake value were fairly high and ^{131}I treatment dose can be calculated using the predicted 24-hrs uptake value estimated from the 3-hrs uptake value. The data from our study can be appropriately used in the prediction of 24-hrs uptake value to provide the same-day thyroid uptake test and ^{131}I treatment in Graves' disease population living in the Northeastern part of Thailand.

REFERENCES

1. Wartofsky L. Treatment options for hyperthyroidism. Hosp Prac 1996; 31(9): 69-84.
2. Clarke SM. Radioiodine therapy of the thyroid. In: Murray IPC, Ell PJ, Strauss HW, eds. Nuclear medicine in clinical diagnosis and treatment. New York: Churchill Livingstone 1994: 1833-45.
3. Hayes AA, Akre CM, Gorman CA. Iodine 131 treatment of Graves' disease using modified early iodine-131 uptake measurements in therapy dose calculations. J Nucl Med 1990; 31: 519-22.

4. Hennessey JV, Berg LA, Ibrahim MA, Markert RJ. Evaluation of early (5 to 6 hours) iodine uptake for diagnosis and treatment planning in Graves' disease.
5. Vemulakonda US, Atkins FB, Ziessman HA. Therapy dose calculation in Graves' disease using early I-123 uptake measurements. Clin Nucl Med1996; 21: 102-5.
6. Solomon B, Glinoer D, Lagasse R, Wartofsky L. Current trends in the management of Graves' disease. J Clin Endocrinol Metab 1990; 70: 1518-24.
7. Hays MT. Radiation dosimetry of radioiodinated thyroid hormones. J Nucl Med 1985; 26: 1068-74.

PALLIATIVE TREATMENT OF ADVANCED CERVICAL CANCER WITH RADIOTHERAPY AND THAI HERBAL MEDICINE AS SUPPORTIVE REMEDY

Montien PESEE M.D[1] Wichit KIRDPON Ph.D[2] Sukachart KIRDPON M.D[3] Anucha PUAPAIROJ M.D[4] Pongsiri PRATHNADI M.D[5]

ABSTRACT

OBJECTIVE: To evaluate the supportive effect of Thai herbal medicine, Vilac Plus (G716/45) on standard radiotherapy in comparison with historic control from the literature reports the results of treatment in stage IIIB-IV cervical cancer.

PATIENTS AND METHODS: During the period of March 2003 to June 2005. Thirty patients in advanced cervical cancer stage IIIB-IV with poor performance status were treated by palliative radiotherapy in adjuvant with the Thai herbal tonic solution (Vilac Plus G716/45) daily dose 15-30 ml orally tid, pc as an additional supportive remedy.

RESULTS: Thirty cases of patients in advanced cervical cancer stage IIIB-IV with poor performance status, the median age in stage IIIB, IVA, IVB were 50 years (range 41-73 years), 50.5 years (45 years, 58 years), 69 years (67 years, 71years) respectively. The analysis were being categorized and performed on stages IIIB, IVA, IVA with bladder cancer and IVB reporting in corresponding number of cases/total subject (percentage) were 25/30 (83.33%), 2/30 (6.67%), 1/30 (3.33%) and 2/30 (6.67%) respectively. The median tumor size for stages IIIB, IVA and IVB were 5 cm (range 2-10 cm), 5 cm (4,6 cm) and 4 cm (2, 6 cm) respectively. The pathological identification had been classified to be squamous cell carcinomas 21/30 (70.00%), adenocarcinomas 7/30 (23.33%), small cell carcinoma 1/30 case (3.33%) and clinically staging IIIB 1/30 case (3.33%). The median time interval between teletherapy and brachytherapy was 22 days (range 7-41 days). Eventually, 84% of the stage IIIB cases were undergone by prolonged gap of more than 2 weeks of time interval between teletherapy and brachytherapy while the rest of the case (16%) received the optimal time gap of treatments. The initial complete response and partial response after 4-6 weeks of radiotherapy were 84% and 16 % respectively. The patterns of failure in stage IIIB revealed in 16 % with residual pelvic diseases (< 6 months), 4% with local pelvic recurrence (> 6 months) and 4% with distant metastases. Median follow-up period in stage IIIB was 22 months (range 2-48 months). Low radiation complications were noted, the severe radiation proctitis (grade 3) was found to

[1] Division of Radiotherapy, Department of Radiology, Srinagarind Hospital, Faculty of Medicine, Khon Kaen University, Thailand 40002

[2] Division of Nuclear Medicine, Department of Radiology, Srinagarind Hospital, Faculty of Medicine, Khon Kaen University, Thailand 40002

[3] Department of Pediatrics, Faculty of Medicine, Khon Kaen University, Thailand 40002

[4] Department of Pathology, Srinagarind Hospital, Faculty of Medicine, Khon Kaen University, Thailand 40002

[5] Department of Surgery, Faculty of Medicine, Chiang Mai University, Thailand 50000

be 3.33%. It was notable results in the declined BUN/Cr level in cervical cancer patients with underlying renal insufficiency/chronic renal failure patients treated by palliative radiotherapy and Thai herbal tonic solution as an additional supportive remedy had been observed in 2 cases of stage IIIB and 1 case of stage IVA with neither surgical intervention nor hemodialysis.

CONCLUSION: Our preliminary study in the treatment of advanced cases of Ca. Cervix with palliative radiotherapy and Thai herbal medicine had shown the evidence of initial complete regression of tumour with disappearance of foul smell discharge as high as 84 % with low rate of local pelvic recurrence, low distant metastases and low rate of radiation complication. However, the study has a limitation on the number of cases and a short follow up period. Moreover, this treatment modality had shown the benefit on the declination of BUN/Cr level in some cases of those locally advanced stages III B-IV in chronic renal failure caused by chronic ureteric obstruction due to lateral spreading of the cancer pressing on both ureters, without neither surgical intervention nor hemodialysis. The declined BUN/Cr levels were the consequence of the relief of pressure effect on the ureters by the decreasing of the tumour volumes. Palliative radiotherapy with Thai herbal tonic as supportive remedy was safe, cost effective, in addition to the benefit of improval of quality of life without the toxicity of herbal medicine. Therefore, this combination of palliative radiotherapy together with Thai Herbal Medicine would be the alternative option for the palliative treatment of advanced cancer cases with poor performance status or in locally advanced cancer cases. Further studies of increasing number of cases with longer follow up period including multicenters studies should be performed in order to confirm this findings with statistical significant conclusion.

Key words : Advanced cervical carcinoma, palliative radiotherapy, Thai herbal medicine.
BUN/Cr = Blood Urca Nitrogen/Creatinine

INTRODUCTION

Carcinoma of the uterine cervix had been recognized to be the major problem of malignant diseases in developing countries particularly in Thai women with an estimated 5,593 new cases in 1990. It was the most common malignancy prevalence in women. In Thailand, the estimated national age -standardized incidence was 23.4: 100,000 which was quite typical comparing to other developing countries in south and southeast Asia, and only a little less than the areas of the world at highest risk (Latin America, the Caribbean, sub-Saharan Africa).[1-2] In Thailand, the incidence was highest in Chiang Mai (age standardized incidence rates(ASR) was 29.7 per 100,000 followed by KhonKaen , the ASR was 23.9 per 100,000).[1-2] The risk factors of the cervical cancer was known to be related to human papilloma virus infection, etc.[1-2] Most of the patients were found to be in advanced stages burdened with large tumor volume at the first visit.[3-7] At these advanced stages of diseases, radiotherapy remained the most general treatment available for controlling inoperable tumors as the palliative treatment. The large tumors volume burden in addition to the advanced stages rendered the consequence of radioresistant tumors that beings the contributing factors on the limitation to achieve the effectiveness of radiation therapy. Currently, the new gold standard is concomitant chemoradiation for dealing with locally advanced cervical carcinoma.[8] But some of our patients were inaccessible to concurrent chemoradiation for the reasons of poor performance status, aging, obstructive uropathy, associated with underlying diseases such as chronic renal failure, etc. Therefore, another alternative approach for the resolution was using Thai herbal medicine (Vilac Plus G716/45) as supportive remedy. The Thai herbal tonic (Vilac Plus G716/45) was proven

to have no acute oral toxicity in animal study.[10] No traces of prednisolone and dexametasone were detected.[11] An In Vitro study, the Vilac Plus(G716/45) presented an important antioxidant capacity.[12] The recipe of the ingredients of the Thai herbal tonic solution (Vilac Plus G716/45) was consisting of three edible plants, the whole part of mushroom namely *Ganoderma lucidum, Houttuynia cordata thunb* (leaves) and the roots of Boesenbergia *Pandurata Holtt* (Kra chai) which were found to be effective anti-tumor activities.[13-14]

OBJECTIVE

To evaluate the supportive effect of Thai herbal medicine, Vilac Plus (G716/45) on standard radiothe rapy compare with historic control from the literature reports in advanced stage IIIB-IV cervical cancer. This study was performed at Radiotherapy Division, Department of Radiology, Faculty of Medicine, Khon Kaen University, Khon Kaen, Thailand 40002.

PATIENTS AND METHODS

During the period of March 2003 to June 2005. Thirty patients in advanced cervical cancer stage IIIB-IV with poor performance status were treated by palliative radiotherapy in adjuvant with the Thai herbal tonic solution (Vilac Plus G716/45) daily dose15-30 ml orally tid, pc, as an supportive remedy. The evaluation parameters before staging were complete history, physical examinations as well as pelvic and rectal examination, routine laboratory investigations, chest X-ray, excretory urography, cystoscopy and proctoscopy. The staging of the diseases had been classified by the tumor clinic committee of gynecologists and radiotherapists according to FIGO recommendations.[8] **Inclusion criteria** were: (1)advanced stages IIIB-IV cervical cancer; (2) poor performance status; (3) minimal response of the tumors after radiotherapy 30-40 Gy /3-4 weeks ; (4) evidence of other underlying diseases; (5) advanced cervical cancer with other malignancies (two malignancies) ; (6) the informed of consent had been signed by the patients. **Exclusion criteria** was: (1) The patients refused this treatment modality. This project was approved by the Human Ethics Committee of Khon Kaen University (HE 480745).

Definition of treatment failure was classified into residual disease and recurrent disease. The residual disease was defined as the present of persistent tumors which were noted 1-6 months after complete treatment while recurrence disease was defined as reappearance of the disease after a complete remission more than 6 months after complete treatment.

Grading of complications was defined according to Perez, et al.[9]

Radiotherapy technique: The treatment planning was done by two-paralleled opposing fields AP-PA with telecobalt-60 or linear accelerator (6 MV).The position for radiotherapy treatment was preferably to be supine. The prescribed dose of teletherapy was 5000 cGy/25 fractions, five fractions per week. Field margins were: anterior and posterior fields 15*15 cms; upper limit: L4-L5; lower limit: the superior two-thirds of the vagina. Brachytherapy was performed by using high dose rate Ir-192 about 2-4 weeks after teletherapy with doses ranges between 500-600 cGy/ fraction to point A for 4-5 fractions, once weekly. The point A. dose was about 8600 cGy. The aim of using this tonic solution was to provide the better well-being condition for the patients, and to enhance the radiotherapeutic effects. The herbal tonic had the positive enhance effect on increasing appetite that may contribute the indirect effect on better nutritional status of the patients, and the better result of radiation therapy was the expected outcome.

RESULTS

During the period of March 2003 to June 2005, Thirty patients in advanced cervical cancer stage IIIB-IV with poor performance status were treated by palliative radiotherapy in adjuvant with the Thai herbal tonic solution (Vilac Plus G716/45) daily dose 15-30 ml orally tid,pc, as an supportive remedy. The following results were obtained in accordance with table 1-9.

1. Age distribution.

The median age in stage IIIB, IVA, IVB were 50 years (range 41-73 years), 50.5 years (45 years, 58 years), 69 years (67 years, 71 years) respectively. There was one case, age 29 years with two primary cancer, stage IVA cervical cancer with bladder cancer. (Table 1)

2. Stage of diseases.

The staging of the diseases had been classified by the tumor clinic committee of gynecologists and radiotherapists according to FIGO recommendations. (8) There were stage IIIB, stage IVA, stage IVA with bladder cancer and stage IVB were 25/30 cases (83.33%), 2/30 cases (6.67%), 1/30 case (3.33%) and 2/30 cases (6.67%) respectively. (Table 1)

3. Median tumor size (range) in cm.

The median tumor size for stage IIIB, IVA and stage IVB were 5 cms (range 2-10 cms), 5 cms (4,6 cms) and 4 cms (2,6 cms) respectively. (Table 1)

4. Pathology

The pathological diagnoses were squamous cell carcinomas 70.00% (21/30), adenocarcinomas 23.33 % (7/30), small cell carcinoma 3.33% (1 case) and clinically staging IIIB 3.33 % (1 case) (Table 1). The pathology of stage IIIB which developed pulmonary metastasis at 10 months after complete treatment was adenocarcinoma, poorly differenciated, while in stage IVB the pulmonary metastases presented at the initial diagnosis. The pathological diagnoses were squamous cell carcinoma, non keratinized and papillary adenocarcinoma, moderately differentiated.

5. Underlying diseases of the patients were diabetes mellitus, hypertention, renal insufficiency, chronic renal failure and HIV. (Table 1)

6. Time interval between teletherapy and brachytherapy.

The median time interval between teletherapy and brachytherapy were 22 days (range 7-41 days). There were 84% having prolonged time interval between teletherapy and brachytherapy, more than 2 weeks in stage IIIB while 16% having optimal time gap of treatment.

7. The initial complete response and partial response after 4-6 weeks of radiotherapy were 84% and 16 % respectively. (Table 3)

8. It was observed that 93.33 % (28/30) of cervical cancer patients, had been found to have clinical improvement according to Karnofsky's performance status (more than 80%). (Table 4-5)

9. Patterns of failure, in stage IIIB, it was found that that 16 % having residual pelvic disease (< 6 months), 4% having local pelvic recurrence (> 6 months) and 4% having distant metastasis. Median follow-up period was 22 months (range 2-48 months). (Table 6 and 1)

10. Low radiation complications were noted while the severe radiation proctitis (G3) was found to be 3.33% and mild radiation proctitis and cystitis were 33.33%. (Table 7)

11. The onset time of the patients who develop severe radiation proctitis G3 was 9 months. (Table 8)

12. The declined BUN/Cr level in cervical cancer patients with underlying renal insufficiency/chronic renal failure patients treated by palliative radiotherapy with Thai herbal tonic solution as an supportive remedy had been observed in 3 cases (stage IIIB 2 cases and stage IVA 1 case) by neither surgical intervention nor hemodialysis. (Table 9)

Table 1 Patient Characteristics

Patient characteristics	
Gender (Female)	Total 30 cases
Age in years	
Median (range)	
Stage IIIB	50.0 (41-73)
Stage IVA	51.5 (45,58)
Stage IVA * with bladder cancer	29
Stage IVB	69.0 (67,71)
Stage of diseases	
Stage IIIB	25/30 cases (83.33%)
Stage IVA	2/30 cases (6.67%)
Stage IVA * with bladder cancer	1/30 case (3.33%)
Stage IVB	2/30 cases (6.67%)
Median tumor size (range) in cms.	
Stage IIIB	5(2-10) cms
Stage IVA	5(4-6) cms
Stage IVA with bladder cancer	7.0 cms
Stage IVB	4(2-6) cms
Median follow-up period (range) in months	
Stage IIIB	22 (2- 48)
Stage IVA	32.5 (17,48)
Stage IVA with bladder cancer	18
Stage IVB	9.5 (4,15)
Pathology	
Squamous cell carcinomas	2 cases
Squamous cell carcinomas, non keratinized *	18 cases
Squamous cell carcinoma , keratinized	1 case
Total squamous cell carcinoma group	21/30 (70.00%)
Adenocarcinomas	3 cases
Adenocarcinomas, moderately differentiated	2 cases
Papillary adenocarcinoma, moderately differentiated	1 case
Adenocarcinoma, poorly differentiated	1 case
Total adenocarcinoma group	7/30(23.33%)
Neuroendocrine group	
Small cell carcinoma	1 case(3.33%)
Clinically advanced cervical cancer stage IIIB (Tumor size 5*5cm with frozen pelvis)	1case (3.33%)

Underlying diseases of the patients	
Stage IIIB with HIV	1case
Stage IIIB with DM	1case
Stage IIIB with DM +CRF	1case
Stage IIIB with CRF	1case
Stage IIIB with HT+CRF	1case
Stage IVA with CRF	1case
Stage IVB with DM+HT+CRF	1case
Stage IVB with DM+HT	1case
Time interval between teletherapy and brachytherapy	
Median (range) days	
Stage IIIB	22(7-41)

DM = Diabetes mellitus
HT = Hypertention
CRF = Chronic renal failure

Table 2 Time interval between teletherapy and brachytherapy (days).

Stage	Time interval (days)	No. of cases (%)
Stage IIIB	1-14	4 (16%)
	15-30	16 (64%)
	31-45	5 (20%)
Stage IVA	16,54	1,1
Stage IVA*	17	1
Stage IVB	16,35	1,1

* Stage IVA 1 case revealed both squamous cell carcinoma, non keratinized and transitional cell carcinima.gr I/III of bladder.

Table 3 Initial complete response rate (CR) and partial response rate (PR) after 4-6 weeks of radiotherapy.

Stages	Initial response rate (cases)	%
Stage IIIB	CR=21/25	84%
	PR=4/25	16%
Stage IVA	CR=1/3	33.33%
	PR=1/3	33.33%
Stage IVA*	PR=1/3	33.33%
Stage IVB	CR=1/2 (local)	50%
Stage IVB	PR=1/2 (local)	50%

* **Stage IVA** 1 case revealed both squamous cell carcinoma, non keratinized and transitional cell CA.gr.I/III of bladder.

Table 4 Subjective response after 4-6 weeks of radiotherapy.

Subjective response	cases	%
Clinical improvement	30/30	100

Table 5 Karnofsky's performance status (KPS) after radiotherapy

KPS	cases	%
70 %	2/30	6.67
80-85%	6/30	20
90%	10/30	33.33
100%	12/30	40

Table 6 Patterns of failure: residual disease (<6 months) & recurrence disease (>6 months)

Stage	Residual disease (<6months)	Recurrence disease (>6months)	
		Pelvic recurrence	Distant metastases
Stage IIIB	4/25 (16%)	1/25 (4%)	1/25 (4%)
Stage IVA	-	-	1 /2case
Stage IVA with bladder cancer	Pelvic +Distant metastases 1 case		
Stage IVB	Pelvic +Distant metastases 1 case		

Table 7 Radiation complications

Radiation complication	No. of cases	%
Radiation proctitis G1	8/30	13.33
Radiation cystitis G1	2/30	6.37
Total proctitis+cystitis G1	10/30	33.33
Radiation proctitis G3	1/30	3.33

Table 8 Onset time to develope radiation complications after complete treatment.

	Onset (months)	No. of cases
Stage IIIB (grade 1)	7-12	3
	13-18	4
	19-25	1
	40-46	1
Stage IIIB (grade 3)	9	1
StageIV (grade 1)	14	1

Table 9 The declined BUN/Cr level in cervical cancer patients with underlying renal insufficiency / chronic renal failure patients treated by palliative radiotherapy and Thai herbal tonic solution as supportive remedy.

Stage	BUN/Cr mg/dl (Before)	BUN/Cr mg/dl (After)
IIIB	51/3.5 (01/12/03)	38.2/2.6 (11/07/05)
IIIB	167/24 (27/02/04)	32.6/3.4 (03/05/05)
IVA	112/1.2 (24/03/03)	13.3/0.9 (01/09/03)

BUN = Blood urea nitrogen
Cr = Creatinine

DISCUSSION

The ten years retrospective study in our institute had been reported on 1,180 cervical cancer cases who had been treated by radiotherapy.[15] The analysis results demonstrated that the factors influencing survival of cervical cancer patients were staging, hemoglobin level, time interval between external and intracavitary radiation and fractionation of brachytherapy. The stage III group was found to be 1.65 fold mortality risk over stage I group. The patients with low hemoglobin level less than 10 g/dl demonstrated a 1.85 fold mortality risk over the high hemoglobin over than 12 g/dl. The time interval between external and intracavitary radiation more than 28 days was associated with 2.28 fold mortality risk over the duration of less than one day. The two fractionations of brachytherapy was associated with 0.25 fold mortality risk over the one fractionation. The overall 5-year survival rate in this study revealed 62.5% and median survival was more than 10 years.[15] The other reports revealed the overall 5 year survival rate of 412 cervical cancer patients in all stages were found to be 51.2% and 39 % in stage IIIB while the 5 year actuarial survival rates for small size tumor less than 2 cm in diameter and tumor size larger than 2 cm in diameter were 74% and 56% respectively.[3-4] The treatment failures with radiotherapy alone were found to be statistically significance correlated with staging, tumor size and time interval between teletherapy and brachytherapy had been reported by Pesee M. et al.[3] According to the pathology 5 year actuarial survival rate of squamous cell carcinoma and adenocarcinoma were 51 % and 58 % respectively.[3]

In radiation complication aspects which had been reported that 39.6 % of 412 cases developed radiation proctitis, 2.7% with radiation cystitis, 3.9 % combined radiation proctitis with cystitis, 0.7 % with recto- vaginal fistula and 1 ileal perforation, occurred during a second course of palliative treatment for lumbar metastasis, causing death had been reported by Boonvisuth V. et al.[16] From the literature reviews of 212 cases of stage III cervical cancer patients treated with radiotherapy alone had been reported that the incidences of pelvic recurrence, pelvic recurrence plus distant metastases, total pelvic recurrence and distant metastases only were 14.6%, 21.2%, 35.8% and 18.4% respectively.[17] The other reports of the incidences of local pelvic recurrence, recurrence outside the pelvis and metastatic failure in stage III cervical cancer patients treated with radiotherapy alone were 12.0% -13.6%, 24.0%, and 15.8% respectively.[18-19] In radiation complication aspects which had been reported by Perez CA, et al. that 9.2 % of 271 stages III cervical cancer cases treated with radiotherapy alone developed grade 2 and 10.7% of grade 3 radiation complication.[9] The absolute 5 year survival rates of 515 cases in stage IIIB and 104 cases in stages IVA and IVB disease treated with radiotherapy alone were 52.2%, 24.1% and 13.3% respectively. The patterns and severity degree of complications were reported as grade 3 and 4 where the complications involved in 4.1% for rectosigmoid colon, 1.2% for bladder, and 1.1% for small intestine in accordance to the report by Arai T, et al.[20] Perez CA .et al reported of 1054 cervical cancer patients that the controlling of the tumor in the pelvis was crucial to the survival of the patients in all stages. The results of complete tumor regression within 30 days after completion of radiation therapy had not only substantialling lower number of pelvic recurrence but also fewer distant metastases.[21] The high incidence of distant metastases had been found in stage III-IV.[21] Pelvic tumor control of stages III-IVA cervical cancer patients treated with concurrent chemoradiation and radiotherapy alone were 62% and 59% respectively had been reported by Perez, et al.[22] The incidence of pelvic failure in concurrent chemoradiation and radiotherapy alone were 41% and 39% while the combined pelvic failure plus distant metastases were 24% and 19% respectively. In addition, the distant metastases only in concurrent chemoradiation and radiotherapy alone were 29% and 11% respectively.[22] In another study of locally advanced stage III-IV cervical cancer treated with combination chemotherapy followed by surgery or radiotherapy revealed complete response was 10.6% and complete response plus partial response were 66% and median survival was 88 weeks had been reported by Kirsten F, et al.[23] The complete response rates and the rates of pelvic recurrence in advanced cervical cancer treated stage IIIB -IVA with chemotherapy (CMT) plus radiation (RT) compared with radiotherapy alone (RT) were found to be 53% (CMT+RT) / 57%(RT) and 60%(CMT+RT) / 47% (RT) respectively while the rates of distant metastases were 19% (CMT+RT) / 35% (RT) respectively had been reported by Sundfor K, et al[24] The complete response and partial response in advanced stages III-IVA treated with chemotherapy plus radiotherapy were found to be 53% had been reported by Symonds RT, et al.[25] The complete response and partial response in advanced stages IIIB treated with chemotherapy plus radiotherapy were found to be 62.5% had been reported by Lara PC, et al.[26] The four randomized trial of neoadjuvant chemotherapy and irradiation in stage IIB-III cervical cancer patients were found to be 30-85% of the response rates and none of the studies showed an advantage to pelvic control or survival had been reported by Thomas GM.[27]

Our cervical cancer patients in this study demonstrated having several poor factors such as advanced stage IIIB-IV, large tumor size (median 5 cm, range 2-10 cm.), prolonged time interval between teletherapy and brachytherapy 84 % of cases and associated with poor performance status with or without underlying diseases in table 1. The remarkable of the results of this treatment modality revealed the evidences of:-

1. High initial complete response rate 84% in the stage IIIB-IV locally advanced cervical cancer

2. Low local pelvic recurrence (4%)

3. Low distant metastases (4%) had been observed. The mild radiation complications had been found 33.33%, the moderate radiation complication had not been detected and severe complication was found to be 3.33%. In comparison with historical controls as evidenced in local control and distant metastases had been improved by this modality therapy. Moreover, it had been observed on the benefit with declined BUN/Cr level in some cases of those locally advanced stage IIIB-IV cervical cancer cases with underlying renal insufficiency/chronic renal failure by neither surgical intervention nor hemodialysis. The evidence of declined BUN/Cr level had been observed by this treatment modality in 1 advanced lung cancer case who had underlying chronic renal failure as in our previous report.[28] However, the study had limitation on number of cases and follow-up period (median follow-up period in the stage IIIB was 22 months, range 2-48 months while the stage IVA was 32.5 months, 1 case was 17 months and 1 case was 48 months).

The noteworthy results of this modality therapy were remarkable evidences in the aspects of high initial complete response of the local control of the tumor in contrary to the low distant metastases, low local pelvic recurrence and low radiation complications were observed. Some of them being improved their underlying diseases of renal insufficiency /chronic renal failure. The declined BUN/Cr levels were the consequence of the relief pressure effect on the KUB system by the decreased tumor volume. Therefore the better ability excretory function of kidney had been observed. It seems to be better well being of those patients in the holistic performance status.

The pharmaceutical aspects considerations and explanations should be emphasizing on the "supportive remedy" actions of Vilac Plus® which had been used as adjuvant to the standard radiation therapy compare to the relevance historic control in articles reviewing with other modalities of treatments. The ingredients of the Vilac Plus® tonic consisting of anti-tumor mushroom, LingZhi *(Ganoderma lucidum), Houttuynia cordata, Thunb and Boesenbergia pandurata Holtt* (Krachai). The tonic preparation accomplished by fermentation by using *Lactobacillus casei spp.* (Genebank Reg. No. AF 320255) and *Lactobacillus plantarum spp.* (Genebank Reg. No. AF 320256). An invitro analysis of the Vilac Plus® tonic had been reported by Kirial International Laboratories, France. This analysis reported,[12] the overall antioxidant potency of all ingredients in the mixture of Vilac Plus® which being concurrently bioavailable in the subcellular level represented by the whole blood sample assessment. This was the key and crucial evidence for scientific explanation upon the mechanism and pharmacological action of our clinical studies. The promising supportive adjuvants actions contributed from each composition of the 4 ingredients in Vilac Plus® including the microorganism used in the fermentation proceedings that should be recognized as the "probiotics" which is one key component in the biotechnology procedure of production. The probiotic action and role on cancer therapy could be summarized as follows[31,32]

1. Antitumor and antimetastatic effects[32] by induction or stimulation the synthesis of several cytokines which had been known to be the immunomodulating factor. The small molecular weight cytokines such as IFN-gamma, IL-1 beta and TNF alpha. being one of the enhancement transfer factor to work effectively.
2. Immunomodulation enhancement through the heat-killed lysate in the tonic (Vilac Plus®) that resulting in the delayed or inhibit the process of distance metastases in various cell type of cancers [31] such as colon, liver, lung uterine, cervix and mammary cancers.

The herbal ingredients was world recognition mushroom, Ling Zhi *(Ganoderma lucidum)* or Reishi, where it had been mentioned as sacred mushroom which had been found the 119 different terpinoids, about 80 of which biologically active.[34,35] The role to be the supportive action in cancer treatment was immunomodulation anticancer by protection DNA damage through its powerful antioxidant mechanism by inhibition of tumor necrosis factor (TNF). There were a number of reports that had mentioned the benefit on various cancers.[36,37]

The other herbs were the edible plants *(Houttuynia cordata Thunb* and the root of *Boesenbergia Pandurata Holtt* (Krachai).[37] The role to contribute as supportive remedy was phytosterols in addition to their characteristic of one of the essential antiproliferative of cancer cells such as flavonoids and volatile oil which the strongest one that present this action was linolool.[38] The study had been shown this effective action on various cancers and the best of action was found to be on cervical carcinoma.[38] The co-operative actions of these herbs were reported to be the "interferon-inducing herb" that may contribute some important role to play on antitumor-antiviral activity through the "interferon" molecule.[39,40]

However the outcome of the support remedy by using Vilac Plus® as an adjuvant to standard therapy were very promising in the aspect of the benefit of cost-effectiveness model of cancer therapy. This should be one option of the multimodalities model of treatment that might be useful in the developing countries where the high technology or expensive chemotherapy even concurrent chemotherapy were inaccessible.

In summary, the best strategy approaches to fight with cancer should be achieve only in the holistic considerations. Therefore, this modality would provide the effective local controls, prevent distant metastases and strengthening of the host immunity then encouraging result could be observed.

CONCLUSION

Palliative radiotherapy was the standard treatment for poor performance status, advanced cervical cancer patients with or without underlying diseases. Radiation therapy alone had been reported of disappointing outcome as the results of pelvic failure, paraaortic nodes failure and also distant metastases. Our preliminary study revealed that palliative radiotherapy with Thai herbal medicine (Vilac plus G 716/45) demonstrated of having high initial complete response rate of 84% with low local pelvic recurrence, low distant metastases and low radiation complication. However, the study had limitation on number of cases and follow-up period. Surprisingly, it had been unexpectedly finding that these treatment modality having benefit on declined BUN/Cr level in some cases of those locally advanced stage IIIB-IV cervical cancer cases with underlying renal insufficiency/ chronic renal failure with neither surgical intervention nor hemodialysis. The declined BUN/Cr levels were the consequence of the relief pressure effect on the KUB system by the decreased tumor volume. Nevertheless, palliative radiotherapy with Thai herbal tonic as supportive remedy was safe, cost effective and benefit in the aspect of quality of life by the evidence of high initial complete response rate with poor performance status who could not undergo concurrent chemoradiation. Therefore, this modality would be the alternative option for the palliative cancer cases or one of the multimodality in locally advanced cervical cancer. Further studies deep in details by increasing number of cases, longer follow-up period including multicenter studies are necessary to affirm with statistically significant conclusion, especially in the aspects of the benefit of declined BUN/Cr level in those who have locally advanced cervical cases with underlying renal insufficiency/ chronic renal failure which are very interesting topics for developing country.

ACKNOWLEDGEMENTS

We would like to express our deep appreciation to Associate Professor Nittaya Chamadol, Head, Depertment of Radiology, Associated Professor Vorachai Tungvorapongchai, Mr.Khajornkiat Srichachet of assisting on manuscript editing, and our colleagues, Associate Professor Apinun Aramrat, Professor Maitree Suthajit, Assistant Professor Dusadee Musikapodoke. Appreciations acknowledgement for kind contribution from Lanna Probiotic Company Limited, Thailand, particulary Mr. Suriya Vichitchot who provided the herbal tonic products for clinical trial.

REFERENCES

1. Vatanasapt V, Martin N, Sriplung H, et at. Cancer in Thailand.1988-1991. Khonkaen: Siriphan Press,1993:68-69.
2. Vatanasapt V, Martin N, Sriplung H, et at. Cancer incidence in Thailand. 1988- 1991. Cancer Epidemiology, Biomarkers & Prevention 1995; 4 :475-483.
3. Pesee M, Tangvoraphonkchai V, Boonvisuth V, et al. Radiotherapy alone in the treatment of carcinoma of the uterine cervix in Srinagarind Hospital: Analysis of treatment failure. Thai J Radiol. 1989;26(1):67-70.
4. Pesee M, Tangvoraphonkchai V, Reamsiri T, et al. Low dose rate brachytherapy Caesium -137 afterloading in the treatment of carcinoma of uterine cervix in Srinagarind hospital: Analysis of a actuarial survival rate. Thai J Radiol. 1995;1(3):125-30.
5. Tungsubutra K, Pesi M, Tangvoraphonkchai V. Problems in treatment of cancer in the rural areas and the remedies. In Mould RF, Tungsubutra K, eds. Diagnosis and treatment of carcinoma of the cervix in developing areas. Bristol and Boston: Adam Hilger 1985; 219-22.
6. Tungsubutra K, Tangvoraphonkchai V, Pesi M. Cancer epidemiology in Thailand. In Mould RF, Tungsubutra K, eds. Diagnosis and treatment of carcinoma of the cervix in developing areas.Bristol and Boston: Adam Hilger 1985; 187-90
7. Tangvoraphonkchai V, Pesee M, Boonvisuth V, et al. Tumor registry: An overview of problems shooting in radiotherapy. Thai J Radiol 1989; 26(1): 95-8.
8. Chao K.S.C , Perez CA, Bradym LW, eds. Uterine Cervix in Textbook of Radiation Oncology. Management Decisions. Lippincott Williams & Wilkins, Philadelphia. 2002;489-509.
9. Perez CA, Breaux S, Bedwinek JM, et al. Radiation Therapy Alone in the Treatment of Carcinoma of the Uterine cervix. II. Analysis of Complication. Cancer 1984;54:235-246.
10. Suntorntanasat T, Banchonglikitkul C, Klungsupaya P, et al. Acute oral toxicity test Herbal tonic solution (G716/45). An analytical report. Thailand Institute of Scientific and Technological Research. September 2003,1-8.
11. Amadi Pirasahid P, Suntorntanasat T, Analytical report on Herbal tonic solution. (G716/45). An analytical report. Thailand Institute of Scientific and Technological Research. September 2004,1-3.
12. Durand Phillippe,Prost Michel. In Vitro study of Vilac Plus analysis. Kirial International laboratories KRL Test (SPIRAL-No. Patent FR 2. 642. 526), 3 rue des Mardors 21560 COUTERNON, France.July 2006,1-4.
13. Lee S-S, Wei Y-H, Chen C-F, et al. Anti -tumor effects of polysaccharides of Ganoderma lucidum. Proc Int Symposium Ganoderma Sci, Auckland, 27-29 April, 2001, 1-6
14. Murakami A, Jiwajinda S, Koshimizu k, et al. Screening for in vitro anti-tumor promoting activities of edible plant from Thailand. Cancer Letters 1995; 95: 139-14
15. Pomros P, Sriamporn S, Tangvoraphonkchai V, et al. Factors Affectng Survival of Cervical Cancer Patients Treated at the Radiation Unit of Srinarind Hospital, Khon Kaen University, Thailand. Asian Pacific Journal of Cancer Prevention 2007; 8: 297-300
16. Boonvisuth V, Pesee M, Tangvophonchai V, et al. Radiotherapy alone in the treatment of carcinoma of the uterine cervix in Srinagarind Hospital: Analysis of Complication. Thai J Radiol. 1989; 26(2): 139-146.
17. Perez CA, Breaux S, Madoc-Jones H et al. Radiation therapy alone in the treatment of carcinoma of uterine cervix.I. Analysis of tumor recurrence. Cancer 1983; 51: 1393-1402
18. Kataoka M, Kawamura M, Nishiyama Y, Hamada K, Hamamoto K, Matsu-Ura S. Results of the combination of external-beam and high-dose-rate intracavitary irradiation for patients with cervical carcinoma. Gynecol Oncol 1992; 44: 48-52.

19. Khoo-Tan HS, Chua EJ. Radical radiotherapy for carcinoma of the uterine cervix using high dose rate brachytherapy--a preliminary report. Ann Acad Med Singapore 1996; 25: 367-70.
20. Arai T, NakanoT, Morita S, et al. High dose rate remote afterloading intracavitary radiation therapy for cancer of the uterine cervix. A 20 -year experience. Cancer 1992; 69:175-180.
21. Perez CA, Kuske RR, Camel HM, et al. Analysis of pelvic tumor control and impact on survival in carcinoma of the uterine cervix treated with radiation therapy alone. Int J Radiat Oncol Bio Phys 1988; 14: 613-621.
22. Perez CA, et al Uterine cervix in textbook of principles and practice of radiation oncology, third edition. Perez CA, Brady LW, eds. Lippincott-Raven publishers.New York. 1997: 1806-1808.
23. Kirsten F, Atkinson Kh, Coppelsen JVM, et al. Combination chemotherapy followed by surgery or radiotherapy in patients with locally advanced cervical cancer. Br. J Obstet Gynaecol 1987; 94: 583-588.
24. Sundfor K, Trope CG, Hogberg T, et al. Radiotherapy and neoadjuvant chemotherapy for cervical cancer. A randomized multicenter study of sequential cisplatin and 5-fluorouracil and radiotherapy in advanced cervical carcinoma stage IIIB and IVA. Cancer 1996; 77: 2371-2378.
25. Symonds RP, Burnett RA, Habeshew T, et al. The prognostic value of chemotherapy given before radiotherapy in advanced cancer of cervix. Br J Cancer 1989; 59: 473-475.
26. Lara PC, Garcia Puche JL, Pedraza V. Cisplatin- ifosfamide as neoadjuvant chemotherapy in stage IIIB cervical uterine squamous cell carcinoma. Cancer chemother Pharmacol 1990; 26: 36-38.
27. Thomas GM. Is neoadjuvant chemotherapy a useful strategy for the treatment of stage IB cervix cancer [Editorial]. Gynecol Oncol 1993; 49: 153-155.
28. Pesee M, Kirdpon W, Puapairoj A, et al. Palliative treatment of advanced lung cancer with radiotherapy and Thai herbal medicine as supportive remedy. The Asean J of Riology 2006; 12(3): 149-176.
29. Pesee M, Kirdpon W, Puapairoj A, et al. Palliative treatment of advanced subependymal oligodendroglioma with radiotherapy and Thai herbal medicine as supportive remedy. The Asean J of Riology 2006;12(3):135-148.
30. Takagi A, Matsuzaki T, Sato M, et al. Enhancement of natural killer cytotoxicity delayed murine carcinogenesis by a probiotic microorganism. Carcinogenesis 2001 ; 22(4): 599-605.
31. Takagi M. Immunomodulation by trestment with Lactobacillus casei strain shirota. Int J Food Microbiol 1998; 41(2): 33-40.
32. Salminen S, Isolauri E , Salminen E. Probiotics and stabilization of the gut mucosal barrier. Asia Pacific J Clin Nutr 1996; 5(1): 53-56
33. Wasser SP. Review of Medicinal Mushrooms Advances: Good news from old allies. Herbalgram 2002; 56: 28-33
34. Kim HW, Kim BK. Biomedicinal triterpenoids of Ganoderma lucidum *(Aphyllophoromycetideae)*. Int J of Med Mushroom 1999; 1:121 -38.
35. Van der Hem LG, Ling Zhi-8. Studies of a new immuno modulating agent. Trasplantation. 1995; 60: 438-443.
36. Wang SY. Anti-tumor effect of Ganoderma Lucidum is mediated by cytokines released from activated macrophages and T-lymphocytes. Int J Cancer 1997;70:699-705.
37. Murakami A, Kondo A , Nakamura Y, et al. Possible antitumor Promoting and identification of Active Constituent Cardomoin of Boesenbergia Pandurata. Biosci Biotech Biochem 1993; 57 (11): 1971-3.
38. Cherng JM, Shieh DE, Chiang W, et al. Chemopreventive effects of minor dietary constitutents in common foods on human cancer cells. Bioscience, Biotechnology and Biochemistry 2007; 71(6): 1500-1504

39. Morita N, Hayashi K, Fujita A, et al. Extraction of antiviral substances from Houttuynia cordata Thunb. Chemical abstract 1995; 123: 93249j.

40. Hayashi K, Kamiya M , Hayashi T. Virucidal effects of the steam distillate from Houttuynia cordata and its components on HSV-1, influenza virus and HIV. Plant Med. 1995; 61 (3): 237-41

RAPID BOLUS SINGLE-VENEPUNCTURE VERSUS TRADITIONAL TWO-VENEPUNCTURE TECHNIQUE IN MODIFIED IN-VIVO RED BLOOD CELL LABELING FOR RADIONUCLIDE VENTRICULOGRAPHY: IS THE IMAGE QUALITY ADEQUATE?

Charoonsak SOMBOONPORN; MD[1], James WESTCOTT; BAppSci[2], Nouria SALEHI; PhD[2], Nathan BETTER; MBBS, FRACP[2], Dan Bing ZHOU; MD[2], Dr. Krisana ROYSRI; MD[1], Meir LICHTENSTEIN; MBBS, FRACP[2]

ABSTRACT

Objective: In modified in-vivo red blood cell labeling, stannous pyrophosphate is traditionally injected through a metal needle, and a plastic catheter is used to take and re-inject the blood. This is problematic in patients with needle phobia or poor veins. To eliminate one venepuncture, the percentage labeling efficiency (% LE) of a new technique was ascertained and image quality of resting radionuclide ventriculography was compared with that of the traditional technique.

Methods: Technique A (n=20) included rapid injection of 20-ml diluted stannous pyrophosphate through an Optiva catheter and this retained catheter was later used for taking and reinjecting the labeled blood. Technique B used a traditional small volume of the stannous agent injected by metal needle and use of an Optiva catheter to manipulate pretinned blood and subsequently reinject it.

Results: The % LE of technique A at the time before reinjection and at the end of image acquisition was 75.0% ± 17.9% and 86.0% ± 11.4%, respectively. Mean left ventricle (LV) count, background (BG) count and LV to BG count was not significantly different between the two techniques (p = 0.414, 0.944, 0.338, respectively). Eighty and 20 percent of images were graded as good and fair quality in both groups, respectively.

Conclusions: This new technique provides a high and acceptable % LE for radionuclide ventriculography but needs only single venepuncture.

Key Words: red blood cell labeling; radionuclide ventriculography; plastic catheter; image quality

%LE = percentage labeling efficiency
LV = left ventricle
BG = back ground

[1] Department of Radiology, Faculty of Medicine, Khon Kaen University, Thailand
[2] Department of Nuclear Medicine, Royal Melbourne Hospital, Victoria, Australia
Author for correspondence: Charoonsak Somboonporn, MD
Address: Department of Radiology, Faculty of Medicine, Khon Kaen University, 40002 Thailand
Phone: 043 363 895 **Facsimile:** 043 202 472 **E-mail address:** charoonsak_s@yahoo.com

INTRODUCTION

Left ventricular ejection fraction (LVEF) is an important and universally accepted physiologic index of cardiac function. Radionuclide ventriculography (RNVG) is a highly reliable, widely accepted and noninvasive method for determining LVEF.[1] Image quality and the accuracy in calculating LVEF depend on the red blood cell (RBC) labeling yields.

Modified in-vivo labeling has been used worldwide with a high labeling yield and is less technical demanding than the classical in vitro method.[2-3] However, to achieve a good labeling, venepuncture is usually has to be done twice. Stannous agent as a reducing agent is intravenously injected by a metal needle to pretin the RBC. Then a plastic catheter is inserted to remove approximately 3 ml of blood to be labeled with ^{99m}Tc pertechnetate and the catheter is retained for injecting the radiolabeled RBC back into the patients. Separate stannous agent injection using a metal needle is mandatory; if injected through a plastic catheter made of teflon, it is postulated to form a complex with a compound leached from teflon of the catheter, resulting in a diminished and potentially insufficient amount of stannous agent to reach RBC in vivo and function as a reducing agent.[4] Although there is no published evidence that this negative effect can be found when a polyurethane catheter is used, this two-venepuncture technique has been adopted to guarantee a good labeling yield for modified in-vivo procedure in many nuclear medicine laboratories worldwide, regardless of the type of plastic catheter used.

A major group of patients referred for RNVG are cancer patients. Baseline study before and interval study during administration of certain chemotherapies to assess cardiac function by RNVG are crucial to early diagnose possible cardiotoxicity.[5-8] However, in cancer patients with poor veins and sometimes needle phobia due to multiple previous venepunctures, it may be difficult to perform a venepuncture procedure twice.

RNVG = Radionuclide ventriculography
LVEF = Left ventricular ejection fraction
% LE = % labeling efficiency

In our Nuclear Medicine Department, we had been using a polyurethane catheter in two-venepucture technique for RBC labeling. In order to eliminate one venepuncture, the performance of a new single -venepuncture technique for modified in-vivo RBC labeling was evaluated. The image quality of RNVG was compared with that of the traditional two -venepuncture technique.

PATIENTS AND METHOD

Patients

A prospective study of the performance of this new technique (technique A) was carried out in 20 consecutive patients referred for resting RNVG at the Department of Nuclear Medicine, Royal Melbourne Hospital during August 2003. The percentage labeling efficiency (%LE) of this technique was determined. The image quality of RNVG was also compared with that performed by the conventional two-venepuncture technique (technique B) in prior 20 consecutive patients. Related demographic data such as age, sex and clinical diagnosis were recorded. Previous chemotherapy administered within three months and concurrent medications taken that have been known to affect RBC labeling were also recorded.[9-10]

Autologous red blood cell labeling method

Technique A: A 22-gauge polyurethane catheter, (Optiva; Johnson & Johnson Medical), attached with a 3-way tap was firstly inserted into an available vein of the patient. Then 1 ml of stannous agent (1.1 mg stannous ion) (PYP; Radpharm Scientific, Australia), diluted with isotonic saline to 20 ml, was rapidly injected through a port of the tap, followed by a thorough flush with 5 ml of isotonic saline via another port of the tap. After 10-15 minutes to allow stannous ion to reduce the RBC, 5 ml of blood was drawn via this retained catheter into a syringe containing freshly

eluted ^{99m}Tc pertechnetate (11.4 MBq per kilogram of body weight) and 10 units of heparin. This syringe was incubated at room temperature for 15-20 minutes.

Before injecting the radiolabeled blood back to the patients through this catheter, 0.5 ml of the labeled blood was separated into a heparinized tube (sample 1) to measure %LE. Cardiac images were then acquired according to our usual RNVG protocol. At the end of image acquisition, 2 ml of blood was drawn via the catheter into another heparinized tube (sample 2) before removing the catheter.

Technique B: The same dose of stannous agent, derived from the same company as in technique A, in a traditional small volume (1 ml) without dilution was injected intravenously in a usual speed through a metal needle. After 10-15 minutes, a 22-gauge Optiva catheter was inserted into another vein for collecting 5 ml of the pretinned blood into a syringe containing the same dose of Tc-99m pertechnetate and heparin as in technique A. After incubation at room temperature for 15-20 minutes, the labeled blood was injected into the patient through the catheter.

RNVG image acquisition and processing

Acquisition was performed 10 minutes later using a Siemens Ecam gamma camera, equipped with a low-energy, all-purpose collimator (with ECG triggering and monitoring), using a 64x64 matrix and 8 frames/cardiac cycle. Three projections, anterior, left anterior oblique (LAO) and left lateral, were imaged for 7,500 Kcount per projection. For each study, the optimal LAO angle with the best visual demarcation of the left ventricle was chosen for positioning the head of the camera, with a caudal tilt of 0 to 10 degrees. Total acquisition time was about 10-15 minutes.

Processing was then performed to calculate LVEF by using a standard area-counts technique, in which background-subtract stroke counts (end -diastolic-end-systolic counts) were divided by end-diastolic counts. An experienced nuclear technologist manually drew separate end-systolic, end-diastolic, and pericardiac background (PCBG) regions of interest from the LAO projection. The region of interest for PCBG was drawn in a curvilinear fashion inferolaterally to the left ventricle. The interpreting physician reviewed region of interest placements and visually confirmed the quantified LVEF value.

Labeling efficiency measurement

Immediately after obtaining sample 2, both sample 1 and 2 were measured for the labeling efficiency. Both samples were diluted to 5 ml with saline solution and then were centrifuged at 3,000 g/ minute for 10 minutes and the plasma was then separated from the cells. In order to exclude technical error, the blood cell sample was washed again by dilution with 5 ml isotonic saline followed by repeated centrifugation. Radioactivity of plasma and cell fractions was counted for 60 seconds for two times in a dose calibrator (Capintec, CRC-120, USA) and the average values were used to calculate % LE according to the following formula:

$$\%\,LE = \frac{\text{radioactivity in RBC fraction}}{\text{radioactivity in RBC fraction+plasma fraction}} \times 100$$

Image quality assessment

The image quality was assessed both semi -quantitatively and qualitatively. For semi-quantitative method, mean left ventricular count, mean PCBG count, and mean left ventricular count to mean PCBG count ratio were used to indicate the image quality. Qualitative assessment was evaluated visually according to the previously published criteria11-12 as "good", "fair" or "poor" quality by two interpreters (CS and DZ) independently, blinded to the labeling technique and relevant clinical data. Any discordant grading was later reviewed and discussed to reach the consensus. Good quality was defined if the boundary of the left ventricle was clearly defined to draw the region of interest. Fair quality was defined if the image quality was reduced but left ventricular edge detection was still possible. Poor quality was defined

PCBG = pericardiac background

if left ventricular edge detection could not be separated completely from surrounding radioactivity.

Statistical analysis

Results were expressed as mean ± SD and percent for continuous and categorical data, respectively. Continuous data including age, LVEF and mean counts were compared using Student's *t*-test. Difference between sex, clinical diagnosis and medications used were evaluated using chi-square analysis or the Fisher exact test when appropriate. A probability value less than 0.05 was considered to be statistically significant.

RESULTS

Patient's characteristics were shown in Table 1. There was no significant difference between age, gender, primary clinical diagnosis and derived LVEF between the groups. Most of the patients in both groups were cancer patients. There was also no significant difference of the prevalence of medications used between the two groups.

Mean % LE (± SD) before re-injecting 99mTc labeled RBC into the patient (sample 1) and immediately after completion of the image acquisition (sample 2) of the technique A was 75.0% ± 17.9% and 86.0% ± 11.4%, respectively. Nineteen out of 20 cases showed a progressively increasing %LE from sample 1 to sample 2. (Figure1).

Table 2 compares the image quality semi -quantitatively between the two techniques. There was no significant difference of the mean left ventricular count, mean PCBG count and mean left ventricular count to PCBG count ratio between the two groups (P = 0.414, 0.944 and 0.338, respectively). In addition, by visual grading the results were equal in both groups. Sixteen of 20 images (80%) were graded as good quality and the other four images (20%) were graded as fair quality. No poor image quality was found in either group. A concordant rate between the two interpreters was found in 18 of 20 images (90%) and 19 of 20 (95%) images from technique A and B respectively. Figure 2 shows an example of a good and fair image quality derived from technique A.

Table 1 Characteristics of patients.

Characteristic	Single-venepuncture (n = 20)	Two-venepuncture (n = 20)
Age (y, mean + SD)	48.9 ± 12.3	47.9 ± 16.0
Gender (M/F)	8/12	12/8
Clinical diagnosis (n, %)		
Leukemia	9 (45)	6 (30)
Lymphoma	4 (20)	6 (30)
Breast cancer	5 (25)	4 (20)
Cardiac diseases	2 (10)	4 (20)
Medications (n)		
Beta-adrenergic blocker	3	1
Calcium-channel blocker	2	1
Furosemide	0	1
Aspirin	1	2
Benzodiazepine	2	2
Lipid lowering drug	1	3
Antibiotic	2	1
Anti-arrhythmic drug	0	2
ACE inhibitor	3	2
Chemotherapeutic agent	4	6
Coumadin	3	2
Iodinated contrast media	3	1
% LVEF (mean ± SD)	59.3 ± 11.7	59.8 ± 19.6

ACE, angiotensin-converting enzyme; LVEF, left ventricular ejection fraction
Data are not statistically significant.

Table 2 Semi-quantitative comparison of image quality between the two techniques.

	Single-venepuncture	Two-venepuncture	p-value
LV count	895.8 ± 132.6	918.9 ± 169.3	ns
PCBG count	439.4 ± 47.2	450.9 ± 68.7	ns
LV/PCBG count	2.0 ± 0.3	2.1 ± 0.3	ns

LV, left ventricle; PCBG, pericardiac background
Values are shown as mean ± SD.
ns, not significant

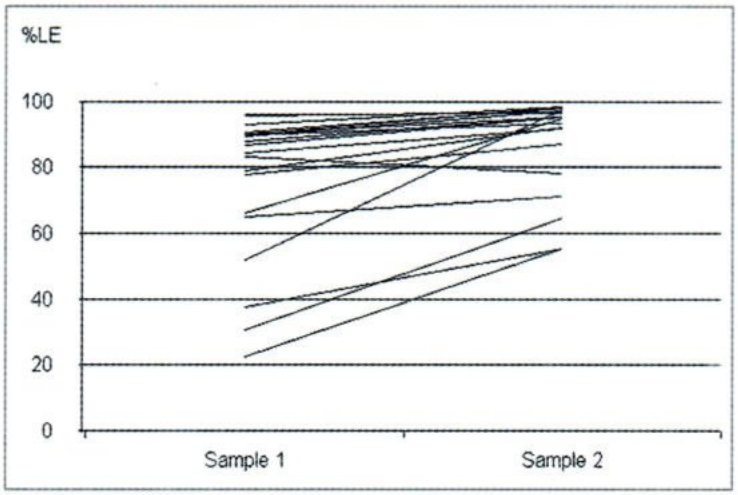

Fig.1 Labeling efficiency of technique A before re-injection of the labeled blood to the patient (sample 1) and after completion of image acquisition (sample 2). The mean %LE increased from 75.0 % to 86.0 % in concordance with similar increase using the two-injections technique in other trials.

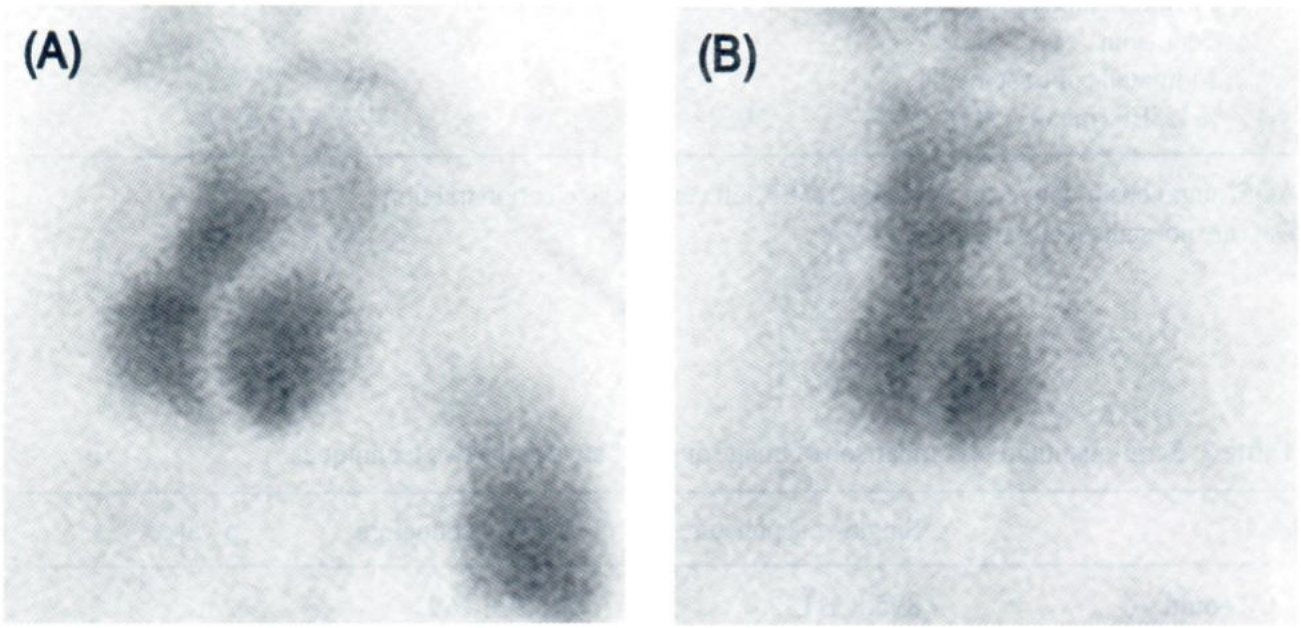

Fig.2 Example of RNVG images of the patients using single-venepuncture technique. (A) Good image quality: clear separation of radioactivity in the left ventricle from surrounding activity. (B) Fair image quality: minimal deterioration of image quality, but left ventricular edge detection was still possible without difficulty.

DISCUSSION

A large number of factors can affect the red cell labeling yield including concurrent medications and iodinated contrast media administered within 24 hours.[9,10,13] For the modified in vivo technique introduced by Callahan et al. in 1982,[2] an intravenous catheter is inserted to withdraw the blood and retained for later reinjecting the labeled blood. This catheter is therefore an inviting route for injection of the stannous agent. However, poor image quality and diminished RBC labeling efficiency was found when injecting the stannous agent through this catheter. Millar et al. reported a poor labeling and rapid clearance of ^{99m}Tc from the bloodstream when stannous agent was injected through a teflon cannula, which was significantly different from those obtained from stannous injection via a metal needle.[4] In addition, the experience of poor labeling and image quality from using the modified in vivo technique with injection of stannous agent through the Hickman catheter was also reported.[14] This had led to the adoption of the two-venepuncture technique to separate the administered route for stannous agent from the route for manipulating the blood.

Our study showed a new technique for such RBC labeling that needed only one venepuncture by inserting a conventional plastic catheter, which was retained for the entire processes of labeling. We prepared a large volume of stannous agent, with rapid injection through a plastic cannula, followed immediately by a thorough flushing the catheter with isotonic saline. We believe that this could reduce the chance of stannous agent to form a complex with the compound that may be leached from the plastic catheter and may also diminish the chance of stannous agent being adsorbed onto the catheter surface.

Since we retrospectively compared this new technique with the data of the prior patients undergoing the traditional two-venepuncture technique in our department, we therefore do not have the data regarding % LE of these prior patients to compare with those of the new technique. However, % LE obtained from this technique was comparable to those performed by traditional two-venepuncture technique reported in the literature.[15]

Regarding the image quality for RNVG, our study showed a satisfactory image quality in most of the patients performed by this new technique. Eighty percent of patients had a good image quality on RNVG and therefore allowed clear and easy delineation of the left ventricular activity for calculating the LVEF. Only a minority of patients was graded as fair image quality, but the left ventricular definition was still sufficient to calculate LVEF in all patients. By comparing this visual grading system between the two techniques, the same results were obtained.

It should be noted that the image quality is not only dependent on %LE but also the stability of the labeling. If significant amount of ^{99m}Tc is discharged from RBC, it can extravasate into the organs surrounding the heart and cause lower left ventricular count to PCBG count ratio and eventually deteriorating image quality. From our single-venepuncture technique, LE after completion of image acquisition was still high suggesting adequate retention time of the labeling for calculation of LVEF in the RNVG procedure.

CONCLUSION

We have shown in a limited number of patients that, a modified in vivo RBC labeling for RNVG can be performed by introducing a retaining polyurethane catheter into the patient, with a rapid bolus of the stannous pyrophosphate. It provides a high and acceptable %LE, without compromising the image quality. It would be very useful in patients with needle phobia or poor venous access. Further study should be carried out to validate this single -venepuncture, high-volume and rapid-injection technique in other kinds of catheter, in particular those made of teflon.

REFERENCES

1. Shaw LJ, Heinle SK, Borges-Neto S, Kesler K, Coleman RE, Jones RH. Prognosis by measurements of left ventricular function during exercise. Duke Noninvasive Research Working Group. J Nucl Med 1998; 39: 140-6.
2. Callahan RJ, Froelich JW, McKusick KA, Leppo J, Strauss HW. A modified method for the in vivo labeling of red blood cells with Tc-99m: concise communication. J Nucl Med 1982; 23: 315-8.
3. Bauer R, Haluszczynski I, Langhammer H, Bachmann W. In vivo/in vitro labeling of red blood cells with ^{99m}Tc. Eur J Nucl Med 1983; 8: 218-22.
4. Millar AM, Wathen CG, Muir AL. Failure in labelling of red blood cells with 99mTc: interaction between intravenous cannulae an stannous pyrophosphate. Eur J Nucl Med 1983; 8: 502-4.
5. Cottin Y, Touzery C, Coudert B, Gilles A, Walker P, Massing JL, et al. Impairment of diastolic function during short-term anthracycline chemotherapy. Br Heart J 1995; 73: 61-4.
6. Ganz WI, Sridhar KS, Ganz SS, Gonzalez R, Chakko S, Serafini A. Review of tests for monitoring doxorubicin-induced cardiomyopathy. Oncology 1996; 53: 461-70.
7. Stuckey SL, Pitman AG, Hicks RJ. Cardiac blood-pool imaging in oncology more than an ejection fraction? Clin Nucl Med 2001; 26: 18-26.
8. Mitani I, Jain D, Joska TM, Burtness B, Zaret BL. Doxorubicin cardiotoxicity: prevention of congestive heart failure with serial cardiac function monitoring with equilibrium radionuclide angiocardiography in the current era. J Nucl Cardiol 2003; 10: 132-9.
9. Tatum JL, Burke TS, Hirsch JI, Millar WW, Fratkin MJ. Pitfall to modified in vivo method of technetium-99m red blood cell labeling. Iodinated contrast media. Clin Nucl Med 1983; 8: 585-7.
10. Sampson CB. Complications and difficulties in radiolabelling blood cells: a review. Nucl Med Commun 1996; 17: 648-58.
11. Neumann P, Schicha H, Schumbrand P, Bahre M, Emrich D. Visualizing cardiac blood pool: comparison of three labeling methods. Eur J Nucl Med 1983; 8: 463-6.
12. Hambye AS, Vandermeiren R, Vervaet A, Vandevivere J. Failure to label red blood cells adequately in daily practice using an in vivo method: methodological and clinical considerations. Eur J Nucl Med 1995; 22: 61-7.
13. Kelly MJ, Cowie AR, Antonino A, Barton H, Kalff V. An assessment of factors which influence the effectiveness of the modified in vivo technetium-99m-erythrocyte labeling technique in clinical use. J Nucl Med 1992; 33: 2222-5.
14. White MP, Mann A, Cross DM, Heller GV. Evaluation of technetium-99m red blood cell labeling efficiency in adults receiving chemotherapy and the clinical impact on pediatric oncology patients. J Nucl Med Technol 1998; 26: 265-8.
15. Kuehne R, Reuter E. High RBC labeling efficiency by controlling pretinning with the modified in vivo/in vitro labeling method. J Nucl Med Technol 1999; 27: 222-6.

STRAIGHT LEG RAISING WHILE PERFORMING ^{99m}TECHNETIUM SESTAMIBI INJECTION AT REST CAN REDUCE INFERIOR WALL ARTIFACT IN PATIENTS WITH A LOW-LIKELIHOOD OF CORONARY ARTERY DISEASE

Charoonsak SOMBOONPORN, MD[1], Nathan BETTER, MBBS, FRACP[2], Dan Bing ZHOU, MD[2], Meir LICHTENSTEIN, MBBS, FRACP[2]

ABSTRACT

Inferior wall artifacts (IWA) are frequently found in 99mTc sestamibi resting myocardial perfusion imaging (MPI) of a low-likelihood of coronary artery disease patients (LCP). Straight leg raising (SLR) relatively decreases proportion of sestamibi in the liver, so it may reduce subdiaphragmatic activity that can potentially cause IWA. Aim of the study is to investigate whether SLR while performing ^{99m}Tc sestamibi rest injection can reduce the incidence of IWA.

Methods: Incidence of hot and cold IWA were compared between 72 LCP performing SLR during ^{99m}Tc sestamibi rest injection and 125 LCP without SLR. Three inferior segments from 20-segment model were used for myocardial grading.

Results: Age, sex, body weight and stress method for MPI were not significantly different between the two groups. The SLR group had a significantly higher incidence of non-artifact patients compared with the non-SLR group (18.1% versus 4.8%, $P = 0.002$). The SLR group also had a significantly lower incidence of hot IWA. (19.4%vs 41.6%, $P = 0.002$). Incidence of cold IWA were not different between the two groups ($P = 0.225$). Analysis of cold IWA patients showed less severe, even not significantly ($P = 0.085$), different, the same as artifact in the SLR group compared with the non-SLR group.

Conclusion: SLR while performing rest injection can reduce the incidence of hot IWA in LCP and may help in the detection of the lesions in the right coronary artery or left circumflex coronary territories.

Key Words: artifact, coronary artery disease, low-level exercise, technetium-99m sestamibi

INTRODUCTION

Prevention and recognition of an artifact occurring both in the process of image acquisition and processing is of paramount importance to improve the accuracy of myocardial perfusion imaging (MPI) interpretation. Since myocardial perfusion agent such as ^{99m}Tc sestamibi is mainly excreted by hepatobiliary system,[1] therefore hepatic activity and also activity in the gastrointestinal tract can cause artifacts during the MPI processes.[2] This may complicate the interpretation of the inferior wall of the myocardium adjacent

[1] Department of Radiology, Faculty of Medicine, Khon Kaen University, Thailand.
[2] Department of Nuclear Medicine, Royal Melbourne Hospital, Victoria, Australia.
Author for correspondence: Charoonsak Somboonporn, MD
Address: Department of Radiology, Faculty of Medicine, Khon Kaen University, 40002 Thailand.
Phone: 043 363 895 **Facsimile:** 043 202 472 **E-mail address:** charoonsak_s@yahoo.com

to these subdiaphragmatic activities.[3]

Low-level exercise has been used in conjunction with pharmacological stress to improve the image quality. Because it can reduce blood flow to the liver and digestive system, resulting in a relatively decreased ^{99m}Tc sestamibi distribution in these organs, therefore it can reduce the inferior wall artifacts.[4-6] Since the artifact seen in patients with a low-likelihood of coronary artery disease (CAD) is likely to be artifactual. In our laboratory, we have observed a significant proportion of a low-likelihood of CAD patients having the inferior wall artifacts on the resting ^{99m}Tc sestamibi myocardial single photon emission computed tomography (SPECT) images. For this reason, we aimed to evaluate whether straight leg raising (SLR) exercise during administration of ^{99m}Tc sestamibi for the resting images can reduce the inferior wall artifacts.

MATERIALS AND METHODS

Patients

This study included two groups of patients referred for rest/stress MPI for the diagnosis of CAD from September 2002 until September 2003, who were categorized as a low-likelihood of CAD. Criteria for low-likelihood of CAD were modified by those of Braunwald E et al.[7] Any patient having any one of the following exclusion criteria was excluded from the study: known CAD; definite angina; probable angina in male older than 60 years or in female older than 70 years; probable angina in patient with diabetes; probable angina in patients with 2 or 3 risk factors including smoking, hypertension and hypercholestero- lemia; hemodynamic change during chest pain; and extracardiac vascular disease.

Patients in the first group (non-SLR) consecutively recruited from September 2002 to April 2003 consisted of 125 patients not performing SLR during administration of ^{99m}Tc sestamibi for the rest study. The second group (SLR) prospectively included 72 nonconsecutive patients from May 2003 to September 2003 who performed SLR while ^{99m}Tc sestamibi was injected for the resting images. Patients who could not do SLR were excluded from the study.

Myocardial perfusion imaging protocol

All patients underwent same-day rest/stress protocol after fasting for at least 6 hours. The rest study was performed first by administration of ^{99m}Tc sestamibi (3.7 MBq per kilogram of body weight) and image acquisition was performed 20-30 minutes later. Three minutes before this injection, a tablet or half a tablet of anginine (600 micrograms of glyceryl trinitrate) was given sublingually to the patient (for body weight > 70 and < 70 kilograms, respectively) who had a history of acute myocardial infarction, coronary artery bypass graft surgery or coronary angioplasty. The stress study began 30 minutes to 2 hours later depending on the availability of the stress laboratory. It was preferably performed by symptom -limited upright bicycle ergometry. At the peak of the exercise, ^{99m}Tc sestamibi (11.1 MBq per kilogram of body weight) was injected and the exercise was continued for further 1 to 2 minutes. The image acquisition was performed about 20 to 30 minutes later. If the exercise was not possible or suboptimal, pharmacologic stress was performed instead with a standard protocol using dipyridamole or dobutamine as appropriate.

Straight leg raising

During lying down on a couch for ^{99m}Tc sestamibi rest injection, patients in the SLR group were asked to raise his/her leg straightly for about 45 degrees, one after the other continuously, beginning one minute before and until two minutes after ^{99m}Tc sestamibi injection.

MPI = Myocardial Perfusion Imaging
CAD = Coronary Arterial Diseases

Myocardial SPECT acquisition, processing and interpretation

The patient was given a cup of water to drink right before the imaging, both in resting and stress studies. Myocardial SPECT was performed with the

patient in the prone position for both acquisitions. Three gamma cameras were used in this study, which included MultiSPECT-3 (Siemens, Hoffman Estate, Ill), E-Cam (Siemens, Hoffman Estate, Ill) and Irix (Marconi Medical Systems, Cleveland, OH). Low -energy, general-purpose collimator was used for all cameras and the matrix size was 64 x 64 pixels.

Images were reconstructed after low-pass prefiltering (Butterworth order, 10; cutoff frequencies, 0.45 for resting and 0.4 for stress studies for Multi SPECT-3 and E-Cam, and 0.2 for resting and 0.25 for stress studies for Irix) and ramp-filtered backprojection. No attenuation correction or scattered correction was applied. Transaxial slices were reoriented by a computer program to obtain oblique angle tomograms parallel to the long axis of the left ventricle.

Gated SPECT acquisition was applied only for the stress study. Eight frames per cardiac cycle were used. The reconstructed electrocardiography (ECG) gated SPECT images were processed and displayed by GS-Quant or QGS software.

MPI interpretation was performed by two experienced nuclear medicine physicians. The cine images were reviewed first to detect artifacts in the reconstructed images during image interpretation. Then the tomographic slices of the myocardium in the short axis, vertical long axis and horizontal long axis were evaluated. Wall motion and thickening of the stress study were also reviewed. Normal scan for this study was defined as absence of perfusion abnormali- ties. Abnormal scans were defined when there was reversible defect (ischemia) or fixed defect (infarct).

Inferior wall grading and definition of artifact

The 20-standard segment model was used to evaluate the degree of myocardial uptake.[8] Three of these 20 segments, representing the inferior wall region, were graded visually by using a 5-point scoring system (0, normal uptake; 1, minimally decreased uptake; 2, moderately decreased uptake; 3, severely decreased uptake; 4, absent uptake) by two other observers, with consensus, blinded to relevant clinical data including SLR performed. Non-artifact patient was regarded when all of three segments were graded as 0. Patient was regarded as having the hot artifact if at least one of the three segments had abnormally high uptake precluding accurate uptake grading. Cold artifact was defined in each segment if it was graded as 1, 2, 3 or 4. For patients having the cold artifact, severity of the artifact was further determined from an average grade of the three segments.

Statistical analysis

Continuous data were expressed as mean ± SD if normally distributed, or as median and range if not normally distributed. Categorical data were expressed as percentage. Age, body weight and severity of cold artifact between the two groups were compared by unpaired Student's *t*-test or Mann-Whitney U test, when appropriate. Difference between gender, the incidence of non-artifact, hot artifact and cold artifact cases used were compared using Fisher's exact test. A probability value less than 0.05 was considered to be statistically significant. The power to detect the reduction rate of the incidence of artifact patients between non-SLR and SLR groups was calculated at a significant level of 0.05 from our sample size of 125 for non-SLR group and 72 for SLR group.

RESULTS

Characteristics of patients were shown in Table 1. There were no significant differences between the two groups in terms of age, gender, body weight, stress method for MPI and percentage of abnormal MPI results. Patients with SLR had a significantly higher proportion of smoking ($P = 0.002$) and family history of heart disease ($P = 0.001$) as the risk factors of CAD compared with those in the non-SLR group.

MPI results were positive in 7 patients (5.6%) without SLR (6 ischemia and 1 infarct) and 5 patients (6.9%) with SLR (4 ischemia and 1 infarct). The follow-up to find if coronary angiography was subsequently performed was not possible in one and

two scintigraphically abnormal patients in the SLR and non-SLR groups, respectively. Apart from these patients, angiogram was performed in only a patient in the SLR group who had anterolateral ischemia on MPI, and was found to have 80% stenosis of the proximal diagonal branch of the left anterior descending coronary artery. We did not find unpleasant symptoms or adverse effects from the SLR in any patient.

Table 2 compares the incidence of artifacts between the groups. Significantly higher incidence of non-artifact patients was found in the SLR group compared with the non-SLR group (18.1% versus 4.8%, $P = 0.002$). In addition, patients with SLR had a significantly lower incidence of hot artifact compared with those in the non-SLR group (19.4% versus 41.6%, $P = 0.002$). However, the incidence of patients with cold artifact was not significantly different between the groups (53.5% versus 62.5%, $P = 0.225$). In patients with cold artifact, severity of the artifact shown by the mean ± SD (range) of average myocardial uptake grade of the three inferior wall segments was 1.209 ± 0.633 (0.333 -2.333) and 1.000 ± 0.599 (0.333-2.667) in non -SLR group and SLR group, respectively ($P = 0.085$).

TABLE 1 Characteristics of patients.

	Non-SLR (n = 125)	SLR (n = 72)	*P*-value
Age (y)	53.2 + 12.6	50.9 + 10.7	NS
Male gender	55 (44.0)	32 (44.4)	NS
Body weight (kg)	79.8 + 19.0	79.9 + 17.8	NS
Risk factor			
Smoking	16 (12.8)	22 (30.6)	0.002
Hypertension	20 (16.0)	19 (26.4)	NS
Hypercholesterolemia	12 (9.6)	4 (5.6)	NS
Positive family history	26 (20.8)	31 (43.1)	0.001
Stress method			
Upright bicycle ergometry	110 (88.0)	64 (88.9)	NS
Dipyridamole	11 (8.8)	8 (11.1)	NS
Dobutamine	4 (3.2)	0 (0)	NS
Abnormal scan	7 (5.6)	5 (6.9)	NS

SLR, straight leg raising; NS, not significant.
Values presented are mean + SD or number of patients (%).

TABLE 2 Comparison of the incidence of each type of artifact between the two groups.

Incidence*	Non-SLR (n = 125)	SLR (n = 72)	*P*-value
Non-artifact patient	6 (4.8)	13 (18.1)	0.002
Hot artifact patient	52 (41.6)	14 (19.4)	0.002
Cold artifact patient	67 (53.6)	45 (62.5)	NS

SLR, straight leg raising; NS, not significant.
* Values in parenthesis are percentages.

From our sample size in both groups, the power to detect the reduction rate of the incidence of artifact patients from non-SLR (95.2%) to SLR (81.9%) groups was 80% at a significant level of 0.05.

DISCUSSION

^{99m}Tc sestamibi is mainly excreted by hepatobiliary system so subdiaphragmatic activity can be found in the liver, gallbladder, small and large intestine and the stomach, the latter due to duodenogastric reflux.[1] The liver activity is particularly prominent at rest and in pharmacologic stress studies. This intense hepatic activity can interfere with the image interpretation in several ways. First, it can give scattered counts to the adjacent inferior wall, creating a hot artifact, and therefore cause underestimation of perfusion defect in this region. Second, a false defect, or cold artifact, in the inferior wall can occur by oversubtraction of the counts from the inferior wall during image processing. In addition, if the images are normalized to the artifactually high counts in the inferior wall, it can create a false defect to the rest of the myocardium, particularly the anterior wall. This can substantially degrade the image quality and can render images uninterpretable.[9]

In patients with a low-likelihood of CAD, the inferior wall defect is likely to be artifactual either from subdiaphragmatic intense activity or diaphragmatic attenuation particularly in male patients. However, the latter cause may be partly resolved by prone imaging as we routinely use.[10-11] In an attempt to reduce subdiaphragmatic activity, apart from keeping the patient fasting before tracer injection, the easiest way may be increasing the interval between tracer injection and imaging. However, this may limit laboratory efficiency in particular for the busy and space-limited department like ours, where the usual time interval between tracer injection and rest imaging was only about 20-30 minutes.

CAD = Coronary Arterial Disease

Low-level exercise or a change in subject's position can rapidly change hepatic blood flow because portal vein, which supplies approximately 80% of the blood to the liver, is a low-pressure system. In addition, the liver as well as the digestive system can alter their plasma volumes almost instantaneously through sympathetic vasoconstriction, mediated by alpha-adrenergic receptors, in reflex response to the stress. This venous constriction causes displacement of a large volume of blood from the liver to the veins in the thorax.[12] After intravenous injection, ^{99m}Tc sestamibi rapidly clears from the blood pool.[1] SLR, as a low-level exercise, during administration of ^{99m}Tc sestamibi, stimulates sympathetic nervous activity and therefore decreases blood flow to the liver and digestive system, while provides a redistribution of blood flow to the leg muscles under activity. These mechanisms result in a lower proportion of ^{99m}Tc sestamibi localizing in the liver. Combination of a low-level exercise to the pharmacological stress has been shown to improve the image quality and reduction of artifacts caused by hepatic activity.[4-6] We adopted this concept to the rest images by introducing SLR exercise during ^{99m}Tc sestamibi injection.

We found that SLR could significantly decrease the incidence of inferior wall hot artifact patients and increase the proportion of non-artifact patients; hence improve the image quality and accuracy of MPI interpretation. Although SLR did not appear to reduce the incidence of cold artifact in our population, it showed a trend to reduce the severity of the cold artifact in these patients.

Our study had some limitations. Since data from the non-SLR group were retrospectively collected. We had to use the criteria for a low-likelihood for CAD only from the itemized data we had recorded. These were purely based on the clinical history without associated ECG data. However, only about 6% of patients in each group had abnormal MPI results and only one of them was confirmed a significant stenosis by coronary angiography. In addition, it seems reasonable to expect differences in terms of body habitus of these patients between the groups, which can cause inferior wall attenuation artifact from the diaphragm in different degrees.[13] Although we did not have the records about the bra-cup size, size and density

of the breast in our female population, and degree of lateral chest wall fat and abdominal protuberance in male subjects,[13] the possible impact of these factors were in part eliminated by the comparable proportion of gender and body weight between the groups and the prone imaging position in our study.

CONCLUSION

We have shown that applying SLR exercise in patients undergoing MPI during ^{99m}Tc sestamibi injection for the rest imaging can reduce the incidence of artifact in the inferior wall of the left ventricular myocardium. Although conducted in the low -likelihood of CAD patients, theoretically it can be generalized to the intermediate and high-likelihood of CAD patients as well. SLR can be incorporated into the protocol for rest injection without difficulty or detrimental effects to the patients. It can reduce the repeated scans and increase the patient throughput of the laboratory. Most importantly, this procedure has a potential to increase the sensitivity in detecting CAD lesions in the right coronary artery and left circumflex coronary artery territories, particularly in patients with multi-vessel disease. Further studies are needed to clarify this issue.

SLR = Straight Lig Raising
MPI = Myocardial Perfusion Imaging
CAD = Coronary Artery Diseases

ACKNOWLEDGMENT

The authors are grateful to James Westcott for excellent technical assistance and Dr. Krisana Roysri for statistical analysis. The authors have indicated they have no financial conflict of interest.

REFERENCES

1. Wackers FJ, Berman DS, Maddahi J, Watson DD, Beller GA, Strauss HW, et al. Technetium -99m hexakis 2-methoxyisobutyl isonitrile: human biodistribution, dosimetry, safety, and preliminary comparison to thallium-201 for myocardial perfusion imaging. J Nucl Med 1989; 30: 301-11.
2. Rehm PK, Atkins FB, Ziessman HA, Green SE, Akin EA, Fox LM, et al. Frequency of extra-cardiac activity and its effect on ^{99m}Tc-MIBI cardiac SPET interpretation. Nucl Med Commun 1996; 17: 851-6.
3. Germano G, Chua T, Kiat H, Areeda JS, Berman DS. A quantitative phantom analysis of artifacts due to hepatic activity in technetium -99m myocardial perfusion SPECT studies. J Nucl Med 1994; 35: 356-9.
4. Cramer MJ, Verzijlbergen JF, van der Wall EE, Vermeersch PH, Niemeyer MG, Zwinderman AH, et al. Comparison of adenosine and high-dose dipyridamole both combined with low-level exercise stress for ^{99m}Tc-MIBI SPET myocardial perfusion imaging. Nucl Med Commun 1996; 17: 97-104.
5. Thomas GS, Prill NV, Majmundar H, Fabrizi RR, Thomas JJ, Hayashida C, et al. Treadmill exercise during adenosine infusion is safe, results in fewer adverse reactions, and improves myocardial perfusion image quality. J Nucl Cardiol 2000; 7: 439-46.
6. Samady H, Wackers FJ, Joska TM, Zaret BL, Jain D. Pharmacologic stress perfusion imaging with adenosine: role of simultaneous low-level treadmill exercise. J Nucl Cardiol 2002; 9: 188-96.
7. Braunwald E, Jones RH, Mark DB, Brown J, Brown L, Cheilin MD, et al. Diagnosing and managing unstable angina. Agency for Health Care Policy and Research. Circulation 1994; 90: 613-22.
8. Germano G, Kavanagh PB, Berman DS. Effect of the number of projections collected on quantitative perfusion and left ventricular ejection fraction measurements from gated myocardial perfusion single-photon emission computed tomographic images. J Nucl Cardiol 1996; 3: 395-402.
9. Jain D. Technetium-99m labeled myocardial perfusion imaging agents. Semin Nucl Med 1999; 29: 221-36.

10. Lisbona R, Dinh L, Derbekyan V, Novales-Diaz JA. Supine and prone SPECT 99mTc MIBI myocardial perfusion imaging for dipyridamole studies. Clin Nucl Med 1995; 20: 674-7.
11. Hayes SW, De Lorenzo A, Hachamovitch R, Dhar SC, Hsu P, Cohen I, et al. Prognostic implications of combined prone and supine acquisitions in patients with equivocal or abnormal supine myocardial perfusion SPECT. J Nucl Med 2003; 44: 1633-40.
12. Widmaier EP, Raff H, Strang KT, editors. Vander, Sherman, and Luciano's Human physiology: the mechanisms of body function. 9th ed. New York: McGraw-Hill, 2004.
13. Araujo W, DePuey EG, Kamran M, Undavia M, Friedman M. Artifactual reverse distribution pattern in myocardial perfusion SPECT with technetium-99m sestamibi. J Nucl Cardiol 2000; 7: 633-8.

RETROPERITONEAL NEURILEMMOMA: A CASE REPORT

Daranee PITANUPONGSA, M.D.[1]

ABSTRACT

Neurilemmoma is a rare retroperitoneal tumor. A case of retroperitoneal neurilemmoma was reported from Trang Hospital, diagnosed by CT as a mass located at the pelvic brim right side. A 41 years old female patient was admitted because of a palpable abdominal mass with referred pain into her right lateral thigh on compression. CT revealed a rim enhancing mass with central hypodensity. After surgical removal, histopathological examination confirmed a neurilemmoma.

Key words : retroperitoneal neoplasms, neurilemmoma

INTRODUCTION

Neurilemmomas, or schwannomas, are benign neurogenic tumors that arise from the nerve sheaths of peripheral nerves. They may occur nearly anywhere in the body but have a predilection for the head, the neck, and the flexor surfaces of the upper and lower extremities. The retroperitoneal localization of a neurilemmoma represents an unusual occurrence (0.5%-1.2% of all sites).[1,2]

In the present report, I describe a case of this uncommon retroperitoneal pathology in a female patient.

CASE REPORT

A 41-year-old Thai female patient was requested for CT scan of the abdomen. The patient presented with a three-month history of palpable mass in the right lower quadrant of the abdomen. On compression to the mass, she had referred pain into her right lateral thigh. On abdominal examination, she had a 5-cm palpable mass, firm to hard in consistency with mild tenderness in right lower quadrant of the abdomen. The mass was not mobile.

CT showed a 4.8x3.9x3.5-cm rim enhancing mass with central hypodensity. It was located just lateral to right psoas muscle and anterior to right iliacus muscle (Fig.1, 2).

[1] Department of Radiology, Trang Hospital, Trang, Thailand.

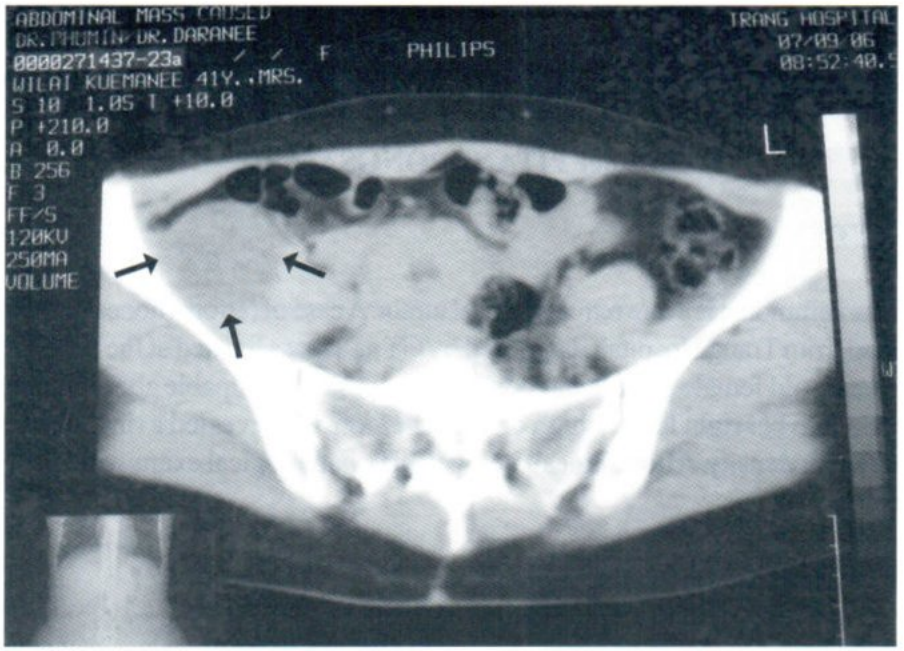

Fig.1 Nonenhanced axial CT scan reveals a well-defined round mass with homogereous hypodensity. The mass is located just lateral to right psoas muscle and anterior to right iliacus muscle.

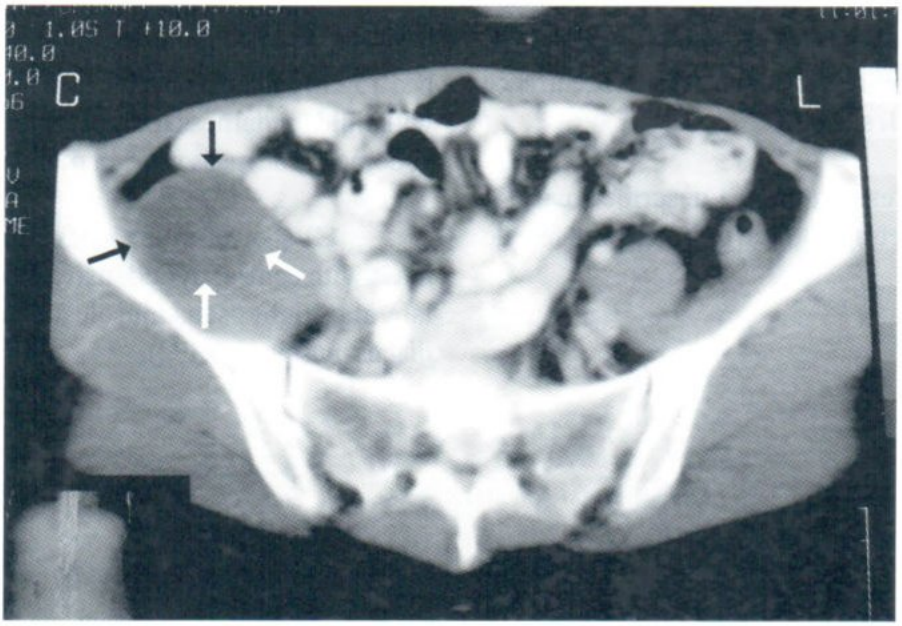

Fig.2 Enhanced axial CT scan reveals rim enhancement of the mass with central hypodensity.

The patient underwent surgery. Surgery revealed retroperitoneal cyst placed on lateral portion of right psoas muscle. Complete excision was performed. Histopathological examination was diagnosed as a neurilemmoma.

DISCUSSION

Neurilemmoma is the most common neurogenic tumor. They are benign, encapsulated tumors of the nerve sheath. They can present in many locations but rarely in the retroperitoneum.[1-11] Only 1% is found in the retroperitoneum, which accounts for 0.5%-1.2% of all retroperitoneal tumor.[2,4,5] Abdominal neurogenic tumors are most commonly located in the retroperitoneum, especially in the paraspinal areas and adrenal glands.[1] Patients with benign retroperitoneal neurilemmomas are predominantly in their second to fifth decade, and women are twice as often affected as men.[1,4,6] Presentation is typically varied and non-specific ranging from low back pain, abdominal pain, abdominal mass or an incidental finding.[1-12] Referred pain and neurological symptoms in the lower extremities have also been described.[3,6,11] As in the presented case, she had abdominal mass with referred pain into her right lateral thigh on compression to the mass. The low frequency of this tumor and the lack of specific signs and symptoms make presurgical diagnosis very difficult.

At CT, a neurilemmoma appears as a well -demarcated round or oval mass that frequently demonstrates prominent cystic degeneration and calcification. At contrast-enhanced CT, they demonstrate variable homogeneous or heterogeneous enhancement. Heterogeneous areas on enhanced CT scans may be due to cystic and hemorrhagic changes.[1,2,5,8,11] Cystic changes occur more commonly in retroperitoneal neurilemmoma (up to 66%) than in other retroperitoneal tumors.[5] It is difficult to identify the peripheral nerve from which retroperitoneal neurilemmoma develop.[1] These features are not pathognomonic images. Therefore, misdiagnosis of retroperitoneal neurilemmoma is not uncommon. It can be confirmed only during surgery and definitive histopathological examination.[1,2,5]

The resection of this tumor is the appropriate treatment. Prognosis is quite good since post-surgical recurrences are unusual.[2-5]

CONCLUSION

Retroperitoneal neurilemmomas are rare tumors arising from the neural sheath of peripheral nerves. Symptoms and CT findings are non-specific and can mimic with different diseases. Diagnosis is based on histopathological examination. The encapsulated cystic mass in retroperitoneum on CT, especially in a patient with a history of referred pain in the lower extremities, should raise the possibility of a neurilemmoma in the differential diagnosis. And it is important to recognize these tumors as benign with excellent prognosis so as to avoid unnecessary extensive radical surgery.

REFERENCES

1. Rha SE, Byun JY, Jung SE, et al. Neurogenic Tumors in the Abdomen: Tumor Types and Imaging Characteristics. RadioGraphics 2003; 23: 29-43.
2. Khan AS, Bakhshi GD, Sankaye PB, et al. Retroperitoneal Schwannoma. Bombay Hospital Journal 2002; 44: 489-490.
3. Dickey ID. Neurilemmoma. eMedicine [WebMD] 2007 March [cited 2007 October 19]. Available from: URL: http :// www. emedicine. com/orthoped/topic 524.htm.
4. Fass G, Hossey D, Nyst M, et al. Benign retroperitoneal schwannoma presenting as colitis : A case report. World J Gastroentorol 2007; 13: 5521-5524.
5. Cury J, Coelho RF, Srougi M. Retroperitoneal schwannoma: case series and literature review. Clinics 2007; 62: 1-9.
6. Schindler OS, Dixon JH, Case P. Retroperitoneal giant Schwannomas: Report on two cases and review of the literature. Journal of Orthopaedic Surgery 2002; 10: 77-84.

7. Rajagopal KL, Lakhkar BN. Solitary giant meurilemmoma in the psoas muscle. Indian J Radiol Imaging 2002; 12: 551-552.
8. Masahiro K, Kiyoshi Y, Takashi E, et al. Six cases of retroperitoneal neurilemmoma. Journal of Japan Surgical Association 2002; 63: 750-754.
9. Sarto G, Lentini S, Patern R, et al. Retroperitoneal neurilemmoma: Clinical case. Urologia [Homepage] 1999 [cited 2007 October 19]. Available from: URL: http:// www. rivistaurologia.net/2_99/articolo 15.htm.
10. Dede M, Yagci G, Yenen MC, et al. Retroperitoneal Benign Schwammoma: Report of three cases and Analysis of Clinico-Radiologic Findings. Tohoku J. Exp. Med. 2003; 200: 93-97.
11. Seok SH, Kim MC, Chung H, et al. Solitary Schwannoma in the Psoas Muscle-A Case Report. Journal of Korean Neurosurgical Society 2001; 30: 1127-1129.
12. Jang CI, Choi JS,Rhee HS, et al. A Case of Retroperitoneal Neurilemmoma Arising from Adjacent to Kidney. Korean J Urol. 1997; 38: 1010-1012.

STUDY OF AMORPHOUS SILICON ELECTRONIC PORTAL IMAGING DEVICE AS A DOSIMETRY FOR DYNAMIC INTENSITY MODULATED RADIATION THERAPY VERIFICATION

Sivalee SURIYAPEE MEng,[1] Nuttakorn PREEDASAK MSc,[1] Sornjarod OONSIRI MSc,[2] Chulee CHAROONSANTIKUL MSc,[2] Taweap SANGHANGTHUM MSc,[2] Chotika JUMPANGERN MSc,[2] Isra ISARANGKUL NA AYUTHAYA MSc.[2]

ABSTRACT

The purpose of this study is to investigate the basic dosimetric characteristics of Varian flat panel amorphous silicon electronic portal imaging detectors (EPID) for the possibility of using a silicon portal imager for absolute dosimetric verification of the delivery of dynamic intensity modulated radiation treatment (IMRT) fields. The measurements were performed with 6 MV X-ray beams from Varian Clinac 23EX. The studies included field size dependence, dose rate, dose response, effect of dead time, relative and absolute dosimetry. The portal dose image was tested by comparing the EPID profiles with the ion chamber both for open and wedge fields. The portal dose image calculated by EPID dosimetry was compared with the EPID measurement for clinical IMRT fields. The results showed field size dependence of EPID, which was more sensitive than ion-chamber for larger field size but less than ion chamber in smaller field size, the maximum deviation of 4.9% was observed. The EPID was linear with dose rate and integral dose. The effect of dead time in frame acquisition due to transfer to the CPU was found to start at 40 MU of field size studied. The dead time resulted in dynamic field caused error that increased with leaf speed, the error was 17.62% for a 1 cm leaf gap moving at 1 cm/s. The comparison of profiles from EPID and ion chamber measurement for 10x10 cm^2 normal field showed the good agreement. For wedge field, both of EPID and ion-chamber profiles showed the agreement in the center part but slightly shift in the penumbra region. The pre-treatment verification for IMRT fields of 15 plans showed the agreement stribution between EPID calculation and EPID measurement within 3% difference in dose and 3 mm. difference in distance. The profile in the direction of MLC movement also showed good correlation between calculation and measurement.

EPID	=	Electronic portal imaging detectors	**PDI**	=	Predicted portal dose image
IMRT	=	Intersity Modulated radiation treatment	**QA**	=	Quality assurance
CPU	=	Central processing unit	**DMLC**	=	Dynamic multileaf collimater
MU	=	Monitor unit	**SDD**	=	Source detector distance
MLC	=	Multileaf collimator	**FF**	=	Flood field
CU	=	Calibration unit	**AM**	=	Acquisition mode
R2	=	The Correlation Coefficient	**DTA**	=	Distance to agreement

[1] Department of Radiology, Faculty of Medicine, Chulalongkorn University, Bangkok, Thailand
[2] Department of Radiology, King Chulalongkorn Memorial Hospital, Bangkok, Thailand

INTRODUCTION

The most widely used form of pre-treatment quality assurance (QA) for IMRT verification generally consists of absolute dose measurements with ionization chamber combined with isodose distribution measurements in a phantom with film, or even by means of gel dosimetry.[1] The data acquisition as well as the data handling for comparison remains a time consuming task.

A new efficient tool for IMRT pre-treatment QA is the electronic portal imaging device (EPID). It was originally designed and developed to replace radiographic films for purpose of geometric verification of patient set-up during treatment. The new current generation of EPID is based on semiconductor materials, namely, amorphous silicon photodiodes.[2] This device is mounted on the linear accelerator providing real-time and digital feedback to the user. EPID showed high quality image than previous devices. Until recently EPID is possible to use as a dosimetry.[3] For pre-treatment verification, the EPID image can be compared to a predicted portal dose image (PDI) calculated from the fluence map from the Eclipse treatment planning. Before using EPID as a dosimetry, the relationship between EPID response and dose delivery parameters, such as dose and dose rate should be understood.

In this study the dosimetric properties of amorphous silicon EPID for verification of dynamic IMRT pre-treatment QA are investigated for 6 MV x-ray beams. The portal dosimetry software is used to measure the clinical IMRT fields. All investigations in this study are used at the dose rate of 300 MU/min.

MATERIALS AND METHODS

1. Electronic portal imaging device (EPID)

The amorphous silicon EPID[4] (aS500, Varian, Palo Alto, CA) consists of a 1 mm copper metal plate, a 134 mg/cm^2 gadolinium oxysulphide phosphor screen (Kodak, Lanex Fast B) that includes a 0.18 mm polyester reflector, and a 40x30 cm^2 (512x384 pixel) a silicon array. Each pixel consists of a light sensitive photodiode and a thin-film transistor with a pixel pitch of 0.78x0.78 mm^2. A 1.6-mm-thick plastic collision cover (epoxy with glass and foam) encloses the detector with an air gap of approximately 1.5 cm between the cover and the detector surface. The EPID was integrated with a 6 and 15 MV x-ray beams from linear accelerator with a dynamic multileaf collimator (DMLC) of 120 leaf (Clinac 23EX, Varian, Palo Alto, CA).

2. AM maintenance mode

This mode is used for tuning and maintaining the PortalVision image acquisition system that can read line profile, pixel value, pixel region of interest, acquisition mode, time/frame and number of frames. Two possible modes of acquisition for the EPID systems are multiple image acquisition and continuous frame averaging. We used continuous mode for the experiments, a single image consisting of the average of many image frames is acquired during radiation delivery. The EPID will average successively acquired frames up to a limit of 9999 frames.

3. Portal dosimetry mode

The portal dosimetry is consisted of Portal Vision hardware (EPID), acquisition module (4DTC/ standalone PV), and algorithm for dosimetric image prediction (Eclipse treatment olanning) and evaluation module (Review). This mode is available for point dose measurement, line dose measurement, isodose overlays, relative and absolute dose comparison with treatment planning, relative and absolute gamma evaluation. The pixel value in term of calibration unit (CU) is shown.

4. EPID calibration

4.1 AM maintenance

The EPID was calibrated by the acquisition of dark field and flood field. The calibration field size was 40x30 cm^2 at isocenter with the detector at a source-detector distance (SDD) of 140 cm. The calibration of the EPID with a flood field (FF) image

is important for accurate signal response as all acquired images are divided by the normalized FF image. This image is acquired to correct for non -uniformities in the EPID response, and after calibration, the input beam profile for the FF acquisition is uniform. The image should be calibrated every month for high quality image.[5]

4.2 Portal dosimetry

The detector was calibrated to yield a predicted portal dose (PD) of 1 CU for a 10x10 cm^2 field size and a dose of 100 MU at SDD = 100 cm. Since in practice, the SDD cannot be reduced beyond 105 cm. when the robotic arm is in clinical mode, the actual calibration was performed at SDD = 105 cm, setting the PD to be 0.90702 CU (i.e. calculated by inverse square law).

5. Parameters influence EPID dosimetry

The EPID was used in AM maintenance program with continuous mode of 10 fixed frames for the parameters studied.

5.1 The response of EPID with field size

In this experiment, the EPID was irradia ted with 50 MU and the field size was varied from 4x4 to 24x24 cm^2. At each field size, three images are acquired and the mean pixel values in a 9x9 pixel region at the center of field size were recorded. The doses were measured for comparison by the 0.13 cc ion-chamber with Dose 1 dosemeter (IC13, Wellhoffer, Schwarzenbruck, Germany) in a solid water phantom at SDD 105 cm, 1.5 cm depth with 5 cm of backscatter at each field size.

5.2 The response of EPID with dose rate

In order to find the relationship between the signal and dose rate, EPID was irradiated with 100 MU at 10x10 cm^2 field size. The changes in dose rate (300-132 MU/min) were the results of changes with SSD (100, 105, 120.2, 130.2, 140 and 151.2 cm). At each distance, three images were acquired and the mean pixel values in a 9x9 pixel region at the center of field size were recorded. To determine the relation of dose rate with distance; the dose rate were measured with ion-chamber in a solid water phantom at a 3.0 cm depth at each SDD.

5.3 The response of EPID with dose

Normally, the total dose in term of pixel values can be found by the average pixel values multiplied by frame number. The experiment was performed at 10x10 cm^2 field size with the varied dose of 10-200 MU. EPID was set at 105 cm SDD. Three images are acquired and the pixel values were recorded from the mean pixel values in a 9x9 pixel region at the center of field size.

5.4 Effect of dead time related to leaf speed

Sliding window deliveries were performed with a uniform 1 cm leaf gap between two banks of multileaf collimator (MLC) and a 10x10 cm^2 field size. The speed of the MLC depended on the MU. The MU used was 50, 100 and 200, so the speeds of MLC were 1.0, 0.5 and 0.25 cm/s, respectively. Reduction in signal from a uniform profile occurred due to dead time in frame acquisition was quantified for each leaf speed. Profiles were obtained along the direction of leaf motion directly under the center of the MLC leaf adjacent to the central axis. The dropping of the profile near the end of the field represented the effect of the dead time.

6. EPID dosimetry

This part has been performed in portal dosimetry mode.

6.1 Relative dose measured for open and wedge fields

The beam profiles at 1.5 cm depth from EPID were compared with the profile measured from ion-chamber in water. Images were acquired with open field and 45 degree wedge of 10x10 cm^2 field size. The EPID was at 105 cm from source. The EPID data were scaled to 101.5 cm for comparison.

b. IMRT pre-treatment verification

For pre-treatment verification of the IMRT fluence, an image of clinical IMRT field of

naspharynx cancer were taken without the patient at zero degree gantry angle. The predicted isodose distribution calculated by treatment planning (Eclipse, Varian, Palo Alto, CA) was compared with the isodose measured from EPID. The gamma value of 3% difference in percentage depth dose and 3 mm difference in distance were selected for analyzing the result.

RESULTS AND DISCUSSION

1. Parameters influence EPID dosimetry

1.1 The response of EPID with field size

The EPID response in term of the mean pixel values in 9x9 pixel region at the center of field and ion-chamber reading with field size normalized to the 10x10 cm^2 values are shown in figure 1. Second -order polynomials were fitted to the data. The EPID response was shown the deviation of 4.09% for a 4x4 cm^2 and 4.90% for a 24x24 cm^2 field size when compared with ion-chamber. The areas which were close to 10x10 cm^2 normalized field had less error.

The graph showed increasing in EPID and ion-chamber responses with field size which means that the scatter radiation was increasing when field size was increased. Since the scatter has a low energy component, its effect on the EPID's phosphor response for field size larger than 10x10 cm^2 was enhanced compared to ion-chamber due to the presence of high atomic number components in the phosphor. The response of EPID was less for small field size.

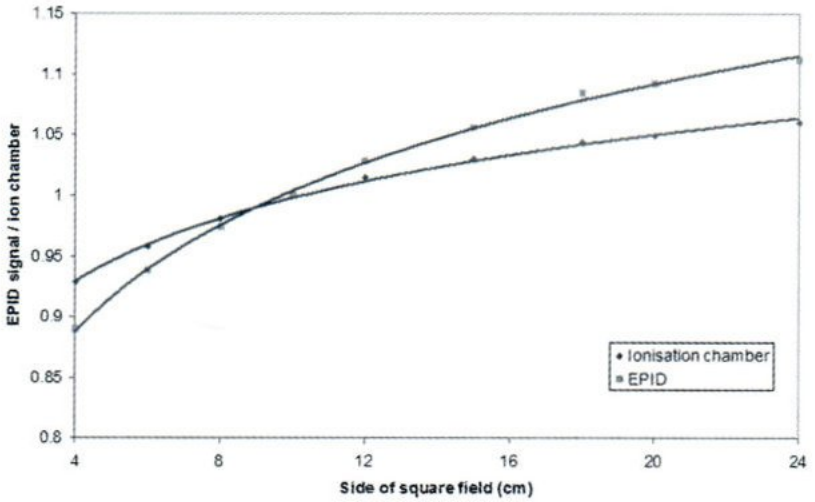

Fig.1 Field size dependence on the EPID and ion-chamber

1.2 The response of EPID with dose rate

The relationships between the dose rate (MU/ min) measured by ion-chamber and mean pixel values are shown in figure 2. The linearity of the EPID with dose rate are shown with $R^2 = 1$. From this result, it can be seen that when the source surface distance was increased which mean that the dose rate was decreased, there would be a decrease in pixel values.

EPID = Electronic Portal Imaging Device

1.3 The response of EPID with dose

The linearity with integral dose had been reported in many researches.[4,6,7] The integral doses of EPID were obtained by multiplication of the pixel values by the number of frames. The experiment's result of the relationship between integral dose in term of MU and the mean values of EPID pixel values multiply by number of frames can be seen in figure 3 for 10x10 cm^2 field sizes. The linearity was shown with $R^2 = 0.9979$. From the results, it can be seen that when doses were increased, there would be an increasing in pixel values and frames. During irradia-

tion, if the dose rate was fluctuated, the pixel values would show slightly non-linearity with dose. When the mean pixel values multiplied by the frames, the result showed linearity with the dose. This is due to the compensation of pixel values with the frame.

The effect of dead time was occurred every 64 frames.[4,6,7] The acquisition time per frame usually is 0.111 sec, therefore we can find the acquisition time per frame dealing with dead time by dividing the total acquisition time reading by number of frame reading. The results showed the acquisition time per frame of greater value than 0.111 sec when the dead time had been occurred. If there was no dead time, the number of frames would be the actual acquisition time divided by 0.111 sec. The frame without dead time showed higher value than the frame with dead time for the dose greater or equal to 40 MU. The frames without dead time multiplied by pixel value were higher when compared with the frame with dead time multiplied by pixel value as shown in figure 4 for 10x10 cm^2 field size. The error signal due to dead time increased when the dose was increasing. So for the static field of 200 MU maximum doses, the error due to dead time were 2.89%.

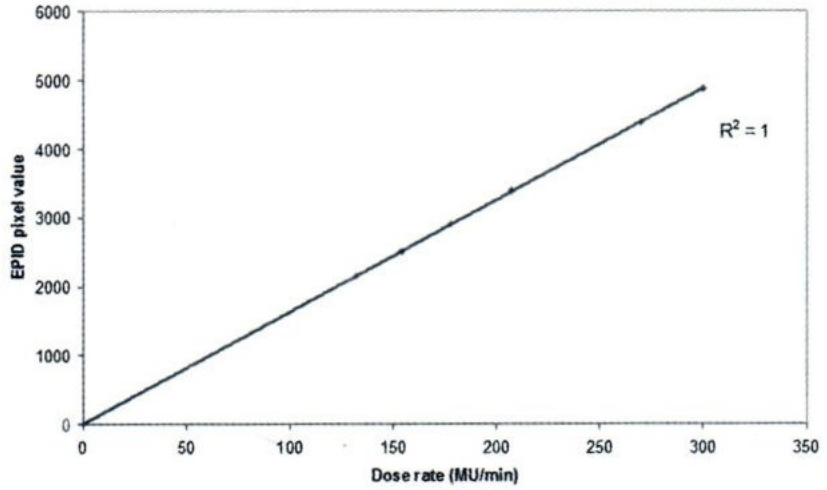

Fig.2 The response of EPID with dose rate for 10 x 10 cm2 field size.

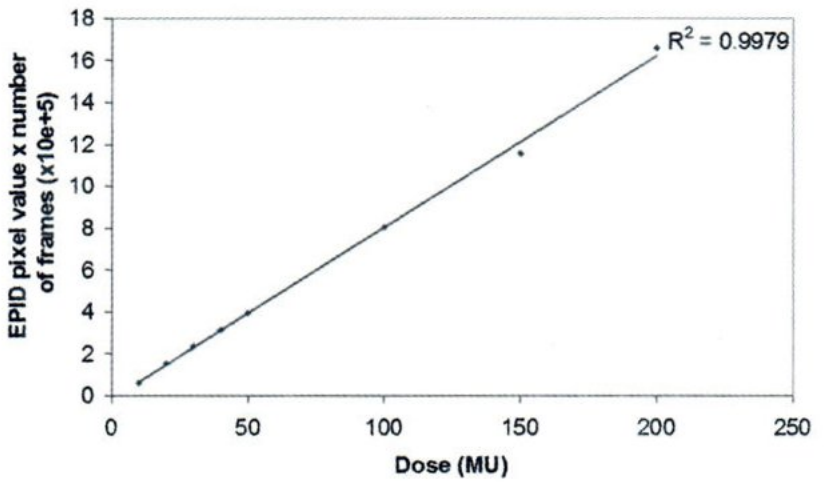

Fig.3 The response of EPID with integral dose for 10x10 cm^2 field size.

1.4 Effect of dead time related to leaf speed in frame acquisition in dynamic field

In the past study on the effect of dead times,[4] it was found that during EPID read out in every 64 frames, there would be data transfer to the CPU (Center Process Unit), with total time loss of 0.28 seconds, which was equal to 2 frames losses. While the data were transferred, EPID will not be able to collect signals, even if radiation were still delivered. Due to effect of dead times, EPID will have loss some signal. The resulted of static field has been shown in 1.3 as mentioned. For dynamic field, the profiles of the EPID are shown at various leaf speeds of 0.25, 0.5 and 1 cm/s in figure 5 by giving the dose of 200, 100 and 50 MU, respectively. The part of profile that shifts from the flat part represented the errors of each leaf speed. From this result, with the increase in leaf speed, there would be an increase in signal errors. The highest signal error value was equal to 17.62% at leaf speed of 1 cm/s and the lowest error value was equal to 3.37% at leaf speed of 0.25 cm/s. Therefore in IMRT treatment, with high leaf speed, the profile could show a higher error signal in EPID. For accurate dosimetry in EPID, the leaf speed should be slower or with larger MU.

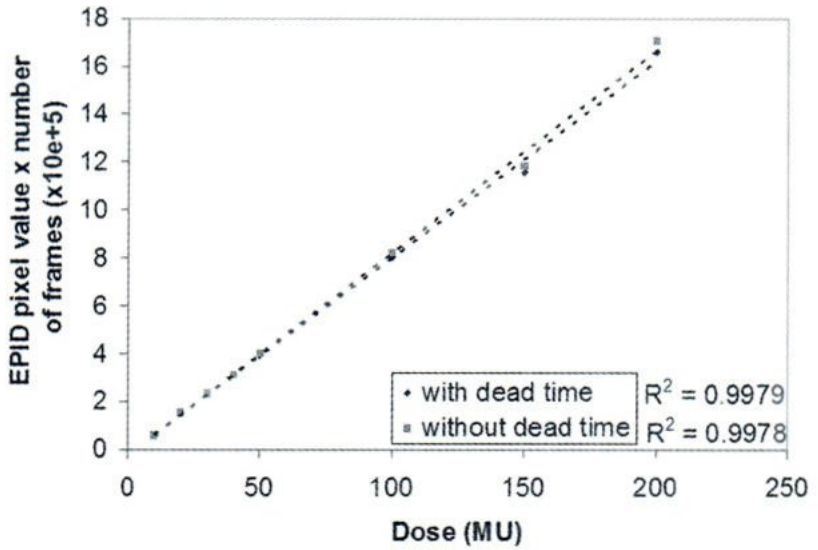

Fig.4 The response of EPID with integral dose in 10 10 cm2 field size with and without dead time.

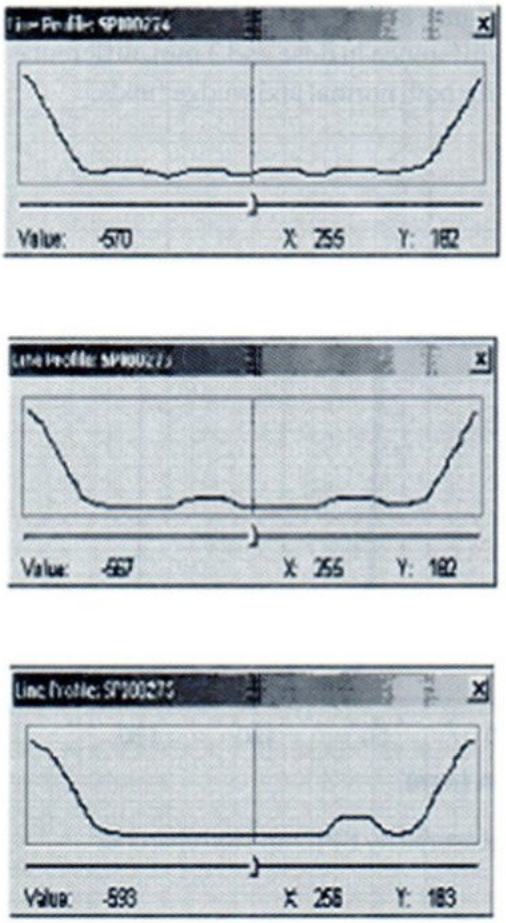

A. 0.25 cm/s leaf speed

B. 0.50 cm/s leaf speed

C. 1.00 cm/s leaf speed

Fig. 5 The profile of sliding window delivery of EPID on x-asix with the effect of dead time for different leaf speed.

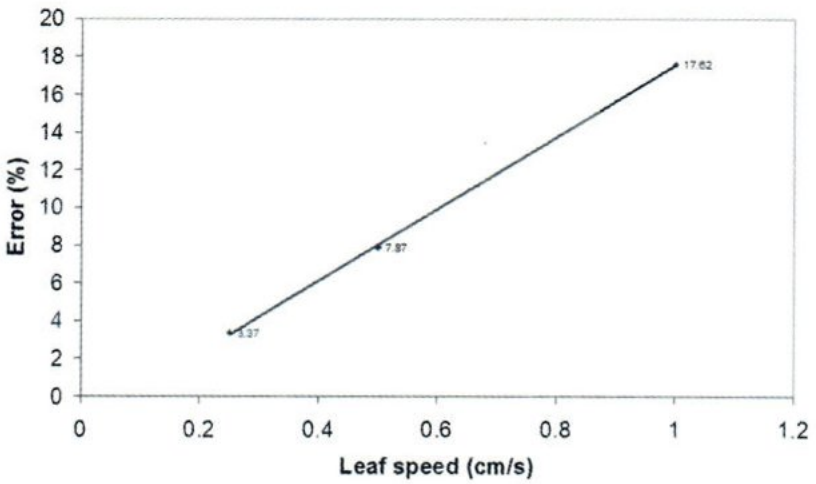

Fig. 6 The percent error due to dead time when increasing the leaf speed.

2. EPID dosimetry

2.1 Relative dose measurement for open and wedge fields

The comparison between the profile measured by EPID and ion chamber[5,6] of 10x10 cm^2 field size is shown in figure 7. The same comparison of 45 of wedge profile of 10x10 cm^2 is shown in figure 8. The profile became agreeable within 3% difference in dose and 3 mm. difference in distance for both normal and wedge fields.

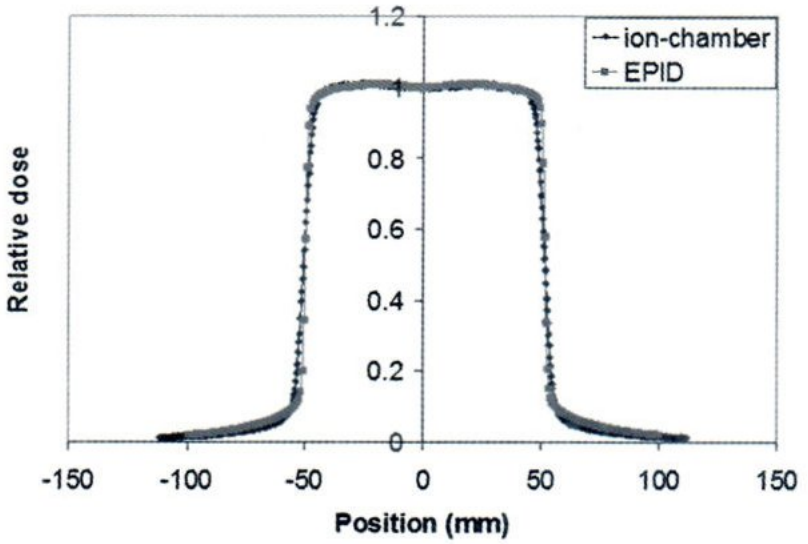

Fig. 7 The comparison of profiles measured by EPID and ion chamber for 10x10 cm^2

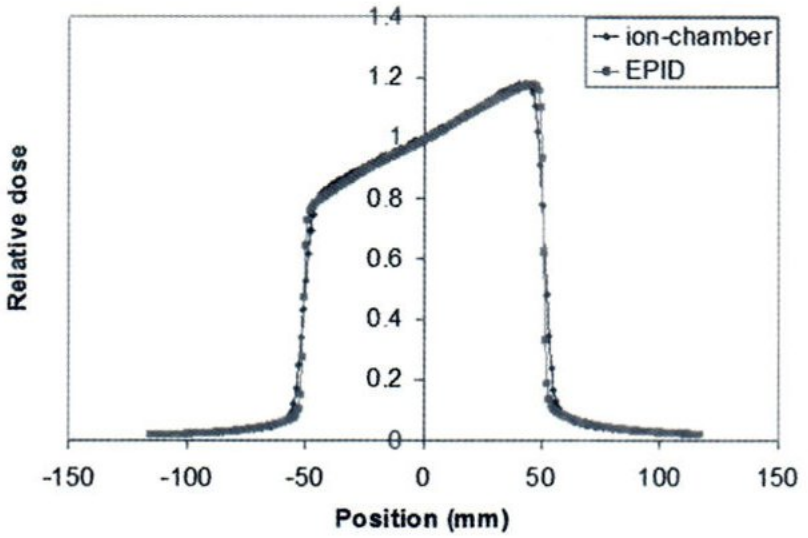

Fig. 8 The comparison of profiles measured by EPID and ion chamber for 10x10 cm^2 of 45^0 wedge.

2.2 IMRT pre-treatment verification

The example of one filed comparison between EPID calculation and EPID measurement in IMRT pre-treatment QA of the nasopharynx plan are shown in figure 9. The absolute isodose distribution showed the agreement of calculation and measurement. The profiles in the direction of MLC in figure10 showed the agreement between EPID calculation and EPID measurement within 3% difference in dose and 3 mm. difference in distance. The verification of 15 IMRT plans which mostly are Nasopharynx plan showed good correlation between measured and calculated.

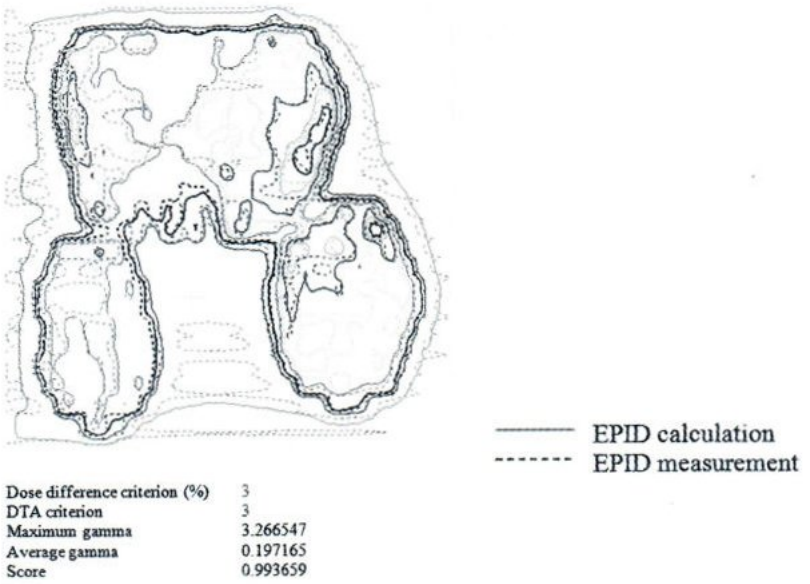

Fig. 9 The comparison of isodose distribution of nasopharynx field EPID calculation and EPID measurement.

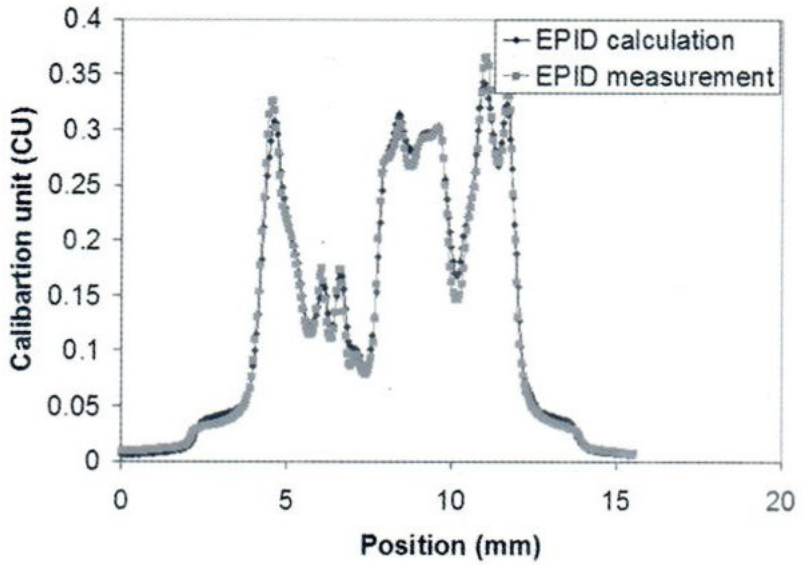

Fig.10 The EPID profile in x direction in a plane as shown in figure 9.

CONCLUSION

The result of dosimetric properties showed that most of the response of EPID are comparable to the response of ion chamber, the only deviation was the field size. This effect was corrected by using field size factor measured by EPID for the predicted dose made by Eclipse treatment planning. The problem of dead time in image acquisition dynamic IMRT delivery was less for IMRT plan used in the clinic due to the high MU of each field. Using EPID as a dosimetry for verification of dynamic IMRT plan showed good result comparable to the film. The process is simple, easy set up and less time consume. However, EPID is limited only for the measurement in air and only at the gantry angle of zero degree.

The research has demonstrated that an understanding of the relationship between pixel value reading and dose or fluence is a prerequisite for portal dosimetry. The EPID is suitable to be used for the IMRT pre-treatment verification. Clinical verification of IMRT plan showed good result with accurate dose measurements.

ACKNOWLEDGEMENTS

The authors would like to acknowledge Varian Medical System and Dr Joseph Y Ting from Melbourne Cancer Center, USA who allowed us to use the portal dosimetry software for this research work.

REFERENCES

1. Esch AV, Bohsung J, Sorvari P, et al. Acceptance tests and quality and control procedures for the clinical implementation of intensity modulated radiotherapy (IMRT) using inverse planning and sliding windows technique. Radiother Oncol 65 (2002): 53-70.
2. Antomuk LE, Boudry J, Huang W, et al. Demonstration of megavoltage and diagnostic x-ray imaging with hydrogenated amorphous silicon arrays. Med Phys 19 (6) (1992): 1455-66.
3. Moran MJ, Roberts DA, Nurushev TS, et al. An active matrix flat panel dosimeter (AMFPD) for in- phantom dosimetric measurements. Med Phys 32 (2) (2005) : 466-72.
4. Greer PB, Popescu CC. Dosimetric properties of an amorphous silicon electronic portal imaging device for verification of dynamic intensity modulated radiation therapy. Med Phys 30 (7) (2003) : 1618-27.
5. Heinrich R. Varian Medical Systems. 2002 Switzerland : Baden.
6. Esch AV, Depuydt T, Huyskens DP. The use of an aSi-based EPID for routine absolute dosimetric pre-treament verification of dynamic IMRT fields. Radiother Oncol 71 (2004): 223-34.
7. Winkler P, Hefner A, Georg D. Dose -response characteristic of an amorphous silicon EPID. Med Phys 32 (10) (2005): 3095-105.